INVESTIGATING NEUROTROPHIC FACTORS THAT REGULATE AXONAL REGENERATION IN MUSCLE LACERATIONS

HAN HWAN CHOUR

A THESIS SUBMITTED

FOR THE DEGREE OF MASTERS OF SCIENCE

DEPARTMENT OF ORTHOPAEDIC SURGERY

NATIONAL UNIVERSITY OF SINGAPORE

2012

PREFACE

This thesis is submitted for the degree of Master of Science in the Department of Orthopaedic Surgery at the National University of Singapore. No part of this thesis has been submitted for any other degree at another university. All the work in this thesis is original. Parts of this thesis have been presented in the following conferences:

1. Han HC, Pereira BP, Yu Z, Tan BL, Nathan SS. intermediate filament proteins and Galectin-1 immunoreactivity in lacerated muscles. **55th Annual Meeting of Orthopaedic Research Society, Las Vegas, Nevada, Feb 2009**.
2. Han HC, Pereira BP, Nathan SS. Nerve-derived R-spondin-1 and Galectin-1 promote functional muscle recovery in lacerated medial gastrocnemius of Sprague-Dawley rats. **Yong Loo Ling School of Medicine, 1st Scientific Conference, Singapore, 2011**.
3. Han HC, Tan BL, Yu Z, Nathan SS, Pereira BP. Laceration-induced expression of R-spondin-1 and Galectin-1 in skeletal muscle regeneration. **58th Annual Meeting of Orthopaedic Research Society, San Francisco, California, Feb 2012.**
4. Pereira BP. Tan BL, Han HC, Yu Z, Aung KZ, Leong DT. Intramuscular nerve damage in lacerated skeletal muscles may direct the inflammatory cytokine response during recovery. **Journal of Cellular Biochemistry. 2012, 113 (7): 2330-45.**
5. Han HC, Pereira BP, Sharma M, Nathan SS. Intact Intra-Muscular Nerve in Lacerated Medial Gastrocnemius of Male Sprague Dawley Rat Improves Muscle Recovery over 12-weeks **Yong Loo Ling School of Medicine, 3rd Scientific Conference, Singapore, 2013**.

ACKNOWLEDGMENTS

Firstly, I am deeply grateful to my Principal Investigator, and co-supervisor, Dr Barry P Pereira for supporting my research work through two research grants (URF Tier-1 grant (T13-0802-P21) and a Biomedical Research Council (BMRC/04/1/21/19/309). He also devoted his time and energy to edit and polished my thesis and related abstracts selflessly.

I also like to thank my main supervisor, Associate Professor Saminathan Suresh Nathan, for his critique and guidance for the project. Next I want to thank Associate Professor Mridula Sharma for her help in the grant application for this project. Finally, a big "Thank You" to all the following individuals working in neighbouring laboratories who have always rendered their technical assistance when I am in doubt; from Dr Ratha's Laboratory, Dr Radtha Mahendran, Tham Sin Mun and Juwita Norasmara bte Rahmat; from Dr Phan's Laboratory, Mr Ong Chee Tian and Ms Zhou Yue; from Dr Lim Yoon Pin's Lab, Ms Chong Lee Yee; from Dr Theresa Tan May Chin's lab, Tan Wei Qi; from Dr Victor Lee's Lab, Ms Chin Sze Yung; from Dr Gan Shu Uin's Lab, Ngo Kae Siang, and last, but not least, from Dr Deng Lih Wen's Lab, Ms Liu Jie.

TABLE OF CONTENT

SUMMARY

The functional recovery of lacerated skeletal muscles can be slow and incomplete. A damaged intra-muscular nerve has previously been shown to influence recovery. The study investigates gene and protein expression profiles of neurotrophic factors, atrophic factors and fibrosis factors during the early (2-weeks) and late (12-weeks) phase of repair using the medial gastrocnemius of adult male Sprague-Dawley rats. It is hypothesized that specific endogenous anti-fibrosis, anti-atrophic and anti-re-innervation targets can improve muscle and intra-muscular nerve axonal regeneration in the early phase post-laceration. The gene and protein expression levels of NT4, GDNF, CNTF, IGF1, HGF, Galectin-1 and EGF in lacerated muscle models involving different intramuscular nerve injuries were studied. In the intramuscular nerve preserved intact (PN), there is a greater reduction in collagen (3.25-fold), vimentin (0.21-fold) and aggrecan (0.24-fold) expression than intramuscular nerve cut group (DN) at 12-weeks post-laceration. This correlates positively with a marked increase in AMPK-1a (2.96-fold), decorin (11.28-fold) and EGF (3.24-fold) expression at 12-weeks in PN. Fibrosis in DN (denervated muscle) is driven by high NT4 (24.86-fold) and TGFb2 (0.21-fold) expression. Fibrosis then promotes chronic denervation via up-regulation of collagen-1 and aggrecan, which leads to more atrophy in DN. This is evident as there is a greater increase in atrogin-1 (3.76-fold) and MuRF-1 (3.44-fold) expression in DN than in PN at 12-weeks post-laceration, resulting from higher myogenin (10.81-fold) and myostatin (0.85-fold) expression, and lower IGF1 (0.15-fold), CNTF (1.34-fold), GDNF (17.78-fold) and EGF (2.44-fold) expression. DN also has abundant immature muscle fibers with small size and central nuclei at lacerated site, while PN had more mature, fully differentiated adult muscle fibers with large cross-sectional area and multiple nuclei at the periphery. The decrease in myogenesis in DN is mediated by high TGFb2 and myostatin expression. Chronic denervation in DN leads to incomplete differentiation of young myofibers into

mature adult muscle fibers to replace dead muscle fibers. DN suffered more permanent fiber type transformation, with lower fast myosin heavy chain (0.043-fold) and fast troponin-I (0.14-fold). This re-distribution of myosin heavy chains and troponin-I is responsible for the loss of muscle force and power in DN rats. Intra-muscular nerve regeneration in PN is better than DN as PN has the highest GAP43 expression level at 12-weeks (0.85-fold) while DN has the lowest GAP43 expression (0.59-fold). This great reduction in GAP43 activity in DN is due to aggressive fibrosis which inhibited axonal regeneration and high complement-3 (6.61-fold) expression which destroyed the newly regenerating axons. Our results showed that the integrity of the intra-muscular nerve can regulate fibrosis, atrophy, intra-muscular nerve regeneration, fiber type transformation, and myogenesis across the lesion site.

(428 words)

LIST OF TABLES

LIST OF FIGURES AND ILLUSTRATIONS

List of Symbols and Abbreviations Used

Symbol	**Full Name**
AMPK-1a	AMP-activated protein kinase, alpha 1 catalytic subunit
AP-1	Activator Protein-1
α-SMA	alpha-smooth muscle actin
ATF-3	cAMP-dependent activating transcription factor-3
bHLH	basic Helix-Loop-Helix
CBP	cAMP- response element binding protein
cDNA	copy DNA
Col-1a	Collagen-1a
CNTF	ciliary-derived neurotrophic factor

CREB	cAMP response element binding protein
CTGF	Connective Tissue Growth Factor
DAB	Diaminobenzidine
Des	desmin
DN	denervated intra-muscular nerve model
DTT	Dithiothreitol
ECL	Enhanced chemiluminescent
ECM	extra-cellular matrix
EGF	epidermal growth factor
Erk	Extracellular regulated kinase
ER	endoplasmic reticulum
ERR-a	estrogen-related receptor-alpha
Foxo	forkhead box
Gal-1	Galectin-1
GAP43	growth associated protein-43
Gasp-1	growth and differentiation factor associated serum protein-1
GDNF	glial-derived neurotrophic factor
gp130	glucoprotein 130, oncostatin M receptor
GPI	glycosyl-phosphatidyl-inositol
Grb2	Growth factor receptor-bound protein 2
HDAC	histone deacetylase
HGF	hepatocyte growth factor
HN-1	hematological and neurological expressed-1
HRP	Horseradish-peroxidase
IGF-1	insulin-like growth factor-1
IGFBP	IGF-binding protein
IRS-1	Insulin receptor substrate-1
JAK/STAT3	Janus kinase/Signal Transducer and Activators of Transcription-3
JDP2	c-Jun dimerization protein-2
LRP	lipoprotein related protein
MAPK	Mitogen-activated protein kinase
MEF2a	myocyte enhancer factor 2a
MG	Medial Gastrocnemius
MGB	minor groove binding

MMP1	matrix metalloproteinase-1
MuRF-1	Muscle Ring Finger-1
myHC	Myosin heavy chain
myf5	myocyte factor 5
NAD	nicotinamide adenine dinucleotide
NT-4	neurotrophin-4
OD	optical densitometry
PCR	Polymerase chain reaction
PGC-1a	peroxisome proliferator receptor gamma co-activator-1-alpha
PI3K	phosphatidylinositol-3-kinase
PAI-1	plasminogen activator inhibitor-1
PN	preserved intra-muscular nerve model
PPAR	peroxisome proliferator receptor
RAG	regeneration associated genes
RET	Re-arranged during transfection Trk receptor
RN	re-innervated intra-muscular nerve model
RQ	Relative Quantification, means fold change in expression level normalized to lamin A
R-spondin-1	Roof- plate specific- spondin-1
RT	reverse transcription
RXR	retinoid X receptor
SD	Sprague-Dawley
SDS-PAGE	Sodium dodecyl sulphate-polyacrylamide gel electrophoresis
SH2	Src homology 2
Shh	Sonic hedgehog
Sirt-1	Sirtuin-1
Sp-1	Specificity protein-1
TAK1	TGFb activated kinase-1
TGFβ2	transforming growth factor-beta 2
TGIF	TGFb-inducible factor
Trk	tropomyosin related kinase

1) INTRODUCTION

Laceration of skeletal muscle involving the intra-muscular nerve is frequently encountered in trauma of the extremities. The muscle lacerations are repaired by epimysial suturing, followed by immobilization (Kragh et al, 2005). Although it is possible to repair damaged the intra-muscular nerves in lacerated skeletal muscle following traumatic injury by micro-anastomosis, this is technically difficult. Also, micro-anastomosis of the intra-muscular nerve cannot prevent the formation of fibrosis at the lesion site. These results in irreversible atrophy with muscle mass and function not fully returned as the muscle remained permanently denervated.

The re-innervation of lacerated skeletal muscle is tightly regulated by an orchestrated expression of growth factors, cell adhesion molecules, extracellular matrix proteoglycans and axonal guidance molecules during different phases of muscle regeneration. This process involves re-connection of alpha motor neurons to their endplates, re-connection of gamma motor neurons to spindles, and re-growth of sensory axons into muscle. The latter comprise several types of axons such as unmyelinated nociceptive axons and large myelinated axons that re-innervate muscle spindles. After injury, terminal Schwann cells first cluster at denervated endplates to facilitate reconnection. Regenerating motor axon terminals are then guided to denervated endplates initially by growing along a lining of old Schwann cells from the proximal stump of the cut nerve.

Another potential source of growing axons is from axonal sprouts from adjacent intact muscles. This may take more than 3-4 months because few regenerating axons can successfully cross the gap between the proximal and distal nerve stumps if the gap is more than 3mm even after micro-surgical repair. Hence the lacerated muscle may be innervated by several sprouts (polyneuronal innervations). Polyneuronal innervation is eventually pruned

when functional neuromuscular synapse is established.

Not all of the regenerating axons will achieve the desired re-innervation of the limb skeletal muscles. Those that do reach the muscle can prevent denervation-induced atrophy (Borisov et al, 2001). Some axons will fail to reach their targets completely whereas others will grow in a misdirected fashion. This inappropriate muscle re-innervation can lead to random nerve sprouting in a mass of scar tissue, resulting in poor functional muscle recovery. The poor muscle recovery can become irreversible with muscle fibers at the lesion site being replaced by non-contractile collagen fibers. This then leads to simultaneous contraction of antagonistic muscles and mass movement, and so effective movement to the traumatised limb cannot be restored (Fu and Gordon, 1995).

Several studies support the proposition that re-innervation of the peripheral nerve at the early repair phase can influence the recovery of the lacerated muscle post-surgery (Fu and Gordon, 1995; Borisov et al, 2001). For example, the range of recovery of the muscle mass in a lacerated muscle (Kragh et al, 2005) or in a denervated muscle (Fu and Gordon, 1995; Borisov et al., 2001) over a period of more than 3-4 months is reported to be between 60% and 80%. In our previous studies (Pereira et al, 2006; Pereira et al, 2010), we reported that the recovery of muscle mass in a lacerated rabbit muscle model with damaged intra-muscular nerve is not more than 80% even up to a period of 7 months. Although several gene expression studies targeted at various muscle injury models have examined various genes involved in improved muscle repair (Zhou et al, 2006), none have looked specifically at the gene expression profiles in lacerated skeletal muscles with damaged intra-muscular nerves.

Thus, the early regenerative response at the lesion site of a lacerated muscle where both the muscle and nerves are damaged has not been completely characterized. It is still unknown if the damaged intra-muscular nerve can influence the acute inflammatory

response, activation of satellite cells, axonal regeneration and re-myelination, and fibrosis formation at the lesion site, and the precise underlying molecular mechanisms involved. Hence having an in-depth knowledge of the role of the integrity of the intra-muscular nerve in muscle regeneration after laceration is important for developing novel therapy to improve muscle repair at the onset of surgical repair.

2) LITERATURE REVIEW

2.1) Neurotrophic Factors

Skeletal muscles initially develop in the absence of neural influence; however, their subsequent growth and survival depends on motor innervation. Many neurotrophic factors regulate the re-innervation of lacerated rat skeletal muscles, but in this study, the focus is on NT-4, GDNF, CNTF, IGF1, HGF, EGF and galectin-1 during the recovery of lacerated skeletal muscle post-surgery at the early (2-weeks) and late (12-weeks) phase. These influence both the myogenic and neurogenic recovery in lacerated muscles affected by a damaged intra-muscular nerve. These neurotrophic factors are also produced by neurons in the central and peripheral nervous systems, as well as the skeletal muscles, to regulate neural survival, axonal and dendritic outgrowth, synapse formation and plasticity, neuron cell migration and proliferation, satellite cell activation and myoblast proliferation and differentitation (Funakoshi et al, 1993).

Neurotrophic factors do not stimulate muscle re-innervation in isolation. Through knockout studies illustrating endogenous actions or investigations using exogenous application, it is evident that the different cells can secrete the same neurotrophic factor or a single cell can synthesise multiple neurotrophic factors and each factor play unique role during different stages of re-innervation of skeletal muscle. There is overlapping expression of neurotrophic factors and their receptors after injury. Binding of the individual neurotrophic factor to specific receptor can activate several downstream intracellular

signaling cascades involving protein kinase A, phospholipase-C gamma, Ras, Mitogen-activated protein kinase (MAPK) and phosphatidylinositol-3-kinase (PI-3-K) (Sofroniew MV et al, 2001). Although some of these neurotrophic factors share common signaling transduction pathways in eliciting their biological actions, distinct mechanisms underlie their actions in different neurons and skeletal muscles. This significantly alters the repertoire of regeneration associated genes (RAGs) such as GAP43, beta-tubulin III, ATF3, Rho kinase and HN-1. While some neurotrophic factors can increase the RAGs expression, others inhibit the expression. The precise molecular mechanism for this differential RAG response is still unclear. The published findings about the signaling pathways and biological functions of the above neurotrophic factors are summarized as follows:

2.1.1- NT-4

NT4 is a member of the neurotrophin family. It is expressed by motor neurons and skeletal muscle (Escandon et al, 1994). NT-4 binds to the tropomyosin-related kinase receptor B (TrkB) with high affinity and the p75 neurotrophin receptor ($p75^{NTR}$) with low affinity (Huang EJ et al, 2001; Lee FS et al, 2001). Binding of the NT4 to TrkB receptor can activate several downstream intracellular signaling cascades involving protein kinase A, phospholipase-C gamma, Ras, Mitogen-activated protein kinase (MAPK) and phosphatidylinositol-3-kinase (PI-3-K) (Sofroniew MV et al, 2001). The activated signaling pathways mediate re-arrangement of the cytoskeleton and neurite formation, growth, survival and differentiation in various neurons (Lentz SI et al, 1999; Goldberg JL et al, 2002). For example, it can activate CREB via the PI3K and MAPK pathways to promote axonal regeneration.

NT4 is initially synthesized and secreted as 30-to 35-kDa precursor proteins. These are cleaved in the middle to release the biologically active 12-to 14-kDa C-terminal mature forms. The N-terminal domain allows for correct protein folding and secretion (Suter U et al,

1991). Both immature and mature NT4 are secreted in high abundance. In addition, neurons can secrete both full length and truncated forms of TrkB receptors. Mature NT4 dimerises and binds to specific TrkB with high affinity, to promote neuron survival whereas the immature NT4 preferentially binds to p75 to induce apoptosis. Thus, the survival or death of neurons that co-express the TrkB receptor and p75 receptor depends on processing of the NT-4 ligands.

The level of NT-4 is increased in the gastrocnemius and soleus muscles after sciatic nerve transaction (Funakoshi et al, 1993; Omura et al, 2005). NT-4 expression is particularly detected in slow type muscle fibres (Funakoshi et al, 1995). Furthermore, the role of NT-4 in muscle fiber type specification has been investigated. Injection of NT-4 into the soleus muscle of neonatal rats accelerates the fiber type transformation from fast to slow type myosin heavy chain. However, NT-4 fails to restore the normal course of this transformation in the denervated muscle, suggesting that its mechanism of action is via a retrograde signal to the motor neuron (Carrasco & English et al, 2003). At the neuromuscular junction, NT-4 inhibits agrin-induced clustering of the acetylcholine receptors, mediated by the TrkB receptor (Wells et al, 1999).

NT-4 also acts as an axonal guidance cue to direct the motor neuron to its target (Paves and Saarma et al, 1997; Tucker et al, 2001). It increases the synthesis of b-actin, peripherin and vimentin, as well as induces the asymmetric distributions of microtubular and actin-associated proteins to determine the direction of growth cone. Also, the use of NT-4 containing conduits resulted in re-innervation of the soleus muscle (Simon et al, 2003).

2.1.2- CNTF

CNTF is expressed throughout the peripheral and central nervous systems, and also in skeletal muscle (Sendtner et al, 1994). While muscle–derived CNTF plays an important role in motor neuron survival (Arakawa et al, 1990), it also induces sprouting at the

neuromuscular junction after injury (Siegel et al, 2000). CNTF has a trophic function in denervated muscles as it can attenuate atrophy and reduce loss of twitch and titanic tensions associated with denervation (Helgren et al, 1994). It also controls protein turnover in muscle (Wang and Forsberg et al, 2000), regulating the synthesis of enzymes such as acetylcholinesterase (Boudreau-Lariviere et al, 1996). Interestingly, recent studies suggest that CNTF can also modulate the differentiation of muscle satellite cells (Chen X et al, 2005) and therefore plays a role in muscle regeneration via activation of STAT3 (Kirsch et al, 2003).

It binds to CNTF receptor which has a glycosyl-phosphatidyl-inositol-anchor (GPI) (Grotzinger et al, 1997). The CNTF receptor is composed of an extra-cellular CNTF-binding subunit, CNTF receptor-α, and two transmembrane proteins, gp130 and leukemia inhibitory factor receptor-b. Through this receptor complex, CNTF elicits its biological actions primarily via the JAK/STAT3 signaling pathway, but it can also activate the PI3K and MAPK pathways.

2.1.3- GDNF

GDNF is abundantly expressed by skeletal muscle (Nagano and Suzuki, 2003), motor neurons and sensory neurons. It protects the survival and promotes the axonal regeneration of both motor neurons and sensory neurons (Matheson et al, 1997) after nerve transaction (Burazin and Gundlach et al, 1998). It is important for the development and function of synaptic connections. GDNF is constitutively supplied to the neuromuscular junction during postnatal development and into adulthood, suggesting its importance in maintenance of the junction (Nagano and Suzuki, 2003). After denervation, there is an up-regulation of GDNF levels in the muscle. Altered production of GDNF in muscle may be responsible for activity-dependent remodeling of the neuromuscular junction (Wehrwein EA et al, 2002). Over-expression of GDNF in skeletal muscle induces multiple endplate

formation and results in hyper-innervation (Zwick M et al, 2001). This is proven using transgenic mice which over-expressed GDNF under the control of the myogenin promoter, where re-innervation is enhanced in the mice after nerve injury but the muscles were not functional due to poly-innervation (Gillingwater TH et al, 2004).

GDNF signals through a multi-component receptor complex that comprises a glycosyl-phosphatidyl-inositol-anchored GDNF Family Receptor-1 (GFR-a1) and a Re-arranged during transfection Trk receptor (RET). Binding of GDNF to the GFR-a1 and RET can activate the PI3K and MAPK pathways to regulate survival, neurite outgrowth and synaptic plasticity. GDNF can also signal through the neural cell adhesion molecule, NCAM, independently of RET. By binding to NCAM, GDNF stimulates axonal growth in hippocampal and cortical neurons via up-regulation of GAP-43 and BII-tubulin.

3) AIM

The first aim was to study the regenerative response at the lesion site of a lacerated muscle where both the muscle and intra-muscular nerve are damaged, with main emphasis on the expression profiles of neurotrophic factors, atrophic factors and fibrosis factors during the early phase (2-weeks) and late phase (12-weeks) of muscle repair using the medial gastrocnemius of adult male Sprague-Dawley rats. At 2-weeks denervation was reversible, while after 12-week, muscle denervation would be permanent and muscle atrophy would be irreversible.

Another goal of the study is to determine if there are specific endogenous anti-fibrosis, anti-atrophic and anti-re-innervation targets to improve muscle and nerve regeneration in the early phase post-laceration, and so we investigated several candidate genes and proteins to assess their mRNA and protein expression levels in various lacerated muscle models involving the intramuscular nerve injury using real-time PCR, western blot and immunohistochemistry.

The rationale for selection of targets to assess the fibrosis, atrophy, myogenesis, isometric contraction, intra-muscular nerve regeneration in this lacerated skeletal model was based on published literature reports on keloid (Ong CT et al, 2010) and lacerated muscle injury models. These factors were to assess the severity of fibrosis formation at the lesion site and to investigate the extent of reversible and irreversible muscle atrophy and denervation at the 2 time points in five different treatment groups. The correlations between the expression trends of selected markers for fibrosis, atrophy, myogenesis, isometric contraction and intra-muscular nerve regeneration in our lacerated rat skeletal muscle model was detected using the Pearson correlation analysis. The targets are classified into several categories based on their biological functions stated in the literature.

4) STUDY HYPOTHESIS

The null hypothesis in this study was that if the integrity of the intramuscular nerve remains intact (PN) or is repaired (RN) in a lacerated muscle, the muscle repair across the laceration will be improved by 12-weeks compared to the denervated skeletal muscle (DN). The alternative hypothesis is that preserving or repairing the intramuscular nerve in lacerated muscles will not improve the muscle repair after 12-weeks. In either case, neurotrophic factors would be secreted from the damaged nerve and lacerated muscle that could direct the neurogenic and myogenic recovery across the lacerated site of the cut muscle.

[Experimental note: In simulating an intact intramuscular nerve, the intramuscular nerve was preserved without damage during the laceration. In simulating a repaired intramuscular nerve, the intramuscular nerve was crushed preserving the nerve sheath but damaging the axons within. In actual clinical practice, it is the nerve sheath that is micro-anastomosed only, not the axons, during nerve repair and therefore this could simulate either a re-innervated nerve, or a repaired nerve.

5) MATERIALS AND METHODS

5.1) Animal Model

The Ethics Committee of the Animal Holding Unit (IACUC) at the National University of Singapore (NUS) approved and monitored the animal surgery protocol (Protocol No:112/08). All animal care and surgery were in accordance with the policies at the NUS, governing the use and care of animals in research and teaching. Experiments were performed on 500g adult SD rats (12-weeks old). All rats were individually housed in a thermo-neutral environment, given food and water ad libitum. The left medial gastrocnemius muscle was chosen as the muscle model as the medial gastrocnemius is a large muscle and is only part of three muscles involved in ankle flexion, together with the lateral gastrocnemius and soleus. Therefore sacrificing of this muscle in this model will not totally disable the animal's mobility. The muscle is also innervated by only one nerve (a branch from the tibia nerve), which makes micro-surgical denervation, repair and subsequent monitoring of isometric contractile properties feasible (Larkin LM et al, 2000). The right limb was used as the control/sham (PosC).

5.2) Surgery

All surgical procedures were performed by the same lab officer (ZouYu), under aseptic conditions. Rats were anaesthetized with intra-peritoneal injection of 3:2 ratio of ketamine and xylazine (0.2mL/100g); placed in a prone position. The lower limb was extended at the hip, knee and ankle to expose the popliteal fossa. After shaving, a skin incision on the posterior aspect of the mid thigh to about 1cm proximal to the calcaneum was made. The skin flap was dissected, exposing the popliteal fat and the two bellies of the gastrocnemius muscle (MG). The bellies are enclosed in a layer of fascia that formed a raphe in the midline, between the two bellies, joining distally at the common calcaneal tendon. The popliteal vein, artery and the sciatic nerve and branches were isolated, exposing the nerve

branches arising from the tibia nerve, to the bellies of the gastrocnemius and soleus. The nerve to the medial belly of the gastrocnemius was seen passing obliquely to its entry point (motor point) between the proximal quarter and distal three quarters of the belly. This branch measured an average 5-6 mm in length, and was on average about 0.4-0.6mm in diameter. For the completely lacerated muscle model, the whole muscle belly of the MG was divided transversely using a sharp scalpel blade, 2-3mm distal to the entry point of the nerve branch. Distal to the laceration site, the nerve was seen at 10X magnification to bifurcate into three branches within the distal segment of the cut muscle belly. The concomitant cut nerve in the proximal segment was observed to have 2 to 3 fascicles. This is a clean-cut laceration model. To avoid variations in muscle damage, a sharp laceration was used over a blunt laceration. The blunt model would have increase damage away from the lacerated site and would have unknown factors involved that can affect the results.

5.3) Experimental Groups

Five groups were assessed at 2-weeks and at 12-weeks post-repair. The groups were as follows:

(a) **Denervated Intramuscular Nerve (DN) Model:** A through-thickness laceration of the MG was done via a sharp dissection across the proximal third of the muscle belly, distal to the entry point of the branch from the tibial nerve (Fig 1B).

(b) **Preserved Intramuscular Nerve (PN) Model:** The nerve branch entering the MG was traced intra-muscularly, and the muscle was lacerated as in (a), but care will be taken to preserve the intra-muscular nerve distal to the motor point (Fig 1B).

(c) **Re-innervated Intramuscular Nerve (RN) Model:** The MG was lacerated as in (b), and the intra-muscular nerve was concomitantly crushed with an arterial forcep to preserve the nerve sheath but damage the axons. No micro-anatomosis was done. This model was to simulate either a re-innervated nerve, or a repaired nerve (Fig 1B).

Electrical stimulation was used to confirm that there was axonal damage, while integrity of the nerve sheath was also assessed to confirm continuity.

(d) **Negative Control (NegC) Model:** The MG was lacerated as in (a), and the peripheral branch from tibia nerve proximal to the motor point was cut and ligated to prevent re-innervation. NegC is a lacerated muscle with the peripheral nerve cut and ligated (i.e the extra-muscular nerve branch that comes from the tibia nerve before it enters the muscle). Similar to DN, but this is with the ligated peripheral nerve – partial denervated with no possibility of re-innervation or sprouting coming from this nerve stump. Any nerve sprouts would therefore have to come from some other neighbouring nerve branch.

(e) **Positive Control (PosC) Model:** The right limb of the rat, with no surgery done on the MG was the Sham operation.

(f) **Modified Kessler suture** is used in all groups (Fig 1A) because it gives the best morphologic and functional healing for management of lacerated skeletal muscle without immobilization, and it ensures that any molecular and histological differences in fibrosis and atrophy among the treatment groups is solely due to integrity of the intra-muscular nerve. Suturing the edges of laceration between two myofibers will reduce the size of the gap and reconstruct the framework for the basal lamina to regenerate. This does not prevent the initial muscle necrosis, fibrosis and the acute inflammatory response induced by the clean cut of the muscle belly.

Immobilisation of lacerated skeletal muscle post-surgery will delay the healing process. It can lead to the development of excessive deep scar between two ruptured myofibers, inhibit angiogenesis between two muscle stumps and result in significant muscle atrophy. This prohibits a fair comparison of the expression profiles of selected markers between the treatment groups and the control group (not

immobilized).

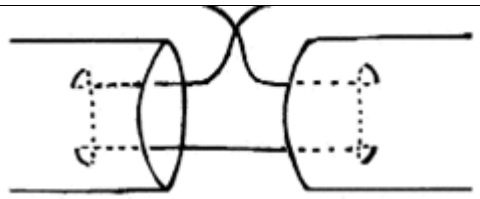

Figure 1A Schematic representation of modified Kessler suture technique. It consists of a two-strand repair with use of a single knot within the repair site. The steps are as follows:
(1) suture needle is inserted into the side of cut muscle end, 1cm from the severed muscle edge, and is passed longitudinally out of the muscle edge (2) needle is then passed into the corresponding severed muscle cut end and is passed longitudinally 1cm out of the side of the muscle (3) suture is then re-inserted a few mm distal to its exit point (no locking), and is directed in a cross-wise fashion to exit in the middle of the muscle laeration site (4) suture is re-introduced into the opposite muscle segment and continues across in crossing direction, and is brought out on the opposite muscle side (1cm from the laceration site) (5) suture is introduced a few

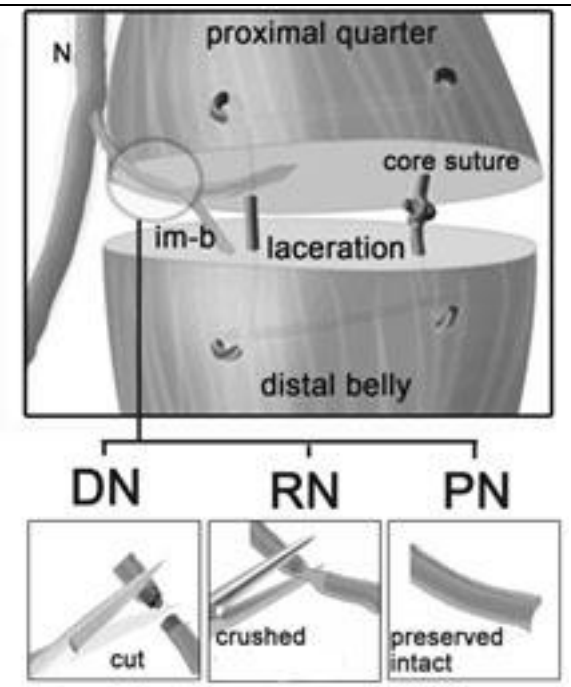

Figure 1B Experimental lacerated skeletal muscle models. A transverse complete laceration was simulated at the proximal quarter of the muscle belly just below the entry point of the peripheral nerve branch supplied by the tibial nerve (N). The peripheral nerve branch enters the muscle at the epimysium and becomes the main intramuscular nerve branch (im-b). The three lacerated skeletal muscle groups simulated were DN, a denervated skeletal muscle, where the im-b was also cut, RN, a re-innervated skeletal muscle group, where the im-b was crushed with the epineurium intact, and PN, where the im-b was preserved intact. All muscle belly lacerations were repaired with core sutures (modified Kessler suture technique).

mm distal (no locking) and is directed longitudinally across the laceration site (6) suture is then passed back crossing the middle of the laceration site to exit next to the free muscle edge (7) make sure the slack is removed with each pass of the suture (8) tighten all the sutures before a knot is tied (9) bury the knot inside the repair site	

5.4) Histology

The MG from both limbs in all rats was then harvested under anaesthesia, and the wet weights measured. The lacerated MG was divided into 3 parts: the mid segment which included the site of laceration (fibrotic zone), the distal segment which was distal to the laceration site and a proximal segment which was proximal to the laceration site. Only the mid segments for all cases were used in histology and immunohistochemistry staining, RNA extraction for real-time PCR analysis, protein extraction for western blot experiments. This is because the proximal and distal segments were reserved for micro-array work in a separate project. The biopsies were snapped frozen in liquid nitrogen, kept in cryovials, and later stored in -80°C freezer. Selected biopsies were later fixed in formalin and paraffin-embedded. Serial sections of 8-um thick were cut from the paraffin blocks and mounted on Matsunami adhesive slides (Unison) for hematoxylin and eosin, and Masson Trichrome staining (Merck).

5.5) Immunohistochemistry

8-µm sections were cut in series from formalin fixed paraffin embedded rat skeletal muscle samples. Paraffin sections were dewaxed in 3 changes of xylene, hydrated in descending grades of ethanol, followed by a short 5min rinse in running tap water. Antigen retrieval was performed using dedicated histology microwave oven, Milestone Mega T/T,

according to the manufacturer's protocol for each antibody (Table 1).

Table 1. Milestones Mega T/T Antigen Retrieval program.

Step	Time (min)	Power (W)	Temperature (˚C)
1	20	600	80
2	0.5	400	85
3	20	200	88
4	1	200	91
5	20	190	96
6	20	150	98

All sections are washed in running tap water for 10 min after antigen retrieval. The Dako Envision+ kit was used for the subsequent IHC steps. Briefly, endogenous peroxidase was blocked in 3% hydrogen peroxide for 30min, and then the slides were washed in 1X TBS-Tween-20 X 3 times, followed by incubation with primary antibody. The secondary antibody was applied after rinsing the slides. Slides were washed sequentially with 1X TBS-Tween-20 and incubated with DAB for 5min. Next, the slides are washed with water to quench the DAB, followed by dehydration in ascending grades of ethanol, drying in the oven for 10min and then clearing in xylene before been mounted with coverslips using Depex (Merck). Non-immunised host serum of the respective primary antibody was used for negative controls. We did not use frozen tissue sections for immunohistochemistry staining because the cryostate in the lab was damaged.

5.6) SDS-PAGE and Western Blot

Frozen rat skeletal muscle was homogenized with a hand-held Polytron in lysis buffer made of 8M urea, 2M thiourea, 4% CHAPS, 0.1M DTT, 0.025M Tris and 0.20M glycine pH8.3. This step is done on ice at 20,000rpm for 5 min, with 30sec break for each min. The lysates were then centrifuged at 14,000g for 5min at room temperature, after which

the supernatant was transferred to new tube and the protein concentration of the total tissue lysate was estimated using the GE 2-D Quant kit. We used BSA as the protein standard in estimation of protein amount because it is cheaper than recombinant proteins, the protocol has been optimized for many other protein targets in other projects and the proteins of interest in this project are not in the immunoglobulin family. The recipe for casting SDS-PAGE gels with added glycerol is listed in Appendix 3. Glycerol in the gels enhances the separation of proteins with high molecular weight and prevents the gels from curling during electro-transfer.

10µg/uL of protein were mixed with appropriate volume of SDS-denaturing loading buffer (8M urea, 2M thiourea, 5% SDS, 0.075M DTT, 0.01% bromophenol blue) in the ratio 1:10 (v/v) (Blough E et al, 1996), then resolved on a mini SDS-PAGE gel at constant 125V for 1h 30min, then the voltage was increased to 250V to flush out the bromophenol dye of the gel. The proteins on the gel are then transferred onto nitrocellulose membranes (Bio-Rad) at constant 100V for 2h in cold room. The amount of protein loaded per well is below 30ug/uL because the skeletal muscle contains high levels of myosin heavy chains and other high molecular weight proteins such as titin and nebulin which are difficult to resolve properly in non-gradient mini SDS-PAGE gels. High loading amount of such high molecular weight proteins will lead to smearing of bands on the nitrocellulose membranes after electro-transfer. After washing the membrane with 1X TBS-Tween-20 for 10min, followed by rinsing with MQ water, the membrane was blocked with 5% non-fat milk in 1X TBS for 2h at room-temperature. Then the membrane is washed with 1X TBS-Tween-20 for 10min X 5, before incubation with the desired primary antibody for 1h at room temperature. The membrane was then rinsed 5 times, 10min each, with 1X TBS-Tween-20 before the secondary antibody-conjugated with HRP was applied. The blots were visualized with ECL Plus chemi-luminescence detection kit according to manufacturer’s instruction (Amersham).

Equal sample loading was monitored using mouse monoclonal anti-rat alpha-tubulin. Alpha-tubulin was chosen as it is expressed by both fast and slow myofibers, and it is present in both developing and adult muscle fibers. In addition, it is commonly used as a loading control in immunoblotting of muscle proteins and hence it is a good choice for comparison. Optical densitometry quantification of the respective intensity of the immunoblot bands was done using GelPro v4.5.

5.7) RNA Extraction

Total RNA was extracted from frozen MG muscle using the Qiagen Mini-RNA for fibrous tissue kit, following manufacturer's instruction. The RNA concentration was determined by optical density at 260nm using NanoDrop. The purity of extract was confirmed based on OD260-to-OD280 ratio of 1.8 to 2.0. The RNA integrity was assessed by agarose gel electrophoresis and GelRed staining of 1μg total RNA. Only intact RNA samples were used for the reverse transcription and subsequent real-time PCR analysis.

5.8) Reverse Transcription

Reverse transcription was performed with High Capacity cDNA Archive kit (ABI) and the ABI 2720 Gene Amp thermal cycler, using 1μg RNA in 20μL reaction volume (Tables 2A and 2B).

Table 2A. First strand cDNA synthesis reaction mix

Component	Volume (uL)
Mix A:	
RNA (1ug/uL)	1.0
10X Random hexamers	2.0
25X dNTPs (100mM)	0.8
Nuclease-free water	12.2
Total	**16.0**

Load Mix A into thermal cycler and denature the RNA at 65˚C for 10 min, then incubate the Mix A at 4˚C for 10 min prior adding Mix B on ice-bath. Vortex and spin down all reaction mixes before loading them in thermal cycler to start the reverse transcription.

Mix B:	
10X Reverse transcriptase buffer	2.0
Multiscribe reverse transcriptase	1.0
RNAse Inhibitor	1.0
Total	**4.0**

Table 2B. High capacity reverse transcription protocol

Thermal Cycler	Steps	Time (mins)	Temperature (˚C)
ABI 2720 Gene Amp	1. Activation of random hexamers annealing to RNA	10	25
	2. Activation of reverse transcriptase	120	60
	3. Inactivation of reverse transcriptase	5	85
	4. Cooling	infinity	4

5.9) Real-time PCR

1μL of cDNA (100 μg) was then mixed with respective TaqMan MGB probes and 1X universal TaqMan PCR mastermix (ABI) for real-time PCR analysis on the 7500HT real-time thermal cycler (ABI), accordingly (Tables 3A and 3B).

Table 3A. Real-time PCR reaction mix

Component	Volume (μL)

Taqman Universal PCR Mastermix, no UNG, 2X	10.0
20X TaqMan Gene Expression Assay Mix	1.0
cDNA (100ng), diluted in nuclease-free water	9.0
Total	**20.0**

Table 3B. Real-time PCR: thermal cycling protocol

Thermal Cycler	Step	Time	Temperature (˚C)	No of cycles
7500HT, ABI	1: Taq Polymerase Activation	10 min	95	1
	2: DNA Denaturation	15 sec	95	40
	3: Annealing and Extension	1 min	60	40

Two negative controls were performed for each sample. In the first negative control, the reverse transcriptase was omitted in the RT-PCR reaction mix. Under these conditions, formation of a product indicates either genomic DNA contamination or reagent cross-contamination. The second negative control consisted of no RT primers when the RNA was reverse-transcribed. This ensures that the cDNA obtained is not due to self-priming of RNA. Each sample was analysed in triplicates following manufacturer's instruction, and lamin A was the endogenous control. Lamin A was chosen as a control as it is expressed by both fast and slow myofibers as well as present in both developing and adult muscle fibers. Its expression level is also within the medium abundance range so using it as a denominator in the relative quantification equation will not mask the genes that are expressed at very low levels or high levels in both regenerating and mature muscle fibers. The relative quantification (**RQ**) equation is given below:

$$RQ = 2^{-(\Delta\Delta Ct)}$$

[where $\Delta\Delta Ct$ = (Ct of target gene) $_{treatment}$ − (Ct of target gene) $_{control}$ / (Ct of endogenous gene) $_{treatment}$ − (Ct of endogenous gene) $_{control}$]

5.10) Statistical Analysis

Gene expression results were analysed with Sequence Detection Software v1.4. Average Ct values with standard error greater than 0.3 are omitted, tests are repeated. RQ values are shown in means and SD, n=3 per treatment group. Optical densitometry quantifications of the respective intensity of the protein bands were done using GelPro v4.5 and expressed as means ± standard errors in arbitrary units. Statistical significance between treatment groups and the control were calculated using SPSS v1.9 with one-way analysis of variance (ANOVA) and Scheffe's post-hoc test, where *p<0.05, for both gene and protein expression assays. For real-time PCR, the calibrator sample was cDNA reverse transcribed from the RNA extracted from the normal medial gastrocnemius muscle from the opposite limbs. All RQ values were then represented as fold-changes ± standard error. There is no significant statistical difference for lamin A gene expression between the treatment groups and the controls (see Appendix 6), and the same applies to that for alpha-tubulin protein expression (see Appendix 7). Pearson's correlation coefficient (*r*) was also calculated to measure the linearity of the relationship between all gene and protein markers**.** All statistical tests were two sided with statistical significance set at $p < 0.05$ (Appendix 12).

6) RESULTS

6.1- Histomorphology Comparison between PN and DN

In all groups, the lesion site remains fibrotic at 12-weeks post-surgery (Fig. 2). Denervation induced significant decrease in the wet weight of the medial gastrocnemius. At 2-weeks post-surgery, all the groups showed a decreased wet weight of about 60% of the control value. After 12-weeks, the PN regained 80% of the wet weight of the control level while DN achieved only 40% of the control value and RN attained about 70% muscle mass of the normal muscle. Differences in the cross-sectional area of scar region and size of myofibers were also noted between the PN, RN and DN. The primary aim of this histo-

morphologic study was to determine these differences between lacerated muscles which had its intramuscular innervations preserved (PN) or damaged (DN). DN showed highly random (mosaic) pattern of immature muscle fibers with small size and central nuclei, and extensive scarring at lacerated site, while PN had more mature, fully differentiated adult muscle fibers with large cross-sectional area and multiple peripheral nuclei, and minimal fibrosis at the lesion site. This indicates that DN, RN and PN have distinct histology features of muscle regeneration, arising from important differences at the gene expression level of unique targets.

Figure 2. Muscle Atrophy. At 2-weeks after repair, all muscles had a significant reduced muscle mass. Masson's Trichrome staining at the lesion site (arrows) showed the repair site at 2-weeks with DN having a discontinuity, while RN and PN having its cuts ends bridged differentially by connective and muscle tissue. At 12-weeks the cut lesion was less visible, yet DN still continued to have a poor repair. (Longitudinal section, original magnification: 100X).

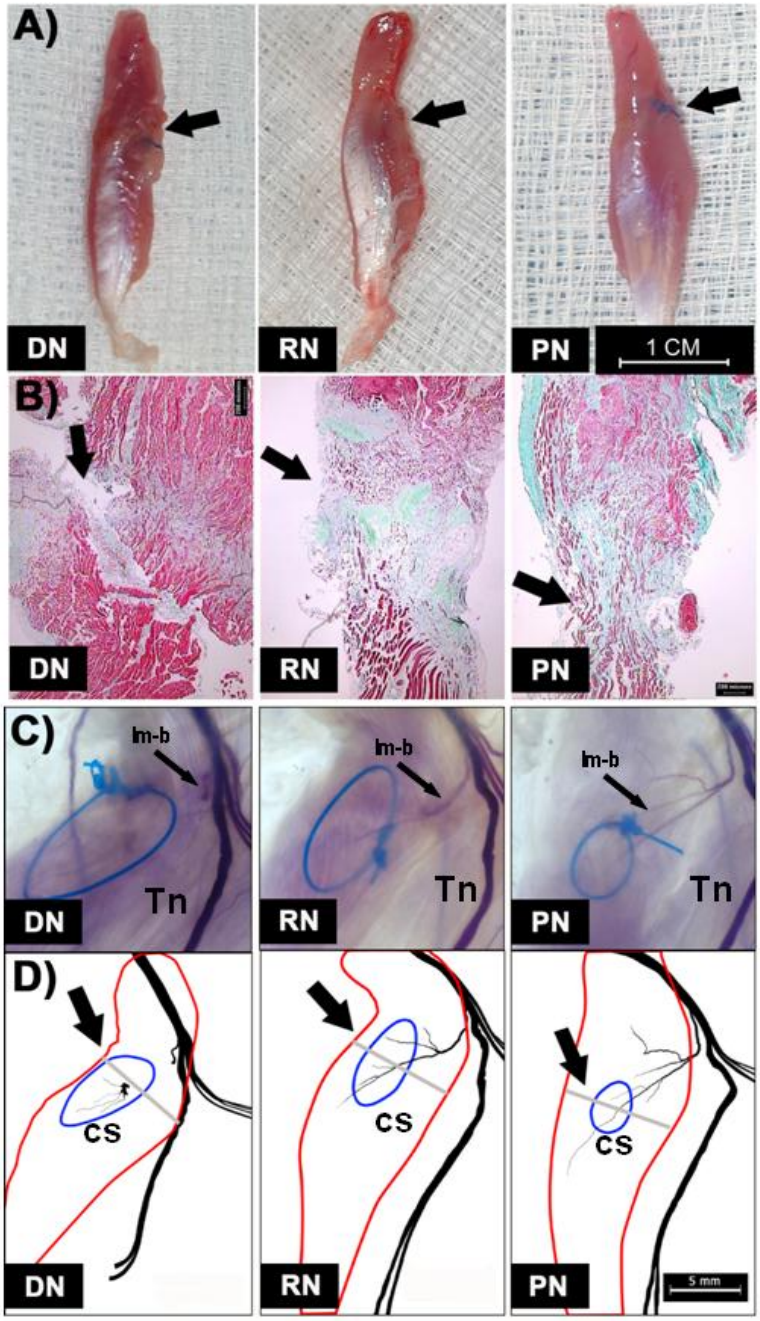
A)
DN
RN
PN
1 CM
B)
DN
RN
PN
C)
Im-b
Tn
DN
Im-b
Tn
RN
Im-b
Tn
PN
D)
CS
DN
CS
RN
CS
PN
5 mm

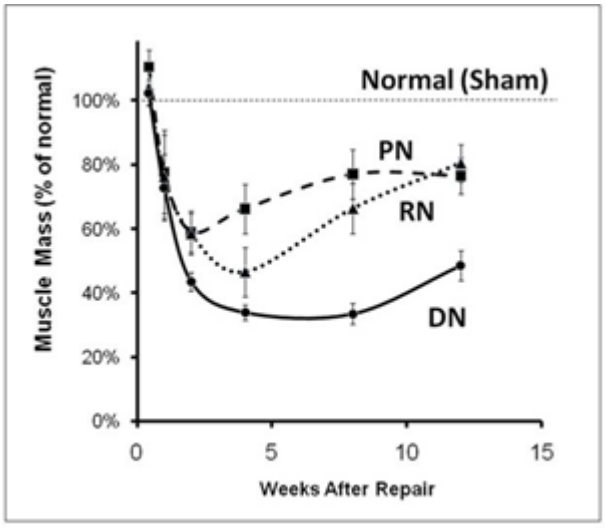

6.1.1- Immunohistochemistry Staining for Intermediate Filaments, Galectin-1 and R-spondin-1

We assessed if the damaged intramuscular nerve in a lacerated muscle contributed to poor muscle regeneration. At 2-weeks post-laceration, there was progressive muscle atrophy and fibrosis in both DN and PN, marked by myofiber size reduction and large collagen deposits at laceration site. Desmin and vimentin were weakly expressed by proliferating myoblasts and immature myotubes in DN but not as obvious in PN. Vimentin was also highly expressed by mononuclear immune cells and fibroblasts in the fibrotic zone. Desmin expression was up-regulated in proliferating myoblasts and mature myofibers but vimentin expression ceased completely after 12-weeks in both DN and PN. Nestin was moderately expressed by proliferating myoblasts in both groups, co-localised with desmin and vimentin at 2-weeks. Minimal nestin expression adjacent to muscle-tendon junctions of mature myofibers was detected after 12-weeks (Fig. 3).

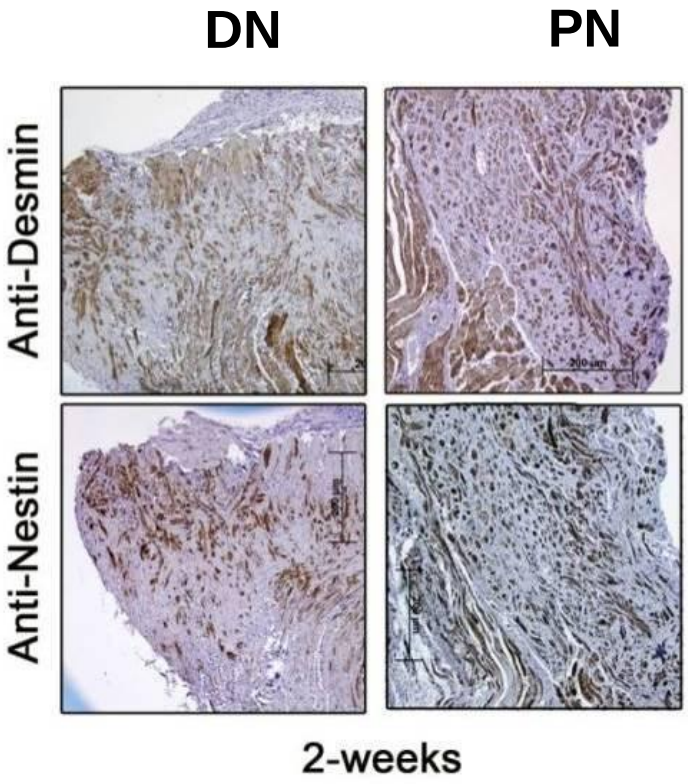

Figure 3. Immunohistochemistry of desmin and nestin expression. Desmin and nestin were expressed by proliferating myoblasts and immature myotubes in DN and PN. Nestin expression co-localised with desmin at 2-weeks post-repair.

R-spondin-1 was strongly expressed by proliferating myoblasts and immature myotubes at 2-weeks in PN, more than DN (Fig. 4). No R-spondin-1 expression was detected in mature myofibers after 12-weeks in both groups and was demonstrated by their protein assays (Fig. 5). Galectin-1 was expressed as organised diagonal rows of large spots in PN, while in DN, it was presented as random diffuse dots (Fig. 6). In addition, fibroblasts and macrophages at the fibrotic zone also displayed both strong galectin-1 and R-spondin-1 expression (Fig. 4, 5).

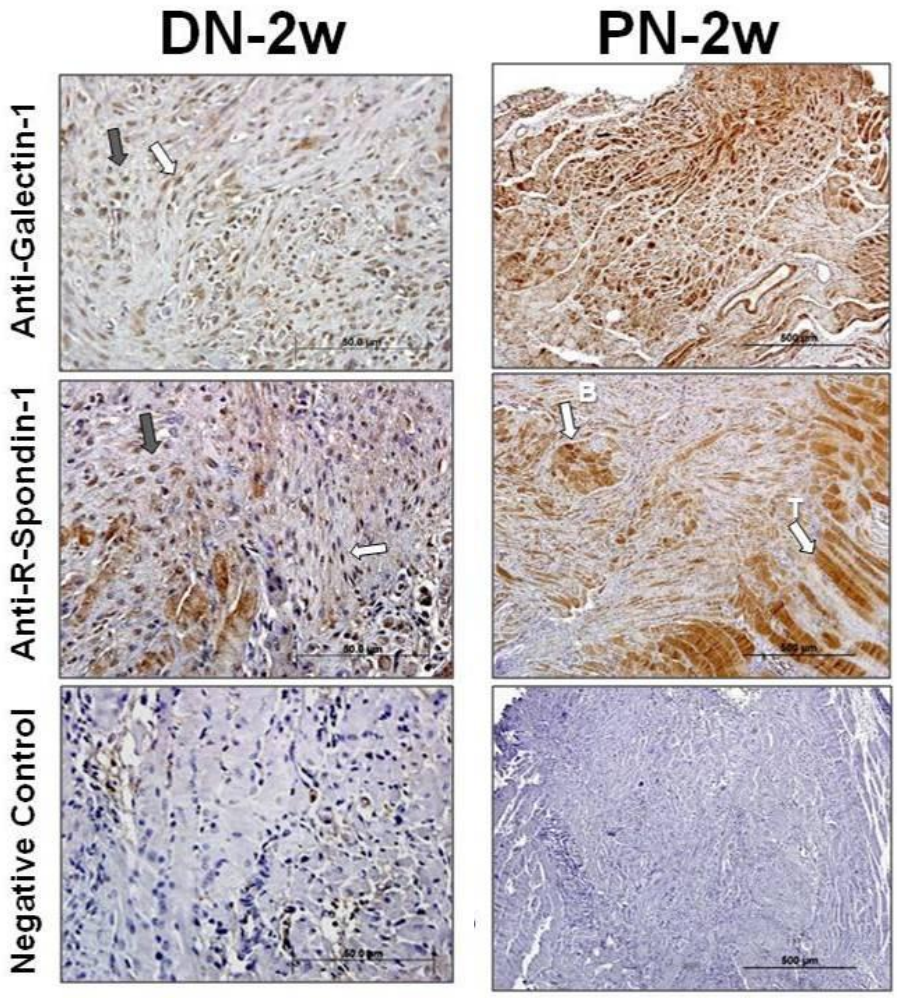

Figure 4. Immunohistochemistry of galectin-1 and r-spondin-1 expression at the lesion site For DN, strong galectin-1 and r-spondin-1 expressions in spindle-shaped fibroblasts (white) at lacerated site, and also in macrophages with plump nuclei (black arrows). While for PN, R-spondin-1 is strongly expressed in proliferating myoblast (B) and immature myotubes (T)

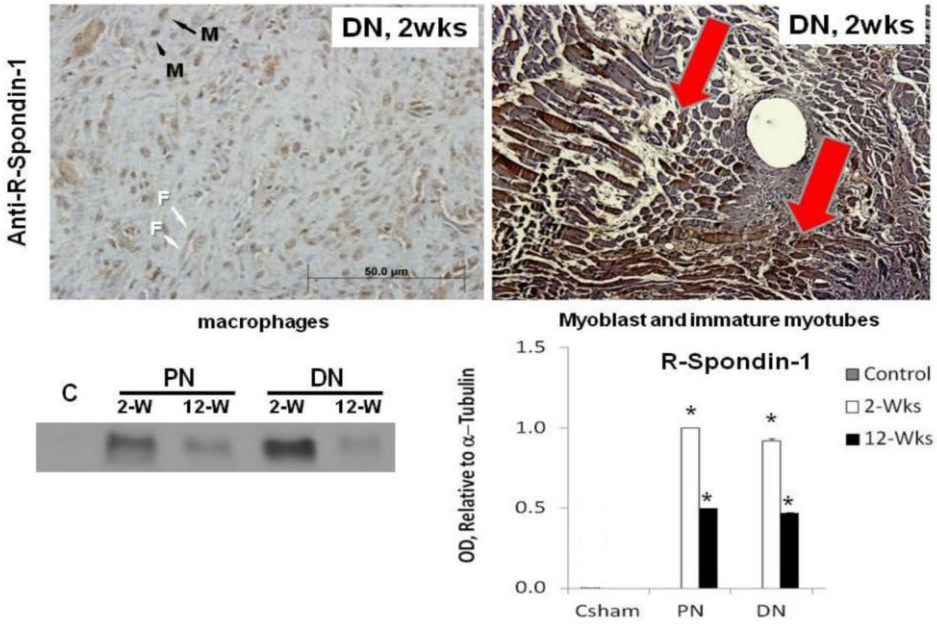

Figure 5. Immunohistochemistry and western blot of R-spondin-1 expression. R-spondin-1 was strongly expressed in macrophages (black arrows with M), fibroblasts (white arrows with F), myoblasts and immature myotubes (red arrows) in DN at 2-weeks post laceration. Optical densitometry quantification of R-Spondin-1 protein expression levels normalized to alpha tubulin, using GelPro v4.5 (arbitrary units) was obtained from three independent experiments with 3 rats. P-values were calculated by Scheffe's post-hoc test, where $p<0.05$ is considered statistically significant. (* - indicates significant difference ($p<0.05$) to Positive Control, Csham).

The strong expression of galectin-1 at 2-weeks for both PN and DN suggest that the myogenic repair process was progressing well (Fig. 4), while at 12 weeks (Fig. 6) the higher and dis-organised expression of galectin-1 in DN is linked to slow myofiber and axonal recovery. It also reflects the random re-innervation of the myofibers distal to the lesion site amidst a mass of collagen scar. The re-innervation of myotubes following muscle injury is important to prevent myotube atrophy and to accelerate myotube growth.

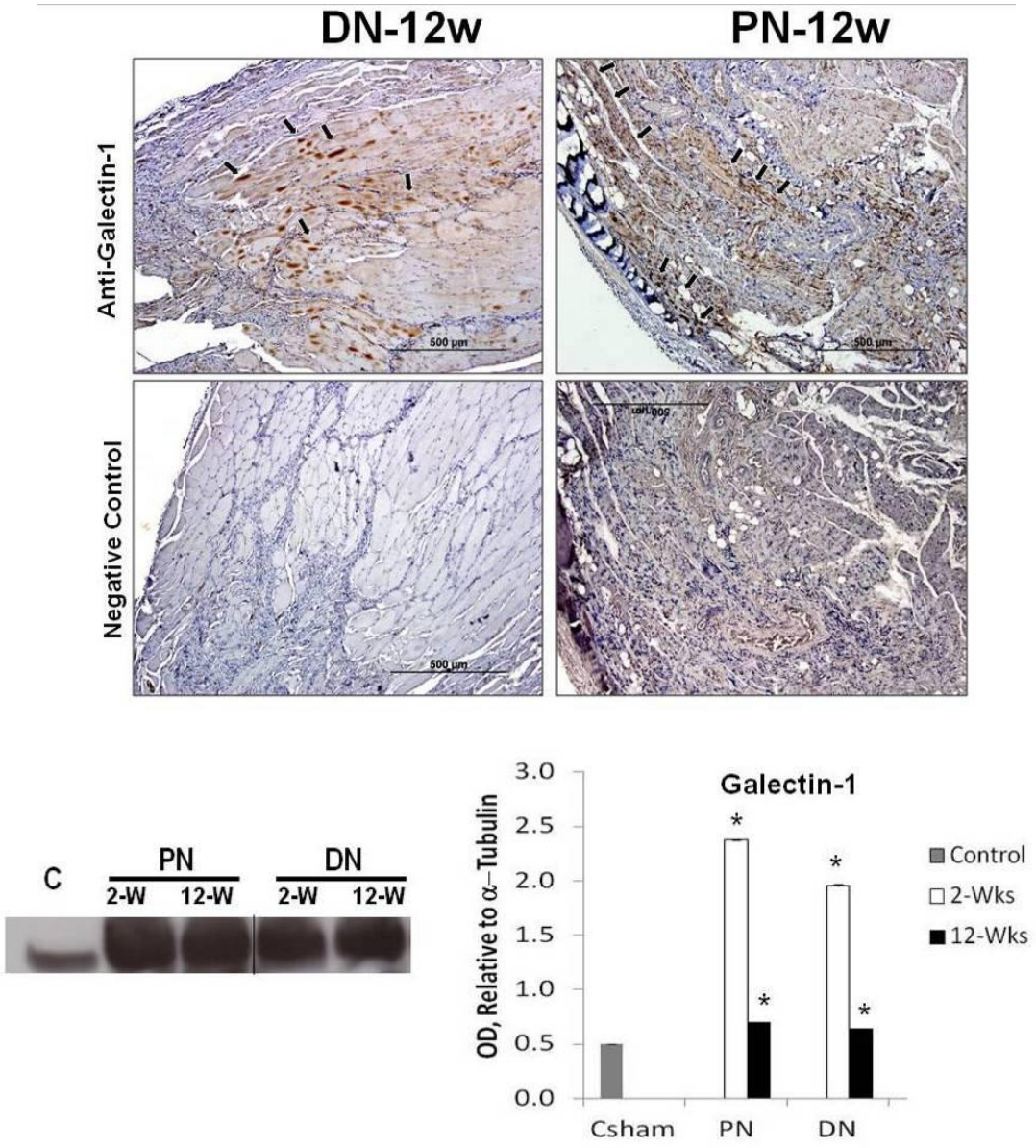

Figure 6. Immunohistochemistry and western blot of galectin-1expression. Comparing DN and PN at 12-weeks post-repair. Galectin-1 was expressed as organised diagonal rows of large spots in PN, while in DN, it was presented as random diffuse dots (arrows). Optical densitometry quantification of Galectin-1 protein expression levels normalized to alpha tubulin, using GelPro v4.5 (arbitrary units) was obtained from three independent experiments with 3 rats. P-values were calculated by Scheffe's post-hoc test, where $p<0.05$ is considered statistically significant. (* - indicates significant difference ($p<0.05$) to Positive Control, Csham).

6.2- Gene and Protein Expression Profiles

6.2.1- Comparing PN, RN, DN and NegC against the sham control, PosC

The gene expression data is presented as mean RQ values based on 3 samples, and for each sample triplicate datasets. The housekeeping gene used for each real-time PCR run is lamin A. The protein expression data is presented as means based on optical densitometry quantification against α-tubulin, which is as loading control. As the study looks at both myogenic and neurogenic recovery in lacerated muscles affected by a damaged intra-muscular nerve, the candidate markers are divided into 5 categories (Table 4).

Table 4. Classification of candidate markers

	Category	Gene or protein markers
1	**Fibrosis markers**	**collagen-1α, aggrecan, vimentin, α-Smooth Muscle Actin**
	pro-fibrosis	TGFβ2, galectin-1, CTGF, R-spondin-1, GDNF, Sonic hedgehog, IGF1, HGF, myostatin, NT4
	anti-fibrosis	decorin, follistatin, EGF, PGC-1α, AMPK-1α, Sirt1, CNTF
2	**Atrophy markers**	**atrogin-1, MuRF-1, complement-3**
	pro-atrophy	myostatin, myogenin, AMPK-1α
	anti-atrophy	calpain-3, IGF1, NT4, GDNF, CNTF, PGC-1α, Sirt1,decorin, follistatin
3	**Myogenesis markers**	**myoD, myogenin, Mef2a, desmin**
	pro-myogenesis	galectin-1, decorin, follistatin, IGF1, HGF, EGF, Sonic hedgehog, NT4, GDNF, CNTF, PGC-1α, R-spondin-1
	anti-myogenesis	TGFβ2, myostatin, CTGF, AMPK-1α
4	**Isometric contraction markers**	**slow troponin-I, fast troponin-I, fast myosin heavy chain, slow myosin heavy chain, embryonic myosin heavy chain**
	pro-slow myosin heavy chain and slow troponin-I (anti-fast myosin heavy chain and fast troponin-I)	myogenin, Mef2a, NT4, Sonic hedgehog, PGC-1α, Sirt1, myostatin
	anti-slow myosin heavy chain and slow troponin-I (pro-fast myosin heavy chain and fast troponin-I)	myoD, IGF1, CNTF
	anti-fast and anti-slow myosin heavy chain, anti-fast troponin-I and anti-slow troponin-I	TGFβ2, complement-3, MuRF-1, atrogin-1
5	**Intra-muscular nerve regeneration marker**	**GAP43**
	pro-axonal regeneration	IGF1, HGF, galectin-1, NT4, GDNF, CNTF, follistatin, decorin, EGF, Sonic hedgehog, HN1
	anti-axonal regeneration	collagen-1α, aggrecan, TGFβ2, complement-3, CTGF
6	**Signaling pathway markers**	**1) MAPK kinase pathway**: p38, Erk1, Erk2

2) SMAD pathway: SMAD2, SMAD3

Each category is further divided into 2 smaller groups, pro- and anti-, depending on specific function of the selected target with respect to the phenotype based on published reports. A few targets will appear in more than one category due to their different functions in different cells and physiological contexts.

6.2.2- Fibrosis markers

Collagen-1α, Aggrecan, Vimentin, α-Smooth Muscle Actin

The expression level of collagen-1α and aggrecan (Fig 7A) was significantly up-regulated in all 4 groups at 2-weeks post-laceration compared against the control ($p<0.05$). DN and RN had the highest collagen-1α expression level (> 20-fold than the control). After 12-weeks, collagen-1α and aggrecan were down-regulated in all groups, but the expression level remained higher than the control ($p>0.05$). NegC and DN had the highest aggrecan expression level (>40-fold greater than the level of the control).

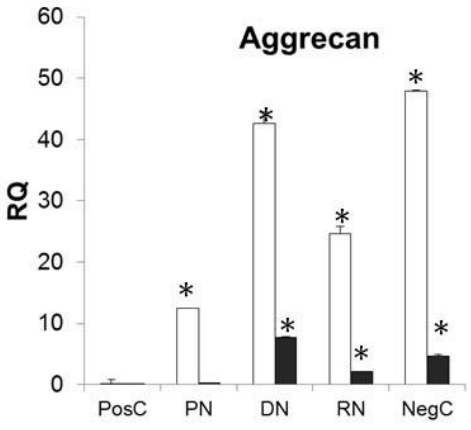

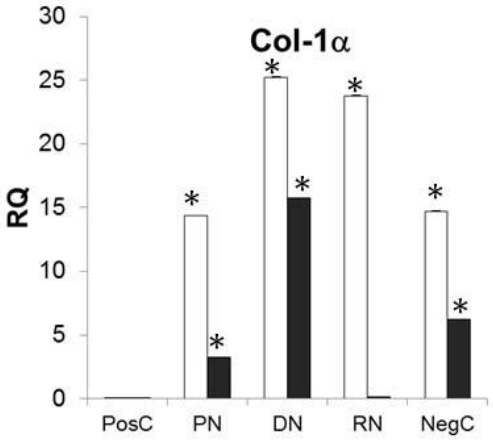

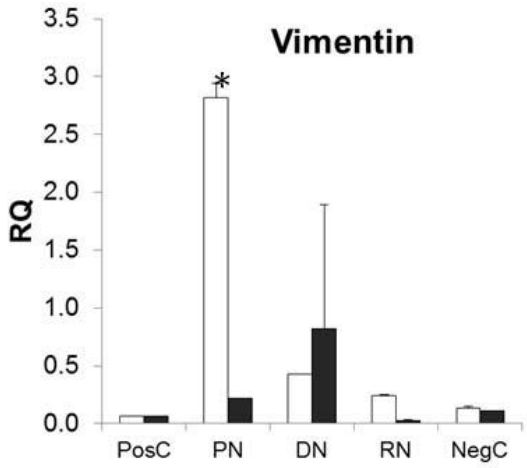

Figure 7A. Fold changes (normalized to Lamin A) of Collagen-1α, Aggrecan and Vimentin. ANOVA and post-hoc tests at 2-weeks (white) and 12-weeks (black) post-repair identified the homogenous sub-sets that were not significantly different (See Appendix 4). Data is expressed as means ± SD of three independent experiments obtained with 3 rats (n=3); p-values were calculated by Scheffe's post-hoc test, where $p<0.05$ is considered statistically significant. (* - indicates significant difference ($p<0.05$) to Positive Control, PosC).

The expression level of the intermediate filament, vimentin was significantly up-regulated in all groups at 2-weeks post-laceration compared against the control. In PN, vimentin expression level were 3.0-fold greater than the control ($p<0.05$). After 12-weeks, vimentin was down-regulated in all, but in DN where the expression remained up by >2.0-fold greater than the control ($p<0.05$). Immunoblotting results showed that vimentin and α-SMA protein expression level (Fig. 7B), both markers for the myofibroblastic phenotype, were significantly up-regulated in all groups at 2-weeks post-laceration compared against the control ($p<0.05$). After 12-weeks, vimentin was down-regulated in all but DN, where its protein level remained highly expressed ($p<0.05$), while α-SMA remained higher than the control ($p<0.05$). The highest mean level of vimentin and α-SMA were in PN at 2-weeks and 12-weeks post-laceration, respectively, compared with the control ($p<0.05$).

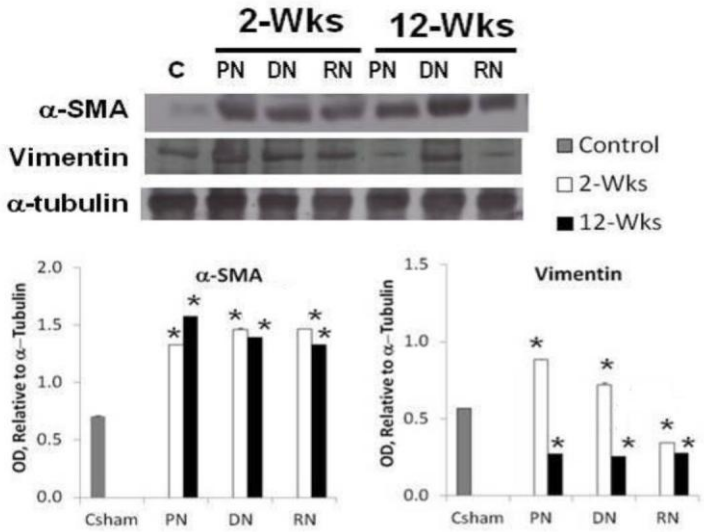

Figure 7B. Optical densitometry quantification of myofibroblast markers - α-SMA and vimentin protein expression levels normalized to alpha tubulin, using GelPro v4.5 (arbitrary units) at 2-weeks (dark bars) and 12-weeks (lighter bars). Data was obtained from three independent experiments with 3 rats. p- values were calculated by Scheffe's post-hoc test, where $p<0.05$ is considered statistically significant. (* - indicates significant difference ($p<0.05$) to Positive Control, CSham).

6.2.2.1- Pro-fibrosis markers

TGFβ2, Galectin-1, Myostatin, CTGF, HGF, R-spondin-1, NT4, GDNF, IGF1, Shh

The expression level of TGFβ2 was significantly up-regulated in PN and DN at 2-weeks post-laceration compared against the control ($p<0.05$). DN has the highest TGFβ2 expression level, about 0.4-fold greater than the level of the control. The expression level of EGF was initially down-regulated in all PN, RN and DN, but not in NegC, at 2-weeks post-laceration (Fig. 15A, $p<0.05$). After 12-weeks, TGFβ2 was down-regulated to the baseline level of the control in all groups ($p>0.05$), except in DN where TGFβ2 remained high, about 0.2-fold higher than in control (Fig. 8A).

The expression levels of galectin-1 and myostatin were up-regulated in all 4 groups at 2-weeks post-laceration compared with the control ($p>0.05$) (Fig. 8A). In PN, the galectin-1 expression level is about 0.60-fold greater than the control ($p<0.05$). After 12-

weeks, galectin-1 expression level in all groups remained higher than the control ($p<0.05$) with PN having a 0.11-fold greater than the control ($p<0.05$); while myostatin further upregulated remaining higher than the control ($P<0.05$). In DN, myostatin protein expression level remained higher than the control by 0.88-fold ($p<0.05$).

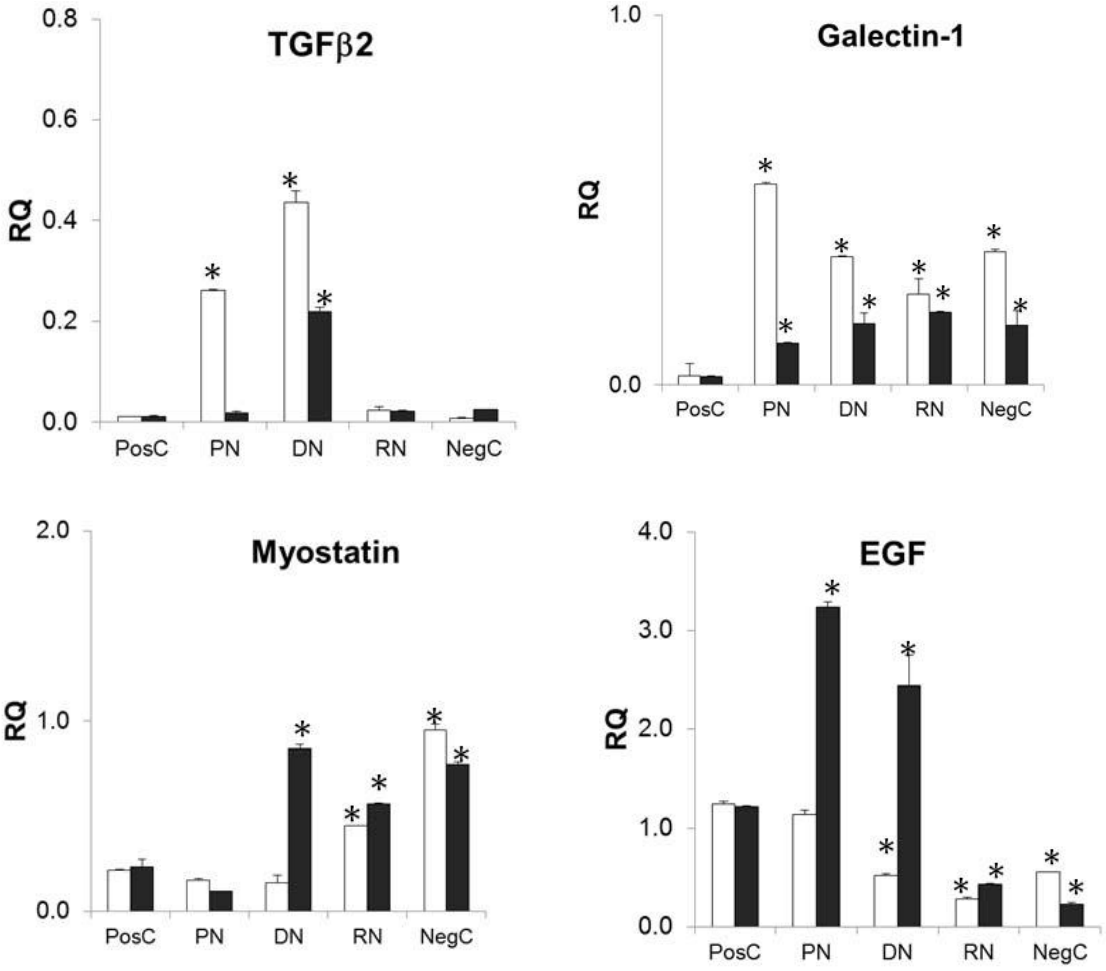

Figure 8A. Fold changes (normalized to Lamin A) of TGFβ2, Galectin-1, myostatin and EGF. ANOVA and post-hoc tests at 2-weeks (white) and 12-weeks (black) post-repair identified the homogenous sub-sets that were not significantly different (See Appendix 4). Data is expressed as means ± SD of three independent experiments obtained with 3 rats (n=3); p-values were calculated by Scheffe's post-hoc test, where $p<0.05$ is considered statistically significant. (* - indicates significant difference ($p<0.05$) to Positive Control, PosC).

Immunoblotting results (Fig. 8B) for galectin-1 protein level showed significantly up-regulated in PN, DN and RN at 2-weeks post-laceration ($p<0.05$). After 12-weeks, galectin-1 protein expression was down-regulated in all groups close to baseline level ($p<0.05$). The highest mean level of galectin-1 was present in PN at 2-weeks post-laceration compared with the control ($p<0.05$). TGFβ2 and CTGF protein level were also significantly up-regulated in PN, DN and RN at 2-weeks post-laceration compared against the control ($p<0.05$). After 12-weeks, TGFβ2 and CTGF level in all groups remained higher than control ($p<0.05$). The data showed that the highest mean level of TGFβ2 was present in DN and for highest CTGF in RN at 12-weeks ($p<0.05$). The stronger expression of galectin-1 at 2-weeks for both PN and DN suggest that the myogenic repair process was progressing well while at 12 weeks, the higher and disorganised expression of galectin-1 in DN is linked to slow myofiber and axonal recovery. It also reflects the random reinnervation of the myofibers distal to the lesion site. The re-innervation of myotubes following muscle injury is important to prevent myotube atrophy and to accelerate myotube growth.

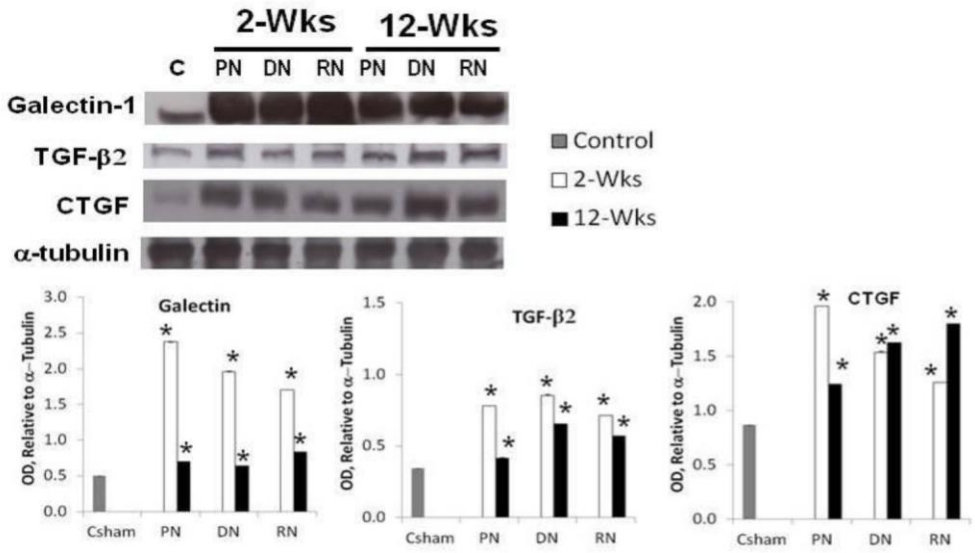

Figure 8B Optical densitometry quantification of Galectin-1, TGFβ2 and CTGF protein expression levels normalized to alpha tubulin, using GelPro v4.5 (arbitrary units). Data was obtained from three independent experiments with 3 rats. P-values were calculated by Scheffe's post-hoc test, where $p<0.05$ is considered statistically significant. (* - indicates significant difference ($p<0.05$) to Positive Control, CSham).

Immunoblotting of R-spondin-1 at 2-weeks (Fig. 8C) showed significantly up-regulation in all groups compared with the controls ($p<0.05$). After 12-weeks, R-spondin-1 protein expression level was down-regulated in all groups, but remained higher than the control ($p<0.05$). The highest mean level of R-spondin-1 were present in PN at 2-weeks post-laceration compared with the control ($p<0.05$).

At 2-weeks post laceration (Figure 12A), IGF1 expression levels were upregulated in all groups, except in NegC ($P<0.05$). After 12-weeks, IGF-1 was down-regulated back to the control levels. At 2-weeks (Fig. 12B), NT-4 was up-regulated in all groups except for NegC ($p>0.05$), with PN having the highest NT-4 level (> 14.0-fold). Similarly, GDNF was up-regulated in all groups ($p<0.05$) with DN having the highest GDNF expression level (>45-fold, $p<0.05$). The expression levels of HGF were significantly up-regulated in all groups at 2-weeks post-laceration ($p<0.05$). After 12-weeks, HGF was down-regulated, but remained higher than the baseline level of the control in all groups ($p<0.05$). RN had the highest level of HGF (>1.7-fold, $p>0.05$). The mRNA expression level of Shh (Fig. 17) were up-regulated

in all 4 groups at 2-weeks post-laceration compared against the control ($p<0.05$). PN has the highest Shh expression level (about 8.0-fold greater, $p<0.05$). After 12-weeks, Shh were down-regulated in all groups, but remained higher than the baseline control ($p<0.05$). Shh expression is the highest in RN ($p<0.05$).

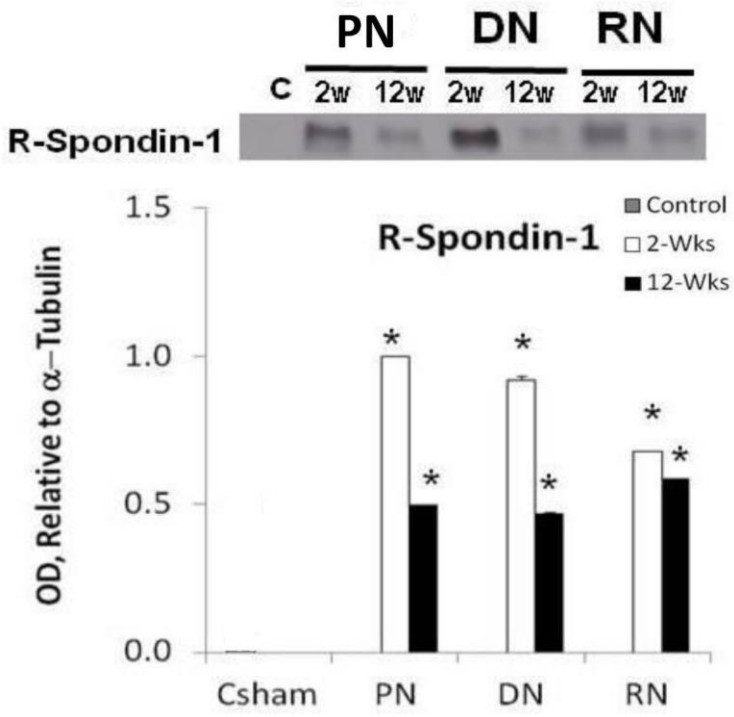

Figure 8C. Optical densitometry quantification for R-spondin-1 protein expression levels normalized to alpha tubulin (arbitrary units). Data was obtained from three independent experiments with 3 rats. p- values were calculated by Scheffe's post-hoc test, where $p<0.05$ is considered statistically significant. (* - indicates significant difference ($p<0.05$) to Positive Control, CSham).

6.2.2.2- Anti-fibrosis markers

Decorin, Follistatin, **EGF, PGC-1α, AMPK-1α, Sirt1, CNTF**

The expression level of follistatin and decorin were up-regulated in all 4 groups at 2-weeks post-laceration ($p>0.05$) (Fig. 9). DN has the highest follistatin expression levels (18-fold at 2 weeks; 7-fold, at 12-weeks, $p<0.05$). Decorin was down-regulated in all groups at 12-weeks, except for PN where it remained higher than the control by 11-fold ($p<0.05$).

At 2-weeks, the expression level of EGF was initially down-regulated in all PN, DN and RN but not in NegC (Fig.15A, $p<0.05$). After 12-weeks, EGF was significantly up-regulated in PN and DN, where PN has about 3.2-fold and DN has about 2.5-fold greater than the control respectively ($p<0.05$). All groups had EGF level lower than the baseline level of the control ($p>0.05$).

At 2-weeks post laceration, mRNA expression of AMPK-1α was up-regulated in all 4 groups (Fig. 11). AMPK-1α expression levels at 12-weeks was down-regulated in all groups, except for PN where AMPK-1α remained higher than the control by 3.0-fold ($p<0.05$). RN had the highest AMPK-1α (4.50-fold, $p<0.05$) expression level.

The gene expression level of PGC-1α (Fig 12A) was up-regulated in all 4 groups at 2-weeks post-laceration compared against the control ($p<0.05$). Sirt-1 was down-regulated in PN and DN but the level was increased in RN and NegC. PN has 0.15-fold lower Sirt-1 level than the control ($p<0.05$). After 12-weeks, PGC-1α was down-regulated in all groups except for DN and RN. In DN, PGC-1α expression level remained higher than the control by 3.5-fold, while RN has PGC-1α expression level of about 15.0-fold greater than the control ($p<0.05$). Sirt-1 was up-regulated to the baseline level of the control ($p<0.05$) with PN having the highest Sirt-1 expression level, about 3.5-fold greater than the control ($p<0.05$).

At 2-weeks (Fig.12B), CNTF was significantly down-regulated in all ($p<0.05$) where RN had the highest CNTF level (>0.55-fold). After 12-weeks, CNTF was up-regulated in all groups except for RN. In PN and DN, CNTF in PN remained higher than the control by 1.93-fold in PN and that in DN by 1.35-fold ($p<0.05$).

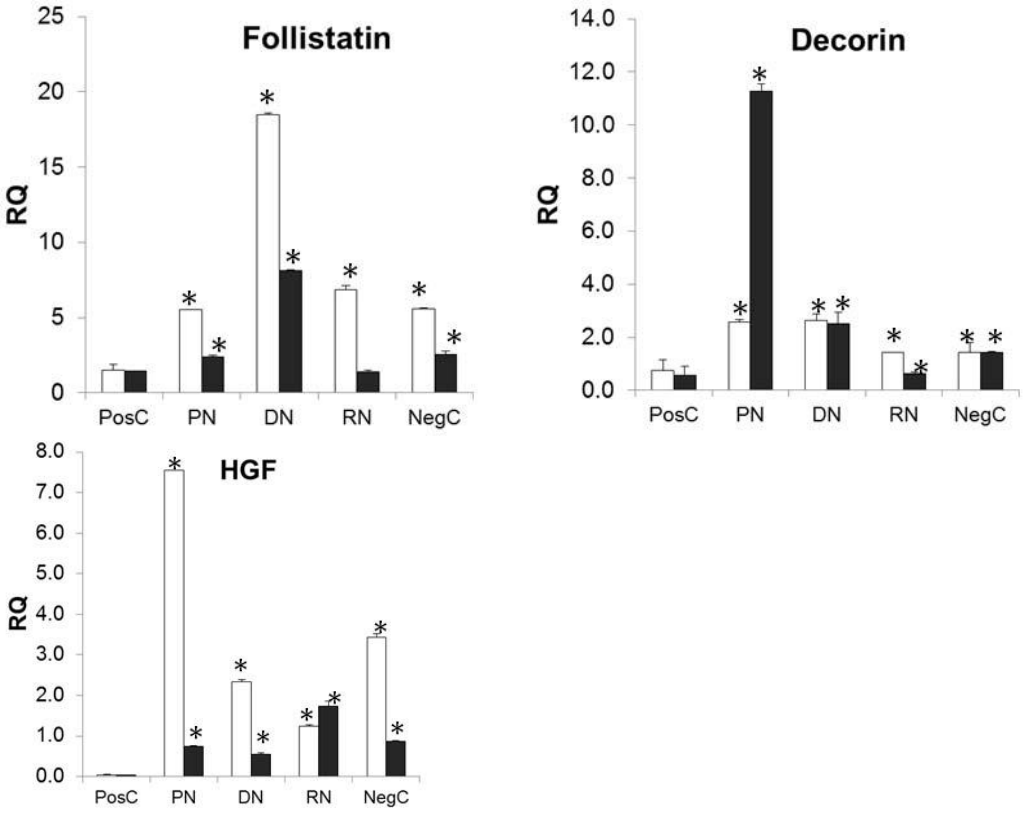

Figure 9 Fold changes (normalized to Lamin A) of Follistatin, Decorin and HGF. ANOVA and post-hoc tests at 2-weeks (white) and 12-weeks (black) post-repair identified homogenous sub-sets that were not significantly different (See Appendix 4). Data is expressed as means ± SD of three independent experiments obtained with 3 rats; P-values were calculated by Scheffe's post-hoc test, where $p<0.05$ is considered statistically significant. (* - indicates significant difference ($p<0.05$) to Positive Control, PosC).

6.2.2.3- Correlations between markers

In PN, the expression of collagen and aggrecan were decreased over 12-weeks to 3.25-fold and 0.24-fold higher than control respectively. It has the lowest aggrecan and second lowest collagen expression level after 12-weeks. This was associated with an increase in AMPK-1a (2.96-fold, $p<0.05$), EGF (3.24-fold, $p<0.05$), Sirt1 (3.43-fold, $p<0.05$), CNTF (1.93-fold, $p<0.05$) and decorin (11.28-fold, $p<0.05$). A corresponding decrease in IGF1 (0.015-fold, $p<0.05$), TGFb2 (0.018-fold, $p<0.05$), galectin-1 (0.11-fold, $p<0.05$), vimentin (0.21-fold, $p<0.05$), R-spondin-1 (0.29-fold, $p<0.05$), CTGF and HGF (0.74-fold, $p<0.05$), and Shh (1.64-fold, $p<0.05$) is observed.

DN has the highest collagen and aggrecan levels at 15.76-fold and 7.69-fold more than the control respectively. This was associated with an increase in the expression of NT4 (24.86-fold, $p<0.05$), myostatin (0.85-fold, $p<0.05$), CTGF (1.62-fold, $p<0.05$), TGFb2 (0.21-fold, $p<0.05$), GDNF (17.78-fold, $p<0.05$), R-spondin-1 (0.46-fold, $p<0.05$), IGF1 (0.15-fold, $p<0.05$) and HGF (0.55-fold, $p<0.05$). There was also a decrease AMPK-1a (0.48-fold, $p<0.05$), EGF (2.44-fold, $p<0.05$), CNTF (1.34-fold, $p<0.05$) and follistatin (8.13-fold, $p<0.05$) expression levels.

RN has the lowest collagen (0.13-fold) and second lowest aggrecan (2.15-fold) levels compared to the control. This corresponds to an increase in PGC-1a (14.99-fold, $p<0.05$), follistatin (1.38-fold, $p<0.05$), AMPK-1a (1.34-fold, $p<0.05$) and CNTF (0.48-fold, $p<0.05$). There is a decrease in CTGF (1.79-fold, $p<0.05$), R-spondin-1 (0.58-fold, $p<0.05$), Shh (6.61-fold, $p<0.05$), IGF1 (0.11-fold, $p<0.05$), HGF (1.73-fold, $p<0.05$) and myostatin (0.56-fold, $p<0.05$) expression levels.

Table 5A Correlation between collagen-1a and other selected fibrosis markers with respect to overall fold change in gene expression in all groups

Gene	**PN**	**DN**	**RN**	**NegC**	**r**
TGFb2	-0.24*	-0.22$^{*,\#}$	-0.01	0.02	0.6407
HGF	-6.81*	-1.78*	0.50$^{*,\#}$	-2.56*	0.3903
GDNF	-2.13	-27.68*	-7.51	-7.00	0.7735
Sonic Hedgehog	-6.68*	-2.62	0.95$^{\#}$	-3.83	0.5246
Galectin-1	-0.43*	-0.18	-0.05	-0.20	0.6537
Aggrecan	-12.17*	-34.89$^{*,\#}$	-22.46*	-43.24*	0.7748
Note: ***** $p<0.05$ at 2-weeks**, #** $p<0.05$ at 12-weeks					

Table 5B Correlation between aggrecan and other selected fibrosis markers with respect to overall fold change in gene expression in all groups

Gene	**PN**	**DN**	**RN**	**NegC**	**r**
TGFb2	-0.24*	-0.22$^{*,\#}$	-0.01	0.02	0.43
HGF	-6.81*	-1.78*	0.50$^{*,\#}$	-2.56*	0.3991
EGF	2.10$^{\#}$	1.92$^{\#}$	0.15	-0.33	-0.4568
IGF-1	-0.37$^{*\#}$	-0.08*	-0.22*	-3.58*	0.6986
GDNF	-2.13	-27.68*	-7.51	-7.00	0.7856
CNTF	1.82$^{*,\#}$	1.09$^{*,\#}$	-1.32*	0.29$^{\#}$	-0.4783
Sonic Hedgehog	-6.68*	-2.62	0.95$^{\#}$	-3.83	0.4969

Galectin-1	-0.43*	-0.18	-0.05	-0.20	0.6324
Collagen-1	-11.10	-9.45	-23.66	-8.50	0.7748
Note: ***** $p<0.05$ at 2-weeks**, #** $p<0.05$ at 12-weeks					

Table 5C Correlation between vimentin and other selected fibrosis markers with respect to overall fold change in gene expression in all groups

Gene	**PN**	**DN**	**RN**	**NegC**	**r**
TGFb2	-0.24*	-0.22$^{*,\#}$	-0.01	0.02	0.5159
HGF	-6.81*	-1.78*	0.50$^{*,\#}$	-2.56*	0.8024
NT-4	-13.71	24.10$^{\#}$	12.43	-0.18	0.5147
CNTF	1.82$^{*,\#}$	1.09$^{*,\#}$	-1.32*	0.29$^{\#}$	-0.4332
Sonic Hedgehog	-6.68*	-2.62	0.95$^{\#}$	-3.83	0.5335
Sirt-1	3.28*	0.92	-1.63	-2.03	-0.4739
Galectin-1	-0.43*	-0.18	-0.05	-0.20	0.6999
Note: ***** $p<0.05$ at 2-weeks, # $p<0.05$ at 12-weeks					

6.2.3- Atrophy markers

Atrogin-1, MuRF-1, Complement-3

The expression level of atrogin-1 and MuRF-1 were up-regulated in all 4 groups at 2-weeks post-laceration compared with the control ($p>0.05$) (Fig. 10). After 12-weeks, atrogin-1 was down-regulated in all groups except for DN. In DN, atrogin-1 expression level remained higher than the control by 4.0-fold ($p<0.05$). On the other hand, MuRF-1 was down-regulated in RN PN and NegC, and up-regulated in DN. In DN, MuRF-1 expression level remained higher than the control by 3.4-fold while in PN, the level is about 0.34-fold greater than the control ($p<0.05$). At 2-weeks, the expression level of complement-3, another atrophy marker which degrades fast ($r = -0.3773$) and slow myosin heavy chains ($r = -0.4383$), was the highest for NegC (about 22-fold greater than the control, $p<0.05$). At 2-weeks post laceration, mRNA expression of complement-3 was up-regulated in all 4 groups, with the highest expression noted with NegC (Fig. 18B). After 12-weeks, complement-3 was down-regulated in all groups, but the expression level remained higher than the control ($p<0.05$).

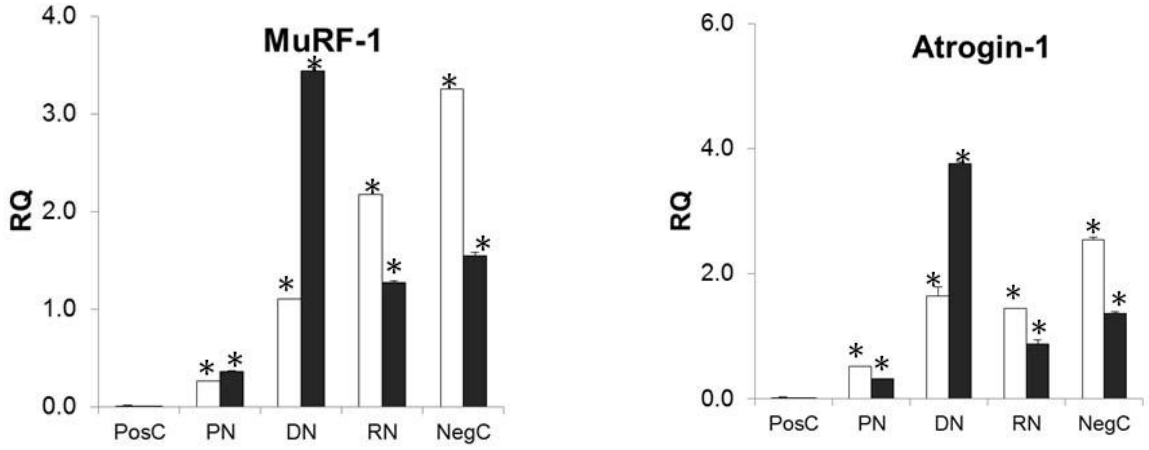

Figure 10. Fold changes (normalized to Lamin A) of MuRF-1 and Atrogin-1. ANOVA and post-hoc tests at 2-weeks (white) and 12-weeks (black) post-repair identified the homogenous sub-sets that were not significantly different (See Appendix 4). P-values were calculated by Scheffe's post-hoc test, where $p<0.05$ is considered statistically significant. (* - indicates significant difference ($p<0.05$) to Positive Control, PosC).

6.2.3.1- Pro-atrophy markers

Myostatin, Myogenin, AMPK-1α

At 2-weeks post laceration, mRNA expression of myostatin, and AMPK-1α were up-regulated in all 4 groups (Fig. 11). After 12-weeks, myostatin was further up-regulated in all groups, except for PN, where it recorded a down-regulation. In DN, myostatin expression level further was up-regulated by 0.88-fold ($p<0.05$). AMPK-1α expression levels at 12-weeks was down-regulated in all groups, except for PN where AMPK-1α remained higher than the control by 3.0-fold ($p<0.05$). RN had the highest AMPK-1α (4.50-fold, $p<0.05$) expression level. The expression level of myogenin was significantly up-regulated in DN, RN and NegC at 2-weeks post-laceration compared against the control ($p<0.05$). In PN, the myogenin expression level was down-regulated but was not statistically significant ($p>0.05$). After 12-weeks, myogenin expression level in RN and NegC remained higher than the control ($p<0.05$) except for PN (1.60-fold less than the control, $p>0.05$).

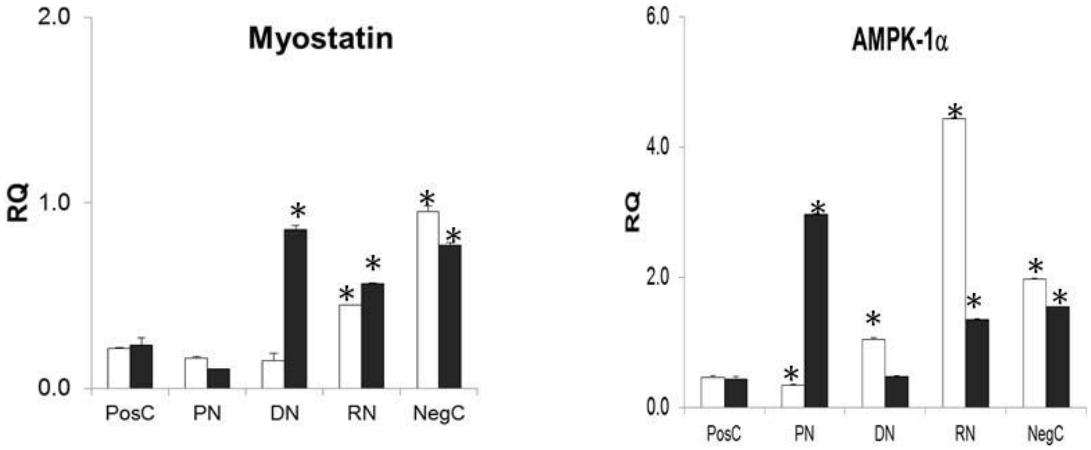

Figure 11. Fold changes (normalized to Lamin A) of Myostatin and AMPK-1α. ANOVA and post-hoc tests at 2-weeks (white) and 12-weeks (black) post-repair identified the homogenous sub-sets that were not significantly different (See Appendix 4). Data is expressed as means ± SD of three independent experiments obtained with 3 rats (n=3); p-values were calculated by Scheffe's post-hoc test, where $p<0.05$ is considered statistically significant. (* - indicates significant difference ($p<0.05$) to Positive Control, PosC).

6.2.3.2- Anti-atrophy markers

Calpain-3, IGF1, PGC-1α, Sirt1, NT4, GDNF, CNTF, **Decorin, Follistatin**

At 2-weeks post laceration (Figure 12A), calpain-3 expression level was down-regulated in all groups except for PN. PN has the highest calpain-3 expression level. In PN the expression level was about 2.0-fold greater than the control ($p<0.05$). IGF-1 expression levels were upregulated in all groups, except in NegC ($P<0.05$). After 12-weeks, IGF-1 was down-regulated back to the control levels. Calpain-3 was noted to be further down-regulated in all groups, except in RN where it was up-regulated compared to the control ($p<0.05$).

The gene expression level of PGC-1α (Fig 12A) was up-regulated in all 4 groups at 2-weeks post-laceration compared against the control ($p<0.05$). Sirt-1 was down-regulated in PN and DN but the level was increased in RN and NegC. PN has 0.15-fold lower Sirt-1 level than the control ($p<0.05$). After 12-weeks, PGC-1α was down-regulated in all groups except for DN and RN. In DN, PGC-1α expression level remained higher than the control by 3.5-fold, while RN has PGC-1α expression level of about 15.0-fold greater than the control

($p<0.05$). Sirt-1 was up-regulated to the baseline level of the control ($p<0.05$) with PN having the highest Sirt-1 expression level, about 3.5-fold greater than the control ($p<0.05$).

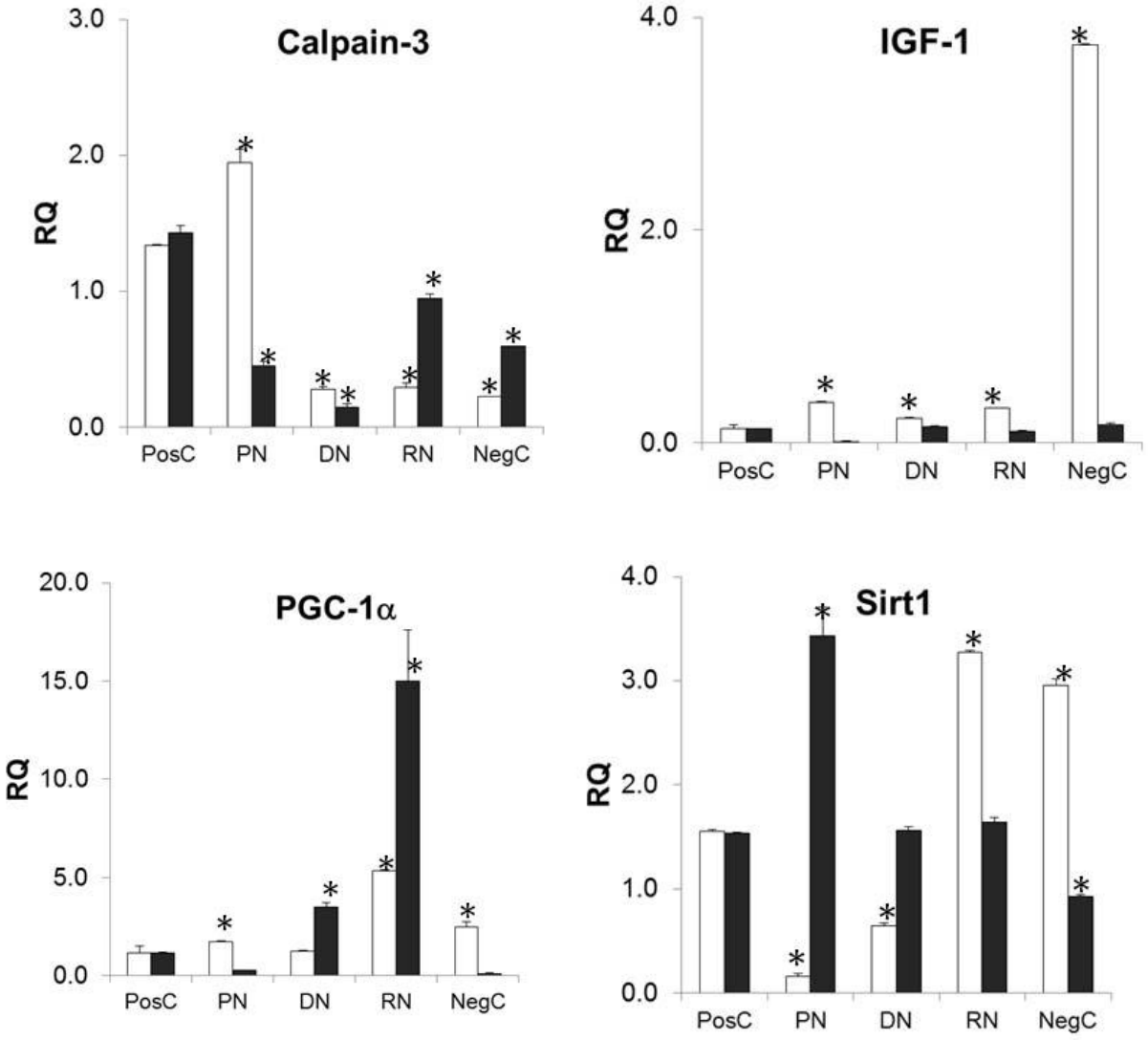

Figure 12A. Fold changes (normalized to Lamin A) of Calpain-3, IGF-1, PGC-1α and Sirt-1**.** ANOVA and post-hoc tests at 2-weeks (white) and 12-weeks (black) post-repair identified the homogenous sub-sets that were not significantly different (See Appendix 4). Data is expressed as means ± SD of three independent experiments obtained with 3 rats; p-values were calculated by Scheffe's post-hoc test, where $p<0.05$ is considered statistically significant. (* - indicates significant difference ($p<0.05$) to Positive Control, PosC).

At 2-weeks (Fig. 12B), NT-4 was up-regulated in all groups except for NegC ($p>0.05$), with PN having the highest NT-4 level (> 14.0-fold). Similarly, GDNF was up-regulated in all groups ($p<0.05$) with DN having the highest GDNF expression level (>45-fold, $p<0.05$).

Conversely, except for RN, CNTF was significantly down-regulated in all ($p<0.05$) where RN had the highest CNTF level (>0.55-fold). Decorin and follistatin which are also anti-fibrosis markers were shown in the previous section to be upregulated in all groups at 2-weeks.

After 12-weeks, NT-4 was down-regulated in all groups except for DN. (Figure 9.) In DN, NT-4 expression levels remained higher than the control (22.0-fold, $p<0.05$). Except for DN, GDNF was down-regulated in all other groups. In DN, GDNF expression level remained high (> 20.0-fold, $p>0.05$). CNTF was up-regulated in all groups except for RN. In PN and DN, CNTF in PN remained higher than the control by 1.93-fold in PN and that in DN by 1.35-fold ($p<0.05$).

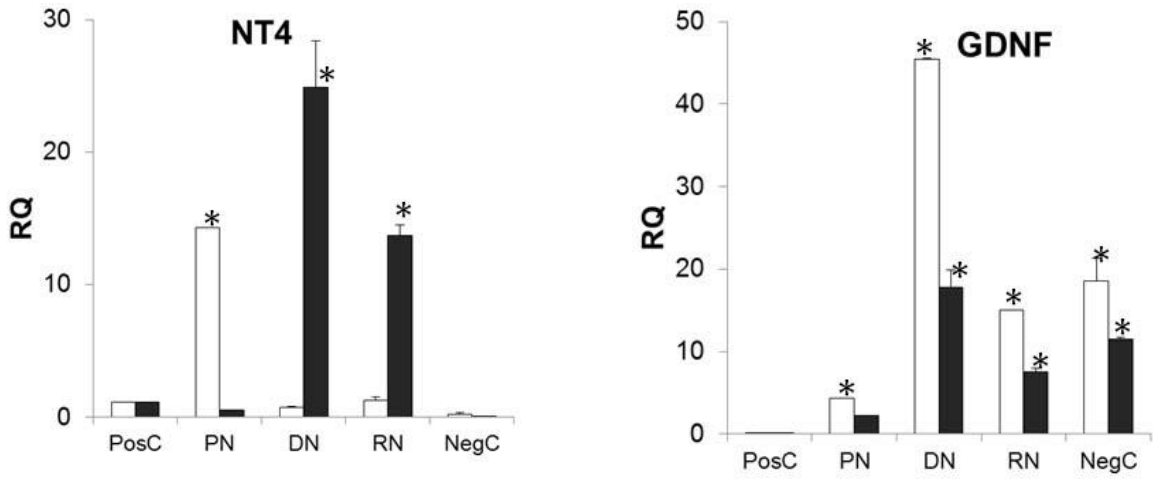

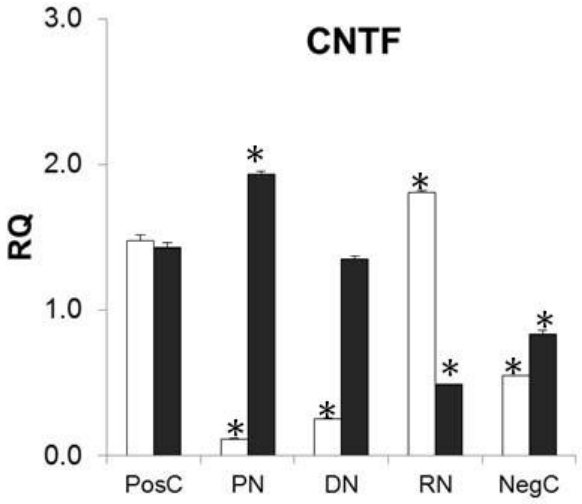

Figure 12B. Fold changes (normalized to Lamin A) of NT-4, GDNF, CNTF. ANOVA and post-hoc tests at 2-weeks (white) and 12-weeks (black) post-repair identified the homogenous sub-sets that were not significantly different (See Appendix 4). Data is expressed as means ± SD of three independent experiments obtained with 3 rats (n=3); p-values were calculated by Scheffe's post-hoc test, where $p<0.05$ is considered statistically significant. (* - indicates significant difference ($p<0.05$) to Positive Control, PosC).

6.2.3.3- Correlations between markers

In PN, the expression of atrogin-1, MuRF1 and complement-3 were decreased to 0.32-fold, 0.36-fold and 1.83-fold lower than the control respectively. It has the lowest atrogin-1, MuRF1 and complement-3 expression levels after 12-weeks. This was associated with an increase in Sirt1 (3.43-fold, $p<0.05$), CNTF (1.93-fold, $p<0.05$) and decorin (11.28-fold, $p<0.05$). A corresponding decrease in pro-atrophy factors AMPK-1a (2.96-fold, $p<0.05$), and anti-atrophy factors calpain-3 (0.45-fold, $p<0.05$), IGF1 (0.015-fold, $p<0.05$) is observed.

The expression of atrogin-1, MuRF-1 and complement-3 in DN were increased to 3.76-fold, 3.44-fold and 6.66-fold higher than the control respectively over 12-weeks.

DN has the highest atrogin-1, MuRF1 and second highest complement-3 expression levels after 12-weeks. This was associated with an increase in myostatin (0.85-fold, $p<0.05$), CNTF (1.34-fold, $p<0.05$) and NT4 (24.86-fold, $p<0.05$). A corresponding decrease in AMPK-1a (0.48-fold, $p<0.05$), IGF1 (0.15-fold, $p<0.05$), GDNF (17.78-fold, $p<0.05$) and

follistatin (8.13-fold, $p<0.05$) is observed.

In RN, the expression of atrogin, MuRF1 and complement-3 was decreased over 12-weeks to 0.87-fold, 1.27-fold and 8.41-fold higher than control respectively. It has the highest complement-3 expression level after 12-weeks, while its atrogin-1 and MuRF1 levels are intermediate between PN and DN. This was associated with an increase in calpain-3 (0.94-fold, $p<0.05$), PGC-1a (14.99-fold, $p<0.05$) and myostatin (0.56-fold, $p<0.05$).

A corresponding decrease in IGF1 (0.19-fold, $p<0.05$), CNTF (0.48-fold, $p<0.05$), follistatin (1.38-fold, $p<0.05$), AMPK-1a (1.34-fold, $p<0.05$) and myogenin (3.54-fold, $p<0.05$) is observed.

Table 6A Correlation between atrogin-1 and other selected atrophy markers with respect to overall fold change in gene expression in all groups

Gene	**PN**	**DN**	**RN**	**NegC**	**r**
MuRF-1	0.10	2.34$^{*,\#}$	-0.90$^{*\#}$	-1.70$^{*,\#}$	0.9471
Myogenin	-0.25	0.45	-3.11$^{*\#}$	-2.98$^{*,\#}$	0.8659
Calpain-3	-1.49*	-0.13	0.65$^{\#}$	0.37	-0.6758
Myostatin	-0.06	0.71$^{\#}$	0.12$^{*,\#}$	-0.18$^{*,\#}$	0.7753
Note: ***** $p<0.05$ at 2-weeks, # $p<0.05$ at 12-weeks					

Table 6B Correlation between MuRF-1 and other selected atrophy markers with respect to overall fold change in gene expression in all groups

Gene	**PN**	**DN**	**RN**	**NegC**	**r**
Atrogin-1	-0.19$^{*,\#}$	2.12$^{*,\#}$	-0.57$^{\#}$	-1.17*	0.9471
Myogenin	-0.25	0.45	-3.11$^{*\#}$	-2.98$^{*,\#}$	0.8476
Calpain-3	-1.49*	-0.13	0.65$^{\#}$	0.37	-0.7066
Myostatin	-0.06	0.71$^{\#}$	0.12$^{*,\#}$	-0.18$^{*,\#}$	0.8712
Note: ***** $p<0.05$ at 2-weeks, # $p<0.05$ at 12-weeks					

Table 6C Correlation between complement-3 and other selected atrophy markers with respect to overall fold change in gene expression in all groups

Gene	**PN**	**DN**	**RN**	**NegC**	**r**
Atrogin-1	-0.19$^{*,\#}$	2.12$^{*,\#}$	-0.57$^{\#}$	-1.17*	0.6389
MuRF-1	0.10	2.34$^{*,\#}$	-0.90$^{*\#}$	-1.70$^{*,\#}$	0.7593
CNTF	1.82$^{*,\#}$	1.09$^{*,\#}$	-1.32*	0.29$^{\#}$	-0.3817
Calpain-3	-1.49*	-0.13	0.65$^{\#}$	0.37	-0.5803
PGC-1a	-1.48	2.24	9.64$^{\#}$	-2.35	-0.4472
Note: ***** $p<0.05$ at 2-weeks, # $p<0.05$ at 12-weeks					

6.2.4- Myogenesis markers

MyoD, Myogenin, Mef2α, Desmin

The expression level of myoD (Fig. 13) was down-regulated in PN and DN at 2-weeks post-laceration ($p<0.05$) with the lowest expression level (0.55-fold lower than the level of the control). After 12-weeks, myoD was up-regulated in all groups, where DN had the highest myoD level ($p<0.05$). The expression level of myogenin was significantly up-regulated in DN, RN and NegC at 2-weeks post-laceration compared against the control ($p<0.05$). In PN, the myogenin expression level was down-regulated but was not statistically significant ($p>0.05$). After 12-weeks, myogenin expression level in RN and NegC remained higher than the control ($p<0.05$) except for PN (1.60-fold less than the control, $p>0.05$).

At 2-weeks, Mef-2α expression level normalized to lamin A (Fig 13) was down-regulated in all groups except for NegC ($p<0.05$). PN has the lowest Mef-2α expression level (about 0.75-fold lower than the control). NegC has the highest Mef-2α expression level (about 2.92-fold higher than the control, $p<0.05$). After 12-weeks, Mef-2α A was up-regulated in all groups with DN having the highest expression level (about 3.15-fold, $p<0.05$).

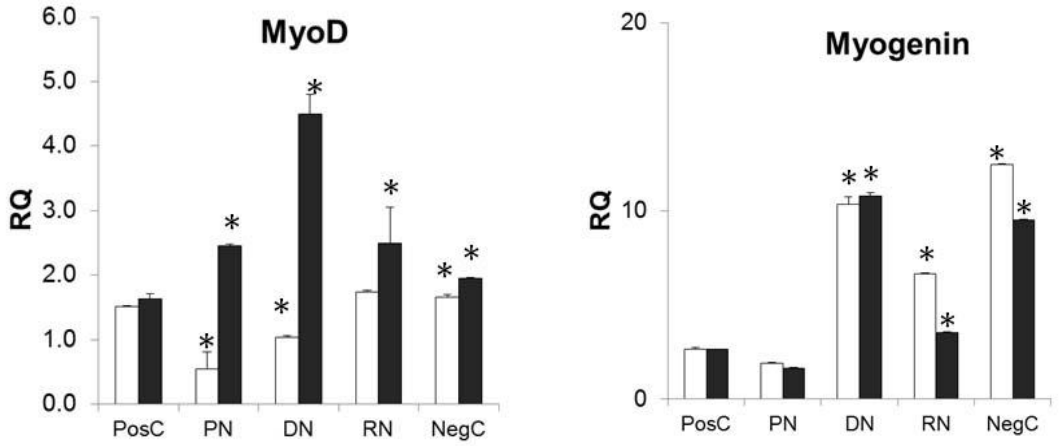

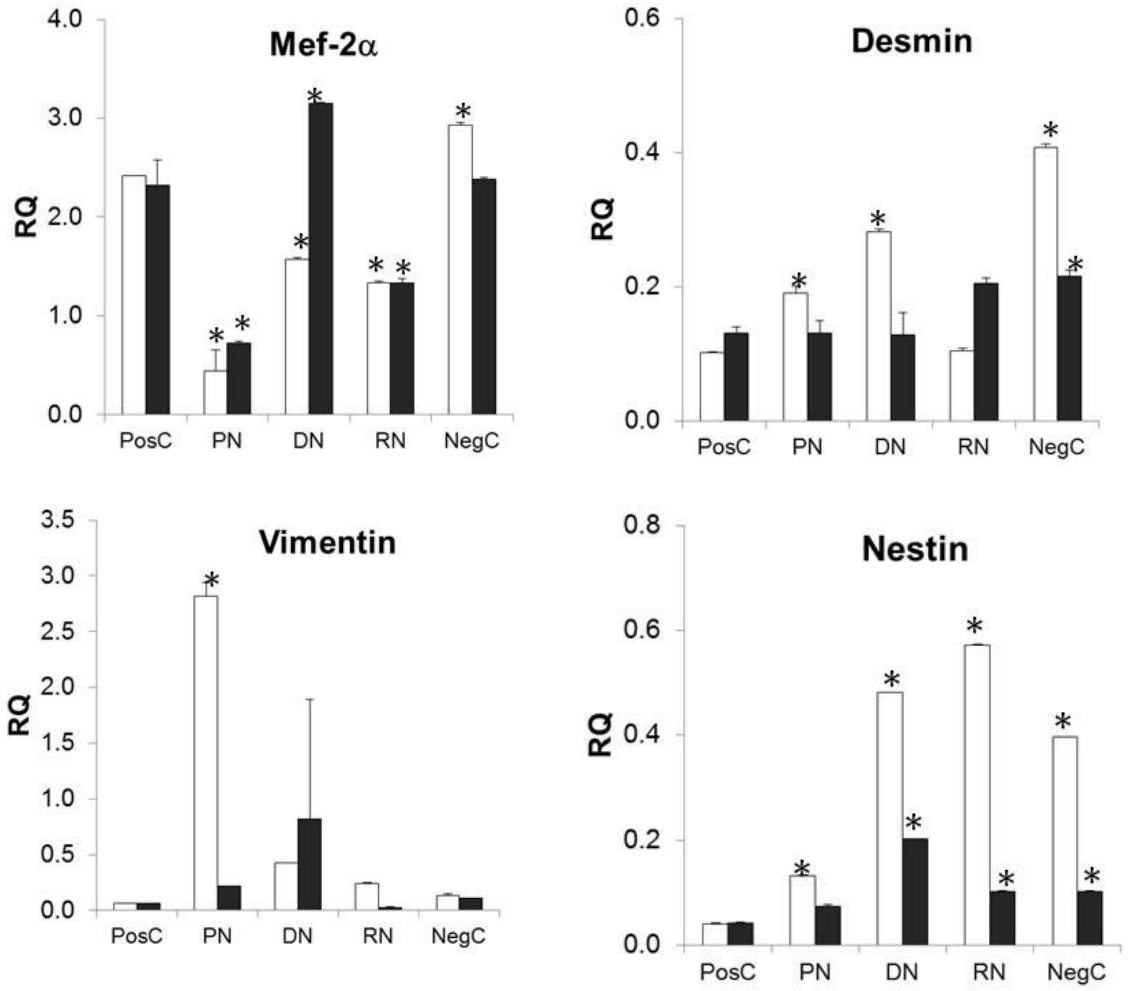

Figure 13. Fold changes (normalized to Lamin A) of myoD, myogenin, Mef-2α and desmin. ANOVA and post-hoc tests at 2-weeks (white) and 12-weeks (black) post-repair identified the homogenous sub-sets that were not significantly different (See Appendix 4). Data is expressed as means ± SD of three independent experiments obtained with 3 rats (n=3); p-values were calculated by Scheffe's post-hoc test, where $p<0.05$ is considered statistically significant. (* - indicates significant difference ($p<0.05$) to Positive Control, PosC).

The mRNA expression levels of the intermediate filaments desmin, vimentin and nestin (Fig. 13) were significantly up-regulated in all groups at 2-weeks post-laceration compared against the control. In PN, the desmin, vimentin and nestin expression level was about 0.26-fold, 3.0-fold and 3.0-fold greater than the control, respectively ($p<0.05$). After 12-weeks, desmin in all groups remained higher than the control ($p<0.05$), where in PN it was about 0.11-fold greater than the control ($p<0.05$). Conversely, vimentin and nestin was down-regulated in PN, DN and NegC, but not in DN where the expression

were >2.0-fold greater than the control ($p<0.05$).

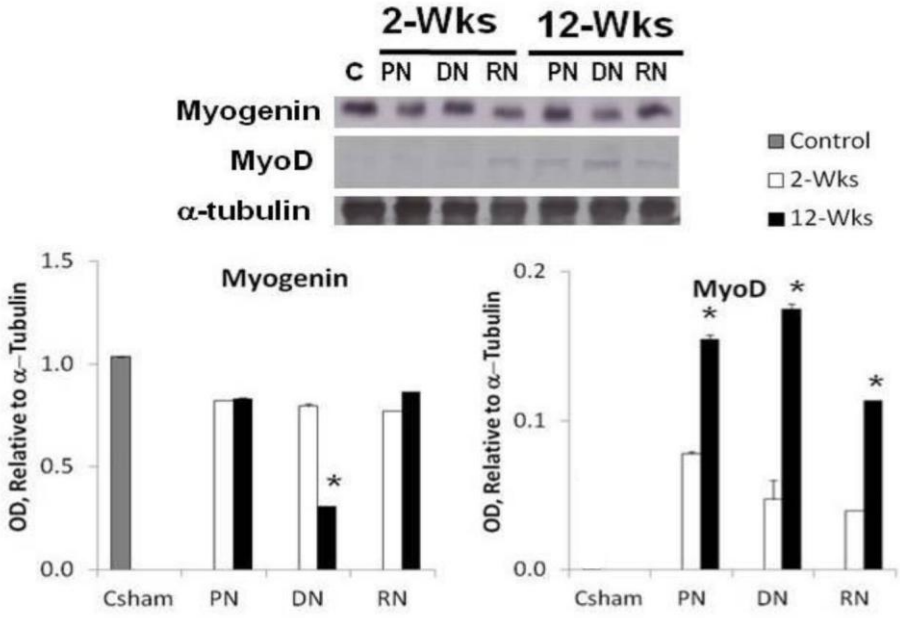

Figure 14A. Western blot analysis of Myogenin and myoD at 2-weeks (white) and 12-weeks (black) post-repair (with alpha tubulin as the loading control). P-values were calculated by Scheffe's post-hoc test, where $p<0.05$ is considered statistically significant. The optical densitometry (OD) quantification of the protein expression level normalized to alpha tubulin, using GelPro v4.5 (arbitrary units).

Immunoblotting results (Fig. 14A) showed that myoD protein expression level was significantly down-regulated in PN and DN at 2-weeks post-laceration but not in RN, compared against the control ($p>0.05$). After 12-weeks, myoD was up-regulated in PN, DN and RN ($p<0.05$). The highest mean level of myoD were in PN and DN at 12-weeks post-laceration compared with other subgroups ($p<0.05$). Myogenin was significantly down-regulated in DN and RN at 2-weeks post-laceration ($p<0.05$). After 12-weeks, myogenin was down-regulated in DN ($p<0.05$). The highest mean level of myogenin were present in PN and RN at 12-weeks post-laceration compared with the control ($p<0.05$). The highest mean level of myogenin were present in PN and RN at 12-weeks post-laceration compared with the control ($p<0.05$). Immunoblotting results for desmin and vimentin (Fig. 14B) showed significantly up-regulation in all groups at 2-weeks post-laceration compared to the control ($p<0.05$). After 12-weeks, desmin expression level in

all groups returned to the baseline level of the control ($p<0.05$). Vimentin was also down-regulated in PN, RN and NegC, but not in DN, where it remained highly expressed ($p<0.05$). The highest mean level of desmin and vimentin was present in PN at 2-weeks post-laceration compared with the control ($p<0.05$).

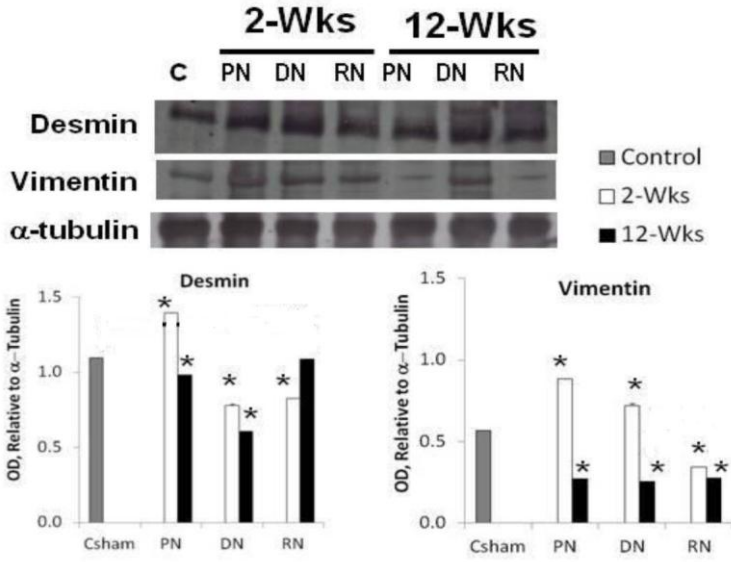

Figure 14B. Western blot analysis of Vimentin and Desmin at 2-weeks (white) and 12-weeks (black) post-repair (with alpha tubulin as the loading control). P-values were calculated by Scheffe's post-hoc test, where $p<0.05$ is considered statistically significant. The optical densitometry (OD) quantification of the protein expression level was normalized to alpha tubulin, using GelPro v4.5 (arbitrary units).

6.2.4.1- Pro-myogenesis markers

Galectin-1, Decorin, Follistatin, IGF1, HGF, EGF, Shh, NT4, GDNF, CNTF, PGC-1α, Sirt1, R-spondin-1

Of the pro-myogenesis markers, galectin-1 (Figs. 8A and B) is a pro-fibrosis marker, while decorin and follistatin (Fig. 9) are anti-fibrosis markers. AMPK-1α (Fig 11) is also a pro-atrophy and anti-fibrosis marker, while IGF-1, PGC-1α, Sirt-1, NT4 GDNF and CNTF (Figs. 12A and 12B) are anti-atrophy markers. NT-4, GDNF and CNTF are also pro-axonal regeneration factors. NT4, GDNF and Sonic hedgehog also have pro-fibrosis actions. All these have been shown above.

The expression level of HGF and IGF-1 (as shown before) were significantly up-regulated in all groups while EGF was initially down-regulated in all PN, RN and DN, but not in NegC, at 2-weeks post-laceration (Fig. 15A, $p<0.05$). NegC had the highest IGF-1 expression level (>4-fold greater than control) while PN had the highest IGF-1 expression level (>7.5-fold).

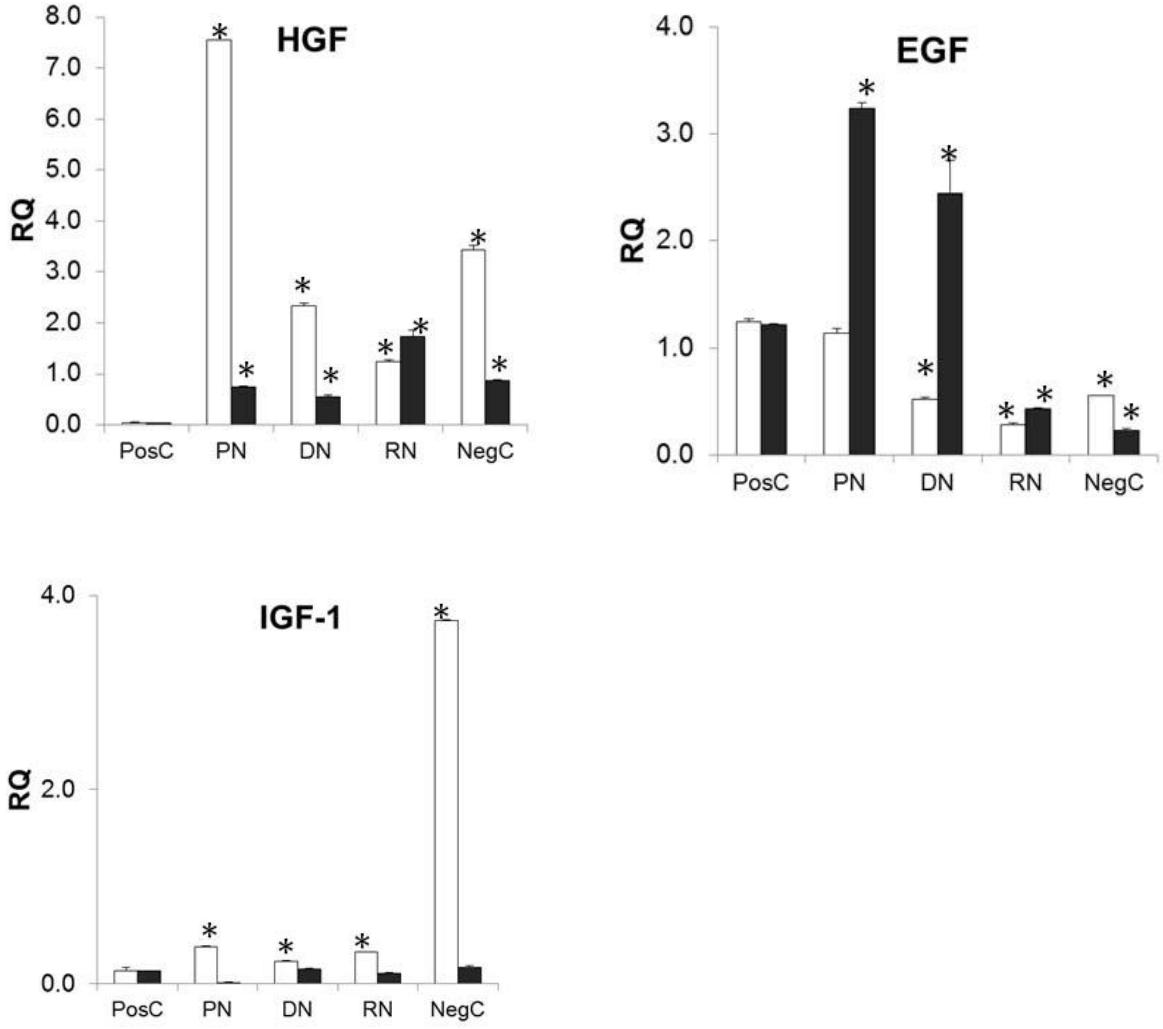

Figure 15A. Fold changes (normalized to Lamin A) of HGF, EGF and IGF. ANOVA and post-hoc tests at 2-weeks (white) and 12-weeks (black) post-repair identified the homogenous sub-sets that were not significantly different (See Appendix 4). Data is expressed as means ± SD of three independent experiments obtained with 3 rats; p-values were calculated by Scheffe's post-hoc test, where $p<0.05$ is considered statistically significant. (* - indicates significant difference ($p<0.05$) to Positive Control, PosC).

After 12-weeks, IGF-1 was down-regulated to the baseline level while HGF was down-regulated, but remained higher than the baseline level of the control in all groups ($p<0.05$). EGF was significantly up-regulated in PN and DN, where PN has about 3.2-fold and DN has about 2.5-fold greater than the control respectively ($p<0.05$). RN has the highest level of HGF (>1.7-fold) while all other groups had EGF level lower than the baseline level of the control ($p>0.05$).

Immunoblotting of R-spondin-1 which is also a pro-fibrosis marker was previously shown (Fig 8C).

6.2.4.2- Anti-myogenesis markers

Myostatin, TGFβ2, CTGF, AMPK-1α

At 2-weeks post laceration, myostatin (Fig. 15B) was up-regulated in all 4 groups. TGFβ2, a pro-fibrosis marker was only up-regulated for PN and DN. After 12-weeks, myostatin was further up-regulated in all groups except for PN. In DN, myostatin expression level remained higher than the control by 0.88-fold ($p<0.05$). On the other hand, TGFβ2 was down regulated to baseline values, in all but DN. AMPK-1a (Fig 11) and CTGF (Fig 8B) have been shown above.

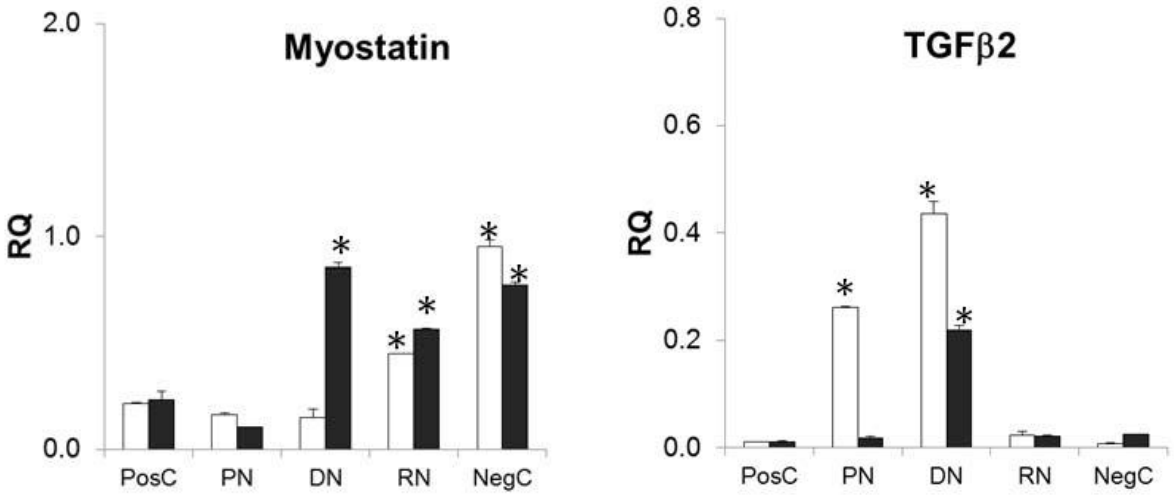

Figure 15B. Fold changes (normalized to Lamin A) of Myostatin, TGFβ2. ANOVA and post-hoc tests at 2-weeks (white) and 12-weeks (black) post-repair identified the homogenous sub-sets that were not significantly different (See Appendix 4). Data is expressed as means ± SD of three independent experiments obtained with 3 rats; p-values were calculated by Scheffe's post-hoc test, where $p<0.05$ is considered statistically significant. (* - indicates significant difference ($p<0.05$) to Positive Control, PosC).

6.2.4.3- Correlations between markers

In PN, the expression of myoD was increased over 12-weeks to 2.45-fold higher than control. It has the lowest myogenin expression level after 12-weeks at 1.66-fold compared to the control. This was associated with an decrease in TGFb2 (0.018-fold, $p<0.05$) and CTGF (0.74-fold, $p<0.05$), galectin-1 (0.11-fold, $p<0.05$), IGF1(0.015-fold, $p<0.05$), HGF (0.74-fold, $p<0.05$), R-spondin-1 (0.29-fold, $p<0.05$), Shh (1.64-fold, $p<0.05$). A corresponding increase in AMPK-1a (2.96-fold, $p<0.05$), decorin (11.28-fold, $p<0.05$), EGF (3.24-fold, $p<0.05$), CNTF (1.93-fold, $p<0.05$) and Sirt1 (3.43-fold, $p<0.05$) is noted.

In DN, the expression of myoD and myogenin were decreased over 12-weeks to 4.49-fold and 10.81-fold higher than control respectively. This was associated with an decrease in TGFb2 (0.22-fold, $p<0.05$) and AMPK-1a (0.48-fold, $p<0.05$), follistatin (8.13-fold, $p<0.05$), IGF1 (0.15-fold, $p<0.05$), HGF (0.55-fold, $p<0.05$), GDNF (17.78-fold, $p<0.05$) and R-spondin-1 (0.46-fold, $p<0.05$). A corresponding increase in myostatin (0.85-fold, $p<0.05$), CTGF (1.62-fold, $p<0.05$), EGF (2.44-fold, $p<0.05$), NT4 (24.86-fold, $p<0.05$) and CNTF (1.34-fold, $p<0.05$) was found.

In RN, the expression of myoD was increased over 12-weeks to 2.48-fold higher than control, while the myogenin level was decreased to 3.54-fold greater than control.
This was associated with a decrease in AMPK-1a (1.34-fold, $p<0.05$) and CTGF (1.79-fold, $p<0.05$), follistatin (1.38-fold, $p<0.05$), IGF1 (0.11-fold, $p<0.05$), CNTF (0.48-fold, $p<0.05$), and R-spondin-1 (0.58-fold, $p<0.05$). A corresponding increase in myostatin (0.56-fold,

p<0.05), HGF (1.73-fold, p<0.05), Shh (6.61-fold, p<0.05) and PGC-1a (14.99-fold, p<0.05) is seen.

Table 7A Correlation between myoD and other selected myogenesis markers with respect to overall fold change in gene expression in all groups

Gene	**PN**	**DN**	**RN**	**NegC**	**r**
TGFb2	-0.24*	-0.22$^{*,\#}$	-0.01	0.02	-0.3873
AMPK	2.61$^{*,\#}$	-0.57*	-3.09$^{*,\#}$	-0.42$^{*\#}$	-0.3653
EGF	2.10$^{\#}$	1.92$^{\#}$	0.15	-0.33	0.4899
IGF-1	-0.37$^{*\#}$	-0.08*	-0.22*	-3.58*	0.3864
NT-4	-13.71	24.10$^{\#}$	12.43	-0.18	0.5492
CNTF	1.82$^{*,\#}$	1.09$^{*,\#}$	-1.32*	0.29$^{\#}$	0.4168
Mef-2a	0.28	1.58	0.01	-0.55	0.3788
Note: ***** p<0.05 at 2-weeks, **#** p<0.05 at 12-weeks					

Table 7B Correlation between myogenin and other selected myogenesis markers with respect to overall fold change in gene expression in all groups

Gene	**PN**	**DN**	**RN**	**NegC**	**r**
Follistatin	-3.15	-10.32$^{*,\#}$	-5.46*	-3.00	0.5833
EGF	2.10$^{\#}$	1.92$^{\#}$	0.15	-0.33	-0.3928
IGF-1	-0.37$^{*\#}$	-0.08*	-0.22*	-3.58*	0.5418
GDNF	-2.13	-27.68*	-7.51	-7.00	0.7514
CNTF	1.82$^{*,\#}$	1.09$^{*,\#}$	-1.32*	0.29$^{\#}$	-0.3479
Mef-2a	0.28	1.58	0.01	-0.55	0.633
Desmin	0.02	-0.15*	0.10	-0.19*	0.6338
Myostatin	-0.06	0.71$^{\#}$	0.12$^{*,\#}$	-0.18$^{*,\#}$	-0.4499
Note: ***** p<0.05 at 2-weeks**, #** p<0.05 at 12-weeks					

6.2.5- Isometric contraction markers

Slow troponin-I, fast troponin-I, slow myosin heavy chain, fast myosin heavy chain, embryonic myosin heavy chain

Quantitative analysis of genes related to isometric contraction including myosin heavy chain -3 (embryonic), -7 (slow) and -4 (Fast); and slow troponin-I and fast troponin-I, were assessed for their expression levels in lacerated medial gastrocnemius of SD rat after 2-weeks and 12-weeks post-surgery, normalised to lamin A (Fig. 16A). This is done to investigate the functional recovery status of the lacerated skeletal muscle in different

treatment groups with respect to the genes involved in synthesis of contractile proteins at the molecular level. The electrophysiologic study about the functional recovery of the lacerated skeletal muscle is done in another project.

The slow troponin-1 and fast troponin-1 expression levels were up-regulated in all groups at 2-weeks post-laceration compared against the control, but were not significantly different from the control ($p=0.07$). After 12-weeks, both slow troponin-1 and fast troponin-1 were down-regulated to the baseline level of the control in all groups except for DN where the slow troponin-1 expression level was 4.5-fold higher than the control and for RN where has the highest expression level was for fast troponin-I, more than 12-fold greater than the control ($p<0.05$).

The expression level of embryonic myosin heavy chain was significantly up-regulated in PN and NegC at 2-weeks post-laceration compared against the control ($p<0.05$). In DN and RN, the embryonic myosin heavy chain expression level are also up-regulated but are not statistically significant ($p>0.05$). After 12-weeks, embryonic myosin heavy chain was significantly down-regulated in PN and DN, where DN has about 29.2-fold and RN has about 17.3-fold greater than the control respectively ($p<0.05$). All other groups have embryonic myosin heavy chain level higher than the baseline level of the control but are not statistically significant ($p>0.05$).

The expression level of slow myosin heavy chain was significantly down-regulated in NegC at 2-weeks post-laceration compared against the control ($p<0.05$). In other groups, the slow myosin heavy chain expression levels are also down-regulated but are not statistically significant ($p>0.05$). After 12-weeks, slow myosin heavy chain expression level in all groups remained lower than the control except for DN, where DN has about 0.45-fold greater than the other groups ($p<0.05$).

Immunoblotting results (Fig. 16B) showed that slow myosin heavy chain was

significantly up-regulated in PN and DN at 2-weeks post-laceration but not in RN, compared against the control ($p>0.05$). After 12-weeks, slow myosin heavy chain was down-regulated to the baseline level of the control ($p>0.05$). The data showed that the highest mean level of slow myosin heavy chain were present in PN and DN at 2-weeks post-laceration compared with other subgroups ($p>0.05$).

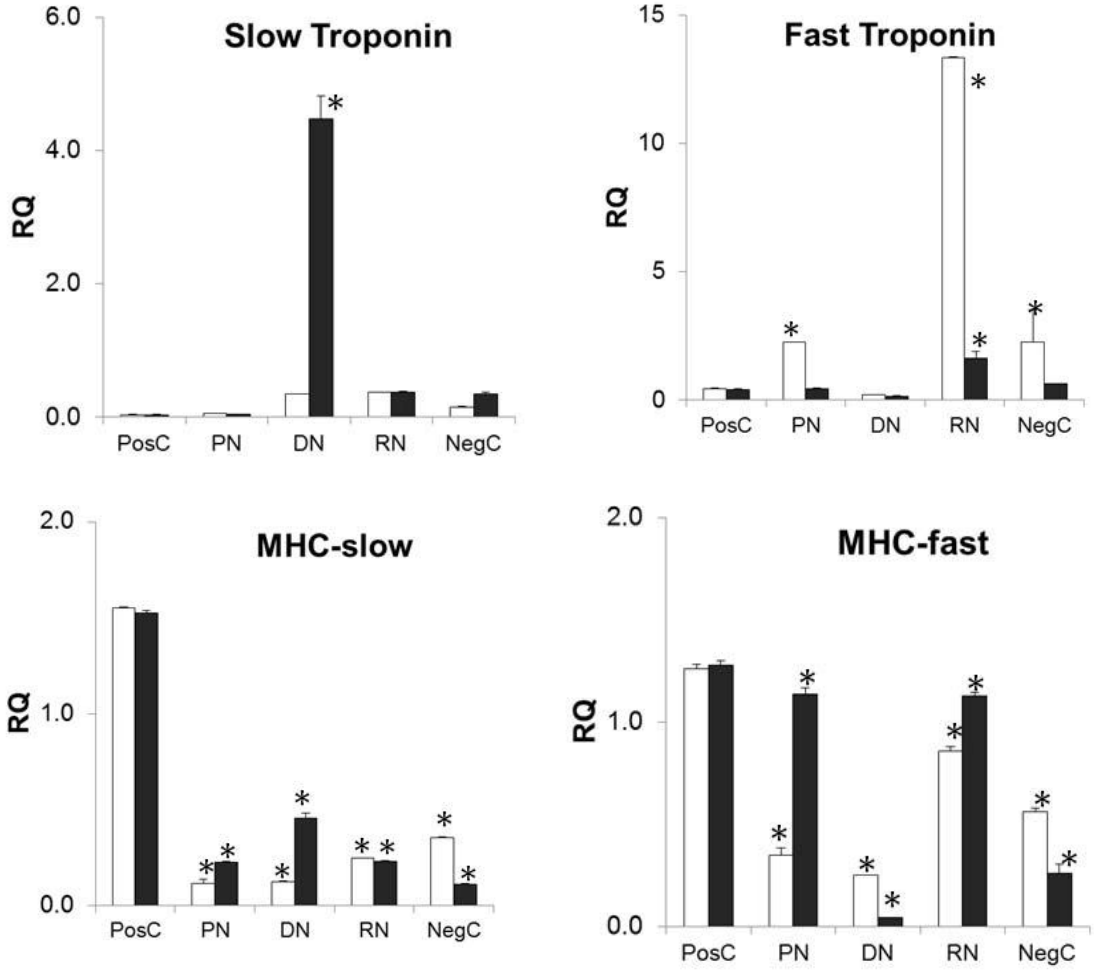

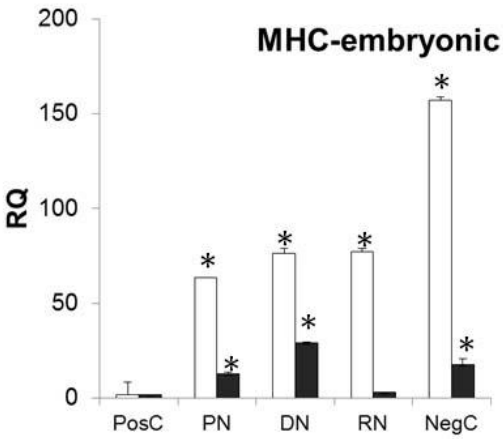

Figure 16A. Fold changes (normalized to Lamin A) of Slow Troponin-I, Fast Troponin-I, Embryonic Myosin Heavy Chain (MHC-embryonic), Slow Myosin Heavy Chain (MHC-slow) and Fast Myosin heavy Chain (MHC_fast). ANOVA and post-hoc tests at 2-weeks (white) and 12-weeks (black) post-repair identified the homogenous sub-sets that were not significantly different (See Appendix 4). Data is expressed as means ± SD of three independent experiments obtained with 3 rats. P-values were calculated by Scheffe's post-hoc test, where $p<0.05$ is considered statistically significant. (* - indicates significant difference ($p<0.05$) to Positive Control, PosC).

The expression level of fast myosin heavy chain was significantly down-regulated in PN, RN and NegC at 2-weeks post-laceration compared against the control ($p<0.05$). PN has about 0.35-fold, RN has 0.85-fold and NegC has about 0.55-fold lower than the control. In DN, the fast myosin heavy chain expression level is also down-regulated but is not statistically significant ($p>0.05$). After 12-weeks, fast myosin heavy chain expression level in all groups increased to the baseline level of the control except for DN. DN has about 0.04-fold lower than the control ($p<0.05$).

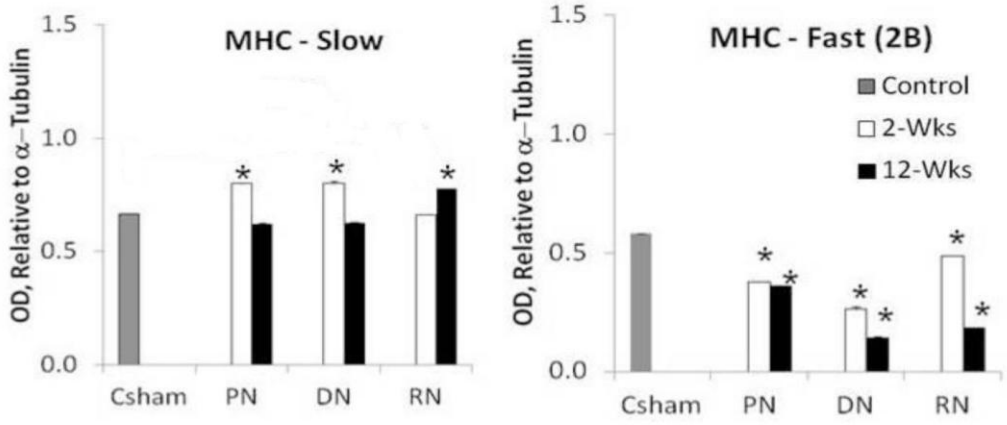

Figure 16B. Optical densitometry quantification of slow (Type 1) and fast (Type 2B) myosin heavy chain protein expression levels normalized to alpha tubulin, using GelPro v4.5 (arbitrary units). Data was obtained from three independent experiments with 3 rats. p-values were calculated by Scheffe's post-hoc test, where $p<0.05$ is considered statistically significant. Non-significant homogenous sub-groups are noted. (* - indicates significant difference ($p<0.05$) to Positive Control, CSham).

Immunoblotting results also showed that fast myosin heavy chain was significantly down-regulated in PN, DN and RN at 2-weeks post-laceration compared against the control ($p<0.05$). After 12-weeks, fast myosin heavy chain was further down-regulated to lower than the control ($p<0.05$). The highest mean level of fast myosin heavy chain was present in RN at 2-weeks post-laceration compared with other subgroups ($p<0.05$).

6.2.5.1- Pro-Slow myosin heavy chain and Slow Troponin-I markers, Anti-Fast myosin heavy chain and Fast Troponin-I markers

Myogenin, PGC-1a, Sirt1, Shh, NT4, CNTF, Mef2a, myostatin

6.2.5.2- Anti-Slow myosin heavy chain and Slow Troponin-I markers, Pro-Fast myosin heavy chain and Fast Troponin-I markers

myoD, IGF1, CNTF

Of the myosin heavy chain isoform regulators for myosin heavy chain proteins, myoD (for fast MHC) and myogenin (for slow MHC) are also myogenesis markers (Figs 13 and 14B); NT4 (for slow MHC), CNTF (for fast MHC) and IGF-1 (for embryonic MHC) are

also anti-atrophy markers as well as pro-re-innervation markers (Figs. 12A and 12B). PGC-1a and Sirt-1 (for slow MHC) are also anti-atrophy (Fig. 12A) as well as mitochondrial biogenesis markers. Myostatin promotes the slow muscle fiber expression after denervation (Fig15B).

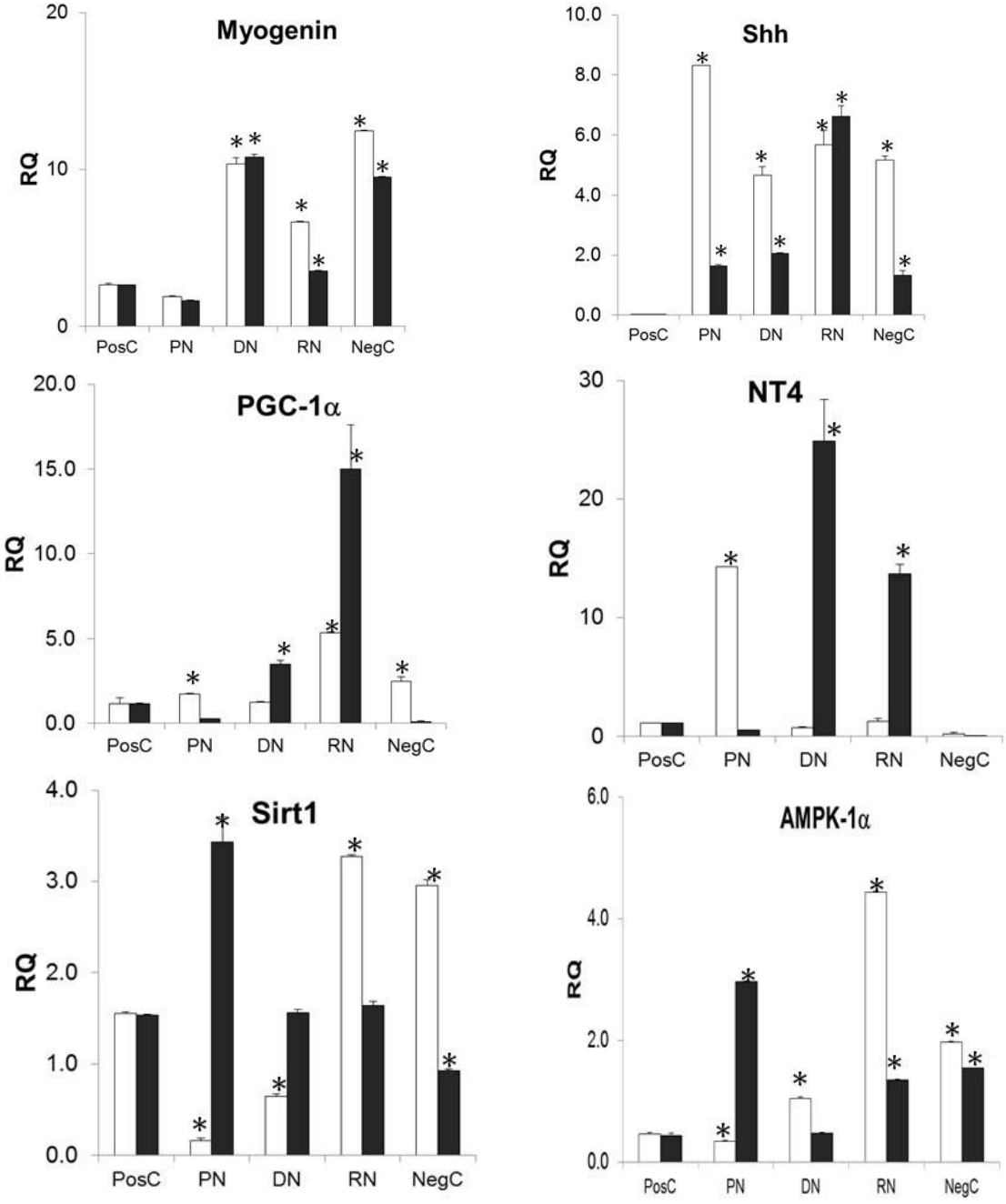

Figure 17. Fold changes (normalized to Lamin A) of myogenin, PGC-1a, NT4, Sonic Hedgehog, Sirt1 and AMPK-1a. ANOVA and post-hoc tests at 2-weeks (white) and 12-weeks (black) post-repair identified the homogenous sub-sets that were not significantly different (See Appendix 4). Data is expressed as means ± SD of three independent experiments obtained with 3 rats. P-values were calculated by Scheffe's post-hoc test, where

$p<0.05$ is considered statistically significant. (* - indicates significant difference ($p<0.05$) to Positive Control, PosC).

6.2.5.3- Anti-fast and anti-slow myosin heavy chain, and anti-fast and slow troponin-I markers, TGFb2, atrogin-1, MuRF-1, complement-3

TGFb2 is described in section 6.2.2.1 (Fig 8A), while atrogin-1 and MuRF-1 are described in section 6.2.3 (Fig10), complement-3 in section 6.2.3 (Fig18B).

6.2.5.4- Correlations between markers

In PN, the expression of embryonic myosin heavy chain was decreased over 12-weeks to 12.83-fold higher than control. This was associated with an increase in CNTF (1.93-fold, $p<0.05$), and a decrease in HGF (0.74-fold, $p<0.05$), Shh (1.64-fold, $p<0.05$) and IGF1 (0.015-fold, $p<0.05$). The expression of fast myosin heavy chain (1.13-fold) was increased but the fast troponin-I (0.45-fold) was reduced over 12-weeks. It has the highest fast myosin heavy chain expression level after 12-weeks. This was associated with an increase in Sirt1 (3.43-fold, $p<0.05$), MuRF1 (0.36-fold, $p<0.05$) and CNTF (1.93-fold, $p<0.05$). A decrease in atrogin-1 (0.32-fold, $p<0.05$), Shh (1.64-fold, $p<0.05$) and TGFb2 (0.018-fold, $p<0.05$) is observed. The expression of slow myosin heavy chain (0.22-fold) was increased but the slow troponin-I (0.042-fold) was decreased over 12-weeks. It has the lowest slow troponin-I expression level after 12-weeks. This was associated with an increase in Sirt1 (3.43-fold, $p<0.05$), MuRF1 (0.36-fold, $p<0.05$), CNTF (1.93-fold, $p<0.05$), and decrease in atrogin-1 (0.32-fold, $p<0.05$), IGF1(0.015-fold, $p<0.05$), TGFb2 (0.018-fold, $p<0.05$), Shh (1.64-fold, $p<0.05$).

In DN, the expression of embryonic myosin heavy chain was decreased over 12-weeks to 29.44-fold higher than control. It has the highest embryonic myosin heavy chain expression level after 12-weeks. This was associated with an increase in CNTF (1.34-fold, $p<0.05$). A corresponding decrease in follistatin (8.13-fold, $p<0.05$), HGF (0.55-fold,

$p<0.05$), GDNF (17.78-fold, $p<0.05$), and IGF1 (0.15-fold, $p<0.05$) is observed.

The expression of fast myosin heavy chain (1.13-fold) and fast troponin-I (0.45-fold) were decreased over 12-weeks. It has the lowest fast myosin heavy chain and fast troponin-I expression levels after 12-weeks. This was associated with an increase in atrogin-1 (3.76-fold, $p<0.05$), MuRF1 (3.44-fold, $p<0.05$), myostatin (0.85-fold, $p<0.05$), NT4 (24.86-fold, $p<0.05$), CNTF (1.34-fold, $p<0.05$), myoD (4.49-fold, $p<0.05$), and a decrease in complement-3 (6.66-fold, $p<0.05$) and TGFb2 (0.21-fold, $p<0.05$). The expression of slow myosin heavy chain (0.22-fold) and slow troponin-I (0.042-fold) were increased over 12-weeks. It has the highest slow myosin heavy chain and slow troponin-I expression level after 12-weeks. This was associated with an increase in atrogin-1 (3.76-fold, $p<0.05$), MuRF1 (3.44-fold, $p<0.05$), myostatin (0.85-fold, $p<0.05$), NT4 (24.86-fold, $p<0.05$), CNTF (1.34-fold, $p<0.05$), myoD (4.49-fold, $p<0.05$), and a decrease in complement-3 (6.66-fold, $p<0.05$), IGF1 (0.15-fold, $p<0.05$), TGFb2 (0.21-fold, $p<0.05$).

In RN, the expression of embryonic myosin heavy chain was decreased over 12-weeks to 3.37-fold higher than control. It has the lowest embryonic myosin heavy chain expression level after 12-weeks. This was associated with an increase in HGF (1.73-fold, $p<0.05$) and Shh (6.60-fold, $p<0.05$). A corresponding decrease in myogenin (3.54-fold, $p<0.05$), CNTF (0.48-fold, $p<0.05$), follistatin (1.38-fold, $p<0.05$), IGF1 (0.10-fold, $p<0.05$) is observed. The expression of fast myosin heavy chain (1.12-fold) was increased but fast troponin-I (1.63-fold) was decreased over 12-weeks. It has the highest fast troponin-I expression level after 12-weeks. This was associated with an increase in Shh (6.60-fold, $p<0.05$), and a decrease in TGFb2 (0.022-fold, $p<0.05$), atrogin-1 (0.87-fold, $p<0.05$), MuRF1 (1.27-fold, $p<0.05$), myogenin (3.54-fold, $p<0.05$), myostatin (0.56-fold, $p<0.05$), complement-3 (8.41-fold, $p<0.05$), CNTF (0.48-fold, $p<0.05$). The expression of slow myosin heavy chain (0.22-fold) and slow troponin-I (0.042-fold) were decreased over 12-

weeks. This was associated with an increase in PGC-1a (14.99-fold, $p<0.05$), Shh (6.60-fold, $p<0.05$), myostatin (0.56-fold, $p<0.05$), and a decrease in CNTF (0.48-fold, $p<0.05$), atrogin-1 (0.87-fold, $p<0.05$), MuRF1 (1.27-fold, $p<0.05$), myogenin (3.54-fold, $p<0.05$), complement-3 (8.41-fold, $p<0.05$).

Table 8A Correlation between fast myosin heavy chain and other selected fiber transformation markers with respect to overall fold change in gene expression in all groups

Gene	**PN**	**DN**	**RN**	**NegC**	**r**
Atrogin-1	-0.19$^{*,\#}$	2.12$^{*,\#}$	-0.57$^{\#}$	-1.17*	-0.7585
MuRF-1	0.10	2.34$^{*,\#}$	-0.90$^{*\#}$	-1.70$^{*,\#}$	-0.6068
Myogenin	-0.25	0.45	-3.11$^{*\#}$	-2.98$^{*,\#}$	-0.7349
TGFb2	-0.24*	-0.22$^{*,\#}$	-0.01	0.02	-0.6738
NT-4	-13.71	24.10$^{\#}$	12.43	-0.18	-0.4297
CNTF	1.82$^{*,\#}$	1.09$^{*,\#}$	-1.32*	0.29$^{\#}$	0.5359
Sonic Hedgehog	-6.68*	-2.62	0.95$^{\#}$	-3.83	-0.3502
Complement-3	-1.12	-4.73$^{\#}$	-3.88$^{\#}$	-18.99*	-0.3773
Mef-2a	0.28	1.58	0.01	-0.55	-0.3777
Myostatin	-0.06	0.71$^{\#}$	0.12$^{*,\#}$	-0.18$^{*,\#}$	-0.4796
Note: ***** $p<0.05$ at 2-weeks**, #** $p<0.05$ at 12-weeks					

Table 8B Correlation between slow myosin heavy chain and other selected fiber transformation markers with respect to overall fold change in gene expression in all groups

Gene	**PN**	**DN**	**RN**	**NegC**	**r**
Atrogin-1	-0.19$^{*,\#}$	2.12$^{*,\#}$	-0.57$^{\#}$	-1.17*	-0.4102
MuRF-1	0.10	2.34$^{*,\#}$	-0.90$^{*\#}$	-1.70$^{*,\#}$	-0.4108
Myogenin	-0.25	0.45	-3.11$^{*\#}$	-2.98$^{*,\#}$	0.9229
TGFb2	-0.24*	-0.22$^{*,\#}$	-0.01	0.02	-0.3466
IGF-1	-0.37$^{*\#}$	-0.08*	-0.22*	-3.58*	-0.3741
NT-4	-13.71	24.10$^{\#}$	12.43	-0.18	0.4504
CNTF	1.82$^{*,\#}$	1.09$^{*,\#}$	-1.32*	0.29$^{\#}$	0.3479
Sonic Hedgehog	-6.68*	-2.62	0.95$^{\#}$	-3.83	0.4912
PGC-1a	-1.48	2.24	9.64$^{\#}$	-2.35	0.3872
Complement-3	-1.12	-4.73$^{\#}$	-3.88$^{\#}$	-18.99*	-0.438
Mef-2a	0.28	1.58	0.01	-0.55	0.4309
Note: ***** $p<0.05$ at 2-weeks, # $p<0.05$ at 12-weeks					

Table 8C Correlation between embryonic myosin heavy chain and other selected fiber transformation markers with respect to overall fold change in gene expression in all groups

Gene	PN	DN	RN	NegC	r
Myogenin	-0.25	0.45	-3.11*#	-2.98*,#	0.6373
Follistatin	-3.15	-10.32*,#	-5.46*	-3.00	0.501
HGF	-6.81*	-1.78*	0.50*,#	-2.56*	0.535
IGF-1	-0.37*#	-0.08*	-0.22*	-3.58*	0.8378
GDNF	-2.13	-27.68*	-7.51	-7.00	0.5478
CNTF	1.82*,#	1.09*,#	-1.32*	0.29#	-0.4195
Sonic Hedgehog	-6.68*	-2.62	0.95#	-3.83	0.5566
Myostatin	-0.06	0.71#	0.12*,#	-0.18*,#	0.3958
Note: ***** p<0.05 at 2-weeks**, #** p<0.05 at 12-weeks					

Table 8D Correlation between fast troponin-I and other selected fiber transformation markers with respect to overall fold change in gene expression in all groups

Gene	PN	DN	RN	NegC	r
Sonic Hedgehog	-6.68*	-2.62	0.95#	-3.83	0.4169
Sirt-1	3.28*	0.92	-1.63	-2.03	0.388
Note: ***** p<0.05 at 2-weeks, # p<0.05 at 12-weeks					

Table 8E Correlation between slow troponin-I and other selected fiber transformation markers with respect to overall fold change in gene expression in all groups

Gene	PN	DN	RN	NegC	r
Myogenin	-0.25	0.45	-3.11*#	-2.98*,#	0.4508
NT-4	-13.71	24.10#	12.43	-0.18	0.7736
myoD	1.91	3.46#	0.75	0.30	0.8113
Mef-2a	0.28	1.58	0.01	-0.55	0.4847
Myostatin	-0.06	0.71#	0.12*,#	-0.18*,#	0.4988
Note: ***** p<0.05 at 2-weeks, # p<0.05 at 12-weeks					

6.2.6- Intra-Muscular Nerve Regeneration marker, GAP43

The expression level of GAP-43 and HN-1 (Fig. 18) were up-regulated in all 4 groups at 2-weeks post-laceration compared against the control (p>0.05). NegC has the highest GAP-43 and HN-1 about 3.3-fold and 5.5-fold, greater than the level of the control, respectively.

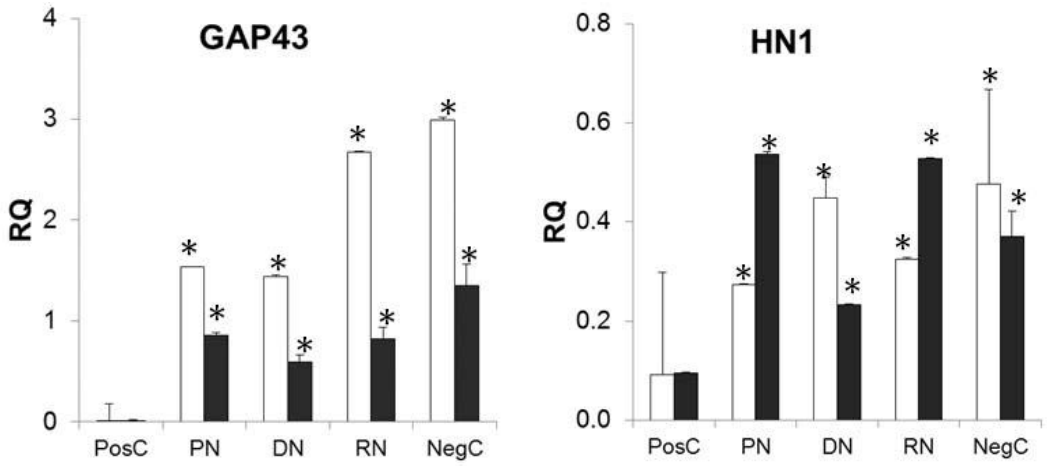

Figure 18A. Fold change (normalized to Lamin A) of GAP43 and HN-1. ANOVA and post-hoc tests at 2-weeks (white) and 12-weeks (black) post-repair identified the homogenous sub-sets that were not significantly different (See Appendix 4). Data is expressed as means ± SD of three independent experiments obtained with 3 rats (n=3); p-values were calculated by Scheffe's post-hoc test, where $p<0.05$ is considered statistically significant. (* - indicates significant difference ($p<0.05$) to Positive Control, PosC).

After 12-weeks, GAP-43 was down-regulate in all groups, but the expression level remained higher than the control ($p>0.05$).

6.2.6.1- Pro-axonal regeneration markers

NT4, GDNF, CNTF, IGF1, HGF, EGF, Galectin-1, Decorin, HN1, Follistatin, Shh

The pro-axonal regeneration markers were grouped into the classical and non-classical neurotrophic factors. The classical neurotrophic factors including NT4, GDNF, CNTF are also anti-atrophy markers, pro-myogenesis markers, as well as myosin heavy chain isoform regulators (Fig. 12B), while the non-classical neurotrophic markers have multiple functions either as anti-fibrosis markers (decorin and follistatin, Fig. 9; EGF Fig 8A), anti-atrophy markers (decorin, follistatin, IGF-1 Fig 12A), pro-myogenesis markers (decorin, follistatin, galectin-1, HGF, IGF-1, Fig 15A) or pro-fibrosis markers (galectin-1, Figs 8A and 8B; Sonic hedgehog Fig 17). All have been demonstrated earlier.

The expression level of HN1 (Fig. 18) was up-regulated in all 4 groups at 2-weeks post-laceration compared against the control ($p>0.05$). NegC has the highest HN1

expression level (5.5-fold, greater than the level of the control). After 12-weeks, the HN1 expression in all groups remained higher than the control ($p>0.05$). Interestingly, histology did not show the presence of any nerve sprouts in PN, DN, RN and NegC.

6.2.6.2- Anti-axonal regeneration markers

Collagen-1α, Aggrecan, TGFβ2, Complement-3, CTGF

The anti-axonal regeneration markers were pro-fibrosis markers as demonstrated earlier (Fig 7A – collagen-1α and aggregan, Fig 8A for TGFβ2 and Fig 8B for CTGF). Complement-3 is an anti-axonal regeneration marker because it destroys newly regenerating axons (Fig.18B).

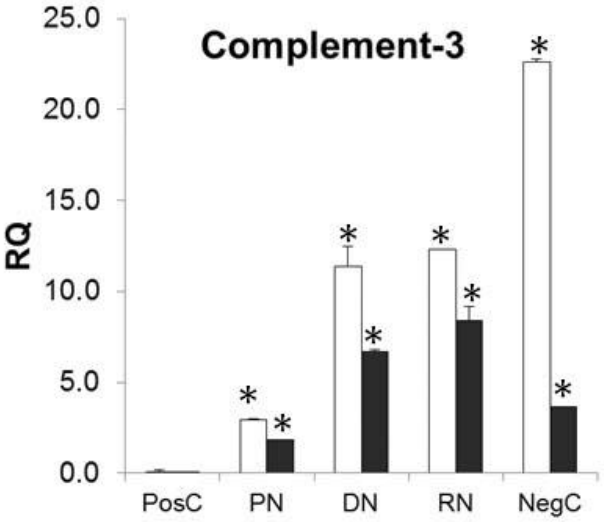

Figure 18B. Fold change (normalized to Lamin A) of Complement-3. ANOVA and post-hoc tests at 2-weeks (white) and 12-weeks (black) post-repair identified the homogenous sub-sets that were not significantly different (See Appendix 4). Data is expressed as means ± SD of three independent experiments obtained with 3 rats (n=3); p-values were calculated by Scheffe's post-hoc test, where $p<0.05$ is considered statistically significant. (* - indicates significant difference ($p<0.05$) to Positive Control, PosC).

6.2.6.3- Correlations between markers

In PN, the expression of GAP43 was 0.85-fold higher than control. It has the highest GAP43 expression level after 12-weeks. This was associated with an increase in pro-axonal regeneration factors EGF (3.24-fold, $p<0.05$), decorin (11.28-fold, $p<0.05$), CNTF (1.93-

fold, p<0.05) and HN1 (0.53-fold, p>0.05) expression respectively. A corresponding decrease in TGFb2 (0.018-fold, p<0.05), aggrecan (0.24-fold, p<0.05), IGF1 (0.015-fold, p<0.05), HGF (0.74-fold, p<0.05), galectin-1 (0.11-fold, p<0.05) and Shh (1.64-fold, p<0.05) was observed.

In DN, the expression of GAP43 was decreased over 12-weeks to 0.59-fold higher than control. It has the lowest GAP43 expression level after 12-weeks. This was associated with an increase in pro-axonal regeneration factors EGF (2.44-fold, p<0.05), NT4 (24.86-fold, p<0.05) and CNTF (1.34-fold, p<0.05), CTGF (1.62-fold, p<0.05). A corresponding decrease in TGFb2 (0.21-fold, p<0.05), complement-3 (6.66-fold, p<0.05), aggrecan (7.69-fold, p<0.05), IGF1 (0.15-fold, p<0.05), HGF (0.55-fold, p<0.05), GDNF (17.78-fold, p<0.05) and follistatin (8.13-fold, p<0.05) is seen.

In RN, the expression of GAP43 was decreased over 12-weeks to 0.82-fold higher than control. This was associated with an increase in pro-axonal regeneration factors HGF (1.73-fold, p<0.05), Shh (6.61-fold, p<0.05), and increase in CTGF (1.79-fold, p<0.05) and PGC-1a (14.99-fold, p<0.05). A corresponding decrease in complement-3 (8.41-fold, p<0.05), aggrecan (2.15-fold, p<0.05), IGF1 (0.11-fold, p<0.05), CNTF (0.48-fold, p<0.05), follistatin (1.38-fold, p<0.05) is observed.

Table 9 Correlation between GAP43 and other selected intr-muscular nerve regeneration markers with respect to overall fold change in gene expression in all groups

Gene	**PN**	**DN**	**RN**	**NegC**	**r**
Follistatin	-3.15	-10.32$^{*,\#}$	-5.46*	-3.00	0.3563
HGF	-6.81*	-1.78*	0.50$^{*,\#}$	-2.56*	0.4788
IGF-1	-0.37$^{*\#}$	-0.08*	-0.22*	-3.58*	0.6643
GDNF	-2.13	-27.68*	-7.51	-7.00	0.4441
Sonic Hedgehog	-6.68*	-2.62	0.95$^{\#}$	-3.83	0.6429
Galectin-1	-0.43*	-0.18	-0.05	-0.20	0.6718
HN-1	0.26	-0.21	0.20	-0.11	0.4349
Note: ***** p<0.05 at 2-weeks, **#** p<0.05 at 12-weeks					

6.2.7- Signaling Pathway Markers:

(a) **MAPK kinase pathway**: p38, Erk1, Erk2
(b) **SMAD pathway**: SMAD2, SMAD3

Optical densitometry quantification showed that the highest mean level of phospho-p38 were present in PN at 2-weeks post-laceration compared with the control ($p<0.05$). Both p38 and phospho-p38 protein expression level normalized to total p38 (Fig. 21) showed that the highest mean level of phospho-p38 were present in RN at 2-weeks post-laceration compared with the control ($p<0.05$). Immunoblotting results also showed that Erk1,2 and phospho-Erk1,2 (Fig 19) and SMAD2, 3 and phospho- SMAD2, 3 (Fig. 20) were significantly up-regulated in all groups at 2-weeks post-laceration compared against the control ($p<0.05$). After 12-weeks, Erk1,2 and phospho-Erk1,2 together with SMAD2, 3 and phospho- SMAD2,3 expression level in all groups remained higher than the control ($p<0.05$).

Optical densitometry quantification of Erk1,2 and phospho-Erk1,2 protein expression level normalized to alpha tubulin (Fig 19) showed that the highest mean level of phospho-Erk1,2 were present in DN at 2-weeks post-laceration compared with the control ($p<0.05$). The highest mean level of phospho-SMAD2 was present in DN at 12-weeks post-laceration compared with the control ($p<0.05$) while the highest mean level of phospho-SMAD3 was present in PN at 2-weeks post-laceration compared with the control ($p<0.05$).

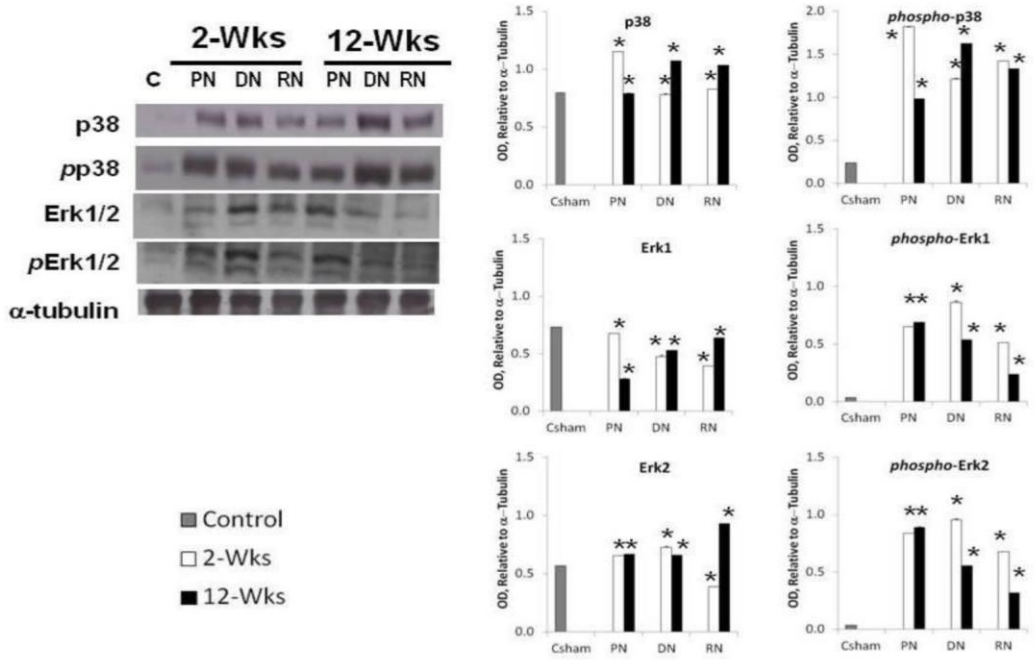

Figure 19. Western blot analysis of p38, phospho-p38, Erk-1, Erk-2 and phospho-Erk-1 and Erk-2 (with alpha tubulin as the loading control). Optical densitometry quantification was obtained from three independent experiments with 3 rats at 2 time points (white bars - 2weeks; black bars – 12weeks). P-values were calculated by Scheffe's post-hoc test, where $p<0.05$ is considered statistically significant. (* - indicates significant difference ($p<0.05$) to Positive Control, PosC).

Erk1,2 and phospho-Erk1,2 protein expression level normalized to total Erk1 and 2 (Fig 21) showed that the highest mean level of phospho-Erk1,2 were present in PN at 2-weeks post-laceration compared with the control ($p<0.05$). For SMAD2, 3 and phospho-SMAD2,3 protein expression level normalized to total SMAD2 and 3 (Fig. 21), the highest mean level of phospho-SMAD2 was present in DN at 2-weeks post-laceration compared with the control ($p<0.05$). The highest mean level of phospho-SMAD3 was present in PN at 2-weeks post-laceration compared with the control ($p<0.05$).

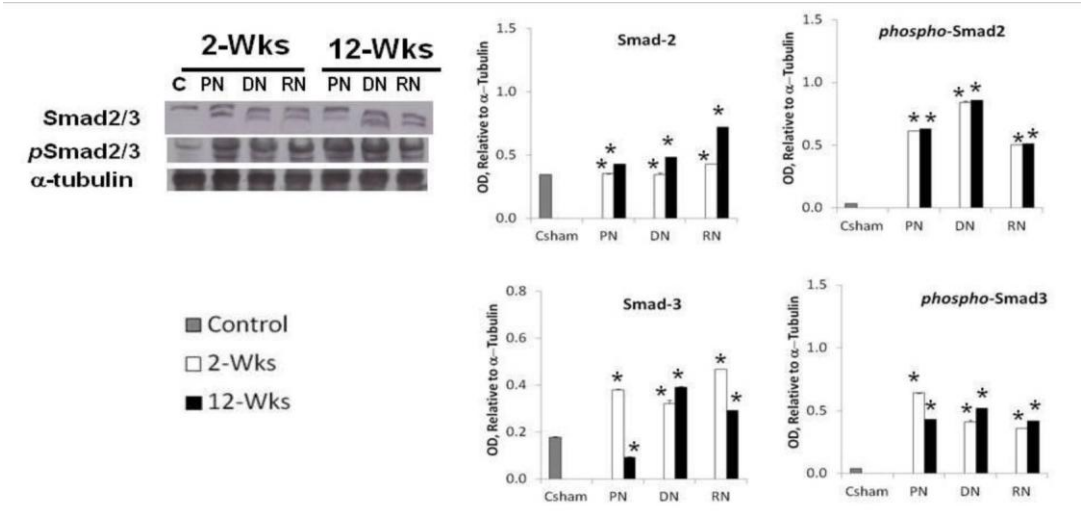

Figure 20. Western blot analysis of SMAD2, SMAD3, phospho-SMAD2 and phospho-SMAD3 (with alpha tubulin as the loading control). Optical densitometry quantification was obtained from three independent experiments with 3 rats at 2 time points (white bars - 2weeks; black bars – 12weeks). P-values were calculated by Scheffe's post-hoc test, where $p<0.05$ is considered statistically significant. (* - indicates significant difference ($p<0.05$) to Positive Control, PosC).

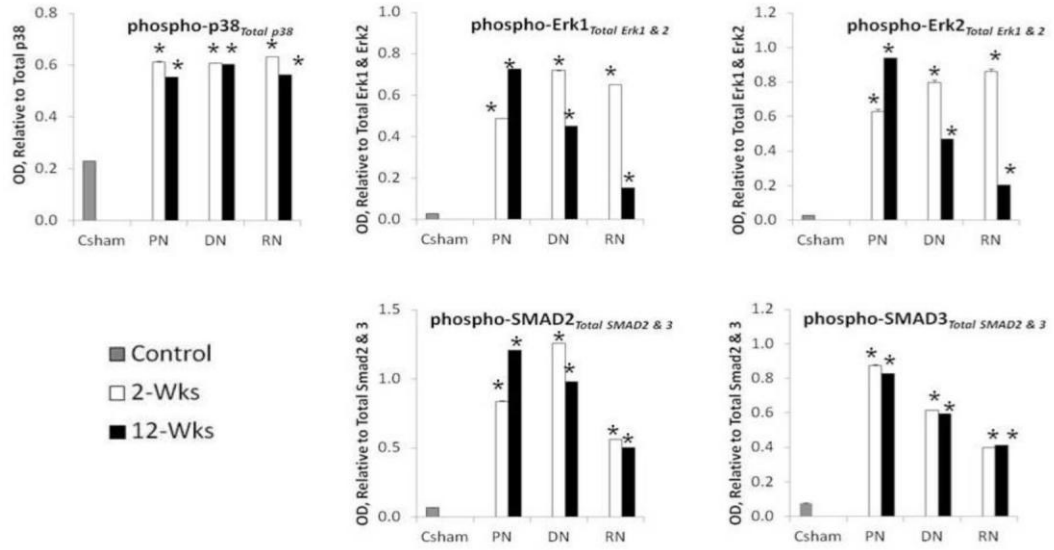

Figure 21. Western blot analysis of phospho-p38 relative to total p38, phospho-Erk1 and phospho-Erk2 relative to total Erk, phospho-SMAD2 and phospho-SMAD3 relative to total SMAD2/3 (with alpha tubulin as the loading control). Optical densitometry quantification was obtained from three independent experiments with 3 rats at 2 time points (white bars - 2weeks; black bars – 12weeks). P-values were calculated by Scheffe's post-hoc test, where $p<0.05$ is considered statistically significant. (* - indicates significant difference to Positive Control, PosC).

7. DISCUSSION

We demonstrated that the temporal gene expression of various neurotrophic factors, anti-atrophic factors and pro-fibrotic factors at 2- and 12-weeks after repair were indeed dictated by the type of denervation injury in surgically repaired lacerated skeletal muscles.

7.1 – Fibrosis

The response to muscle laceration is the development of fibrosis during repair. Fibrosis is a reactive process involving the activation of fibroblasts, endothelial cells and pericytes, leading to excessive collagen and chondroitin sulphate proteoglycan deposition, chiefly type 1 collagen and aggrecan. Collagen-1 and aggrecan is deposited by fibroblasts during repair for wound contraction. The resultant healed skeletal muscle functions well in crude terms representing a contractile structure bridged by a scar. It is not however inherently functional as a contractile structure under neural control.

7.1.1- Preserved Intra-muscular Nerve Model

PN has the lowest aggrecan and second lowest collagen expression level after 12-weeks. This is due to the following factors:

1) Down-regulation of myostatin, TGFb2, CTGF, R-spondin-1, galectin-1, HGF, IGF1 and Shh expression: Significant drop in expression of these proteins lead to reduction in expression of collagen-1 and aggrecan through both Erk1/2 and SMAD2/3 pathways in fibroblasts.

2) Up-regulation of decorin expression: High decorin in PN induces quiescence in fibroblasts via up-regulation of p21. In addition, decorin core protein fragment Leu155-Val260 binds to TGFb and prevents it from binding to the TGFb receptors. Decorin also binds to myostatin with its core protein, suppressing its activity. Similarly, decorin binds to CTGF using its leucine rich repeat residues 10-12 (Vial C et al, 2011). This prevents CTGF from binding to its receptor. All this leads to inhibition of SMAD phosphorylation and

reduction of collagen-1 gene transcription. High decorin expression in PN is induced by TGFb2 via CRE-like element in the P1 promoter of the gene, by CTGF (Vial C et al, 2011), and it is under neural control.

3) Up-regulation of AMPK expression: AMPK disrupts SMAD2/3 association with p300 and promotes proteosomal degradation of p300, thereby inhibiting TGFb-induced SMAD3 phosphorylation and nuclear translocation, leading to reduced aggrecan and collagen production. AMPK is activated by high TAK1 (TGFb activated kinase-1).

4) Up-regulation of EGF expression: EGF can reduce fibrosis via TGIF (TGFb-inducible factor). Activation of the Ras/MAPK pathway by EGF leads to the phosphorylation of the TGIF to inhibit Smads. This suppresses aggrecan and collagen-1 transcription further in PN. EGF also up-regulates MMP1 synthesis to degrade collagen at lesion site.

5) Up-regulation of CNTF expression: CNTF increased acetylcholinesterase expression (Boudrea-Lariviere et al, 1996) to break down excessive acetylcholine released from nerve stumps, so reducing the activation of fibroblasts in vicinity.

6) Up-regulation of Sirt1 expression: Sirt1 deacetylates the p65 subunit of the NFkB complex at lysine 310, and inhibits the NF-κB signaling to activate the synthesis of collagen-1a in fibroblasts and immune cells

7.1.2- Denervated Intra-muscular Nerve Model

DN has the highest collagen and aggrecan levels at 15.76-fold and 7.69-fold more than the control respectively. This is due to the following reasons:

1) Up-regulation of NT4 and GDNF: NT4 can bind to Trk receptors expressed by fibroblasts, stimulating them to proliferate and trans-differentiate into active myofibroblasts, leading to high collagen production via MAPK/Erk pathway (Palazzo E et al, 2012); fibroblasts also express RET receptors which are activated by GDNF binding, leading to increased in collagen-1a and aggrecan production

2) Up-regulation of TGFb2: Pulsatile release of TGFβ2 (Yang et al, 1999) induces the myofibroblast phenotype permanently (Hizz B et al, 2003). The continued maintenance of myofibroblast is due to the epigenetic memory in fibroblasts that have been exposed to TGFb (Chen et al, 2009), resulting in constitutive collagen-1 gene transcription. High TGFb2 expression in DN also attracts phagocytes and monocytes to remove dead cells and initiate muscle fibre regeneration (Ranges et al, 1987; Wahl et al, 1987, Wahl et al, 1988; Adams D et al, 1991; Reibman J et al, 1991). In addition, TGFb2 furthers up-regulates the expression of myostatin by reducing the furin expression in myoblasts, and via Foxo and SMAD2 signaling to promote fibrosis.

3) Up-regulation of CTGF and TGFb2: CTGF protects aggrecan from aggrecanase degradation by binding to its globular domains in the extracellular matrix. This leads to accumulation of aggrecan in skeletal muscle, making the muscle very stiff and rigid and losing its isometric contractile function over time post-laceration. Also, both high TGFb2 and CTGF expression in DN induce the synthesis of collagen-1 and aggrecan through two common Erk1/2 and SMAD2/3 pathways. TGFb2 also induces fibrosis via up-regulation of scleraxis in fibroblasts (Mendias CL et al, 2012). TGFb can further up-regulate the CTGF expression via the TGFb-inducible element in the CTGF-promoter region (Grotendorst, 1997). CTGF expression is upregulated by high mechanical stress induced from muscle laceration via p38 binding to the stretch responsive element, GAGACC (Schild C et al, 2002; Blom IE et al, 2002).

4) Insufficient follistatin expression: Follistatin exerts significant anti-fibrosis effect in DN by sequestering myostatin and TGFb from its receptor and inhibits SMAD signaling. Follistatin expression is under neural control (Armand AS et al, 2003) and it is a downstream target of Wnt signaling. Wnt signaling is greatly reduced in denervated muscles by myostatin, CTGF and short Frizzled proteins (sFRPs). However the high follistatin

expression level in DN is insufficient to reduce the fibrosis-induced by myostatin, CTGF and TGFb2 because other fibrosis-inducing pathways are concurrently activated such as the angiotensin, NFkB and PDGF-α pathways.

5) Up-regulation of myostatin: Stress induced from muscle laceration is transmitted via titin cap and p38 to increase myostatin expression. High myostatin level in damaged muscle can also stimulate fibroblasts to proliferate and differentiate to myofibroblast through SMAD 3 signaling. Thus, the vicious cycle of TGFb2 and myostatin constitutively inducing the myofibroblasts to produce excessive collagen and proteoglycan at lesion site continues after 12-weeks in DN.

6) Leakage of acetylcholine from cut nerve into ECM: The fibroblasts in the endomysium can also synthesize collagen upon stimulation by acetylcholine release from crushed nerve. Expression of choline acetyl tranferase is up-regulated in nerve stumps by NT4 and GDNF but not CNTF, so excess acetylcholine is spontaneously released from nerve stumps; which then constantly activate the fibroblasts to synthesise collagen-1a at lesion site

7) Glutamine release into ECM: Glutamine released from muscle proteolysis can also stimulate the collagen expression in fibroblasts. This is both pyrroline-5-carboxylate-dependent and transport system L-dependent;

8) Leucine release into ECM: Leucine released from protein degradation stimulates HGF production in fibroblasts. This leads to more fibrosis in DN because HGF increases collagen synthesis in fibroblasts through MEKl-mediated phosphorylation on the SSXS motif of Smad2, resulting in its nuclear accumulation and transactivating activity.

9) Down-regulation of decorin expression: Drop in decorin levels increased the bioavailability of CTGF and TGFb2 binding to respective receptors and activation of the downstream SMAD signaling to increase collagen-1a and aggrecan synthesis in fibroblasts.

10) Down-regulation of EGF expression: Reduced levels of EGF lead to the activation of

Smads signaling which then increase aggrecan and collagen-1 synthesis in fibroblasts.

11) Up-regulation of R-spondin-1, Galectin-1, HGF, IGF1 and Shh expression: Fibroblasts in DN proliferate faster than myoblasts and so they produced more collagen-1a and aggrecan due to high levels of myostatin, TGFb2 and CTGF as well as R-spondin-1, galectin-1, HGF, IGF1 and Shh. Galectin-1, a beta galactoside binding protein, binds to cell surface glycoconjugates of the fibroblasts, stimulating them to synthesize collagen-1 via p38 and Erk signaling. IGF1 increases aggrecan transcription in fibroblasts via PI3K signaling while Shh can induce aggrecan synthesis through Gli-mediated phospho-activation of SMAD2 and 3. Vimentin stabilizes the collagen-1a mRNA before it is exported to the Golgi and ER. HGF can also increase collagen synthesis in fibroblasts through MEKl-mediated phosphorylation on the SSXS motif of Smad2, results in its nuclear translocation and transactivating activity. R-spondin-1, heparin-binding protein, binds to the LRP5/6 co-receptor and synergises with the Wnt3a to fibroblast proliferation.

12) Down-regulation of AMPK expression: At low AMPK levels, SMAD2/3 binds to p300 and promotes TGFb-induced SMAD3 phosphorylation and nuclear translocation, leading to more aggrecan and collagen production in fibroblasts.

7.1.3- Re-innervated Intra-muscular Nerve Model

RN has the lowest collagen (0.13-fold) and second lowest aggrecan (2.15-fold) levels compared to the control. This is due to the following reasons:

1) Up-regulation of PGC-1a expression: PGC-1a is a co-activator for PPAR-alpha and gamma. Upon ligand binding, PPAR heterodimerizes with retinoid X receptor and prevents the phosphorylated Smads from undergoing nuclear translocation, thereby intercepting TGFb–mediated signal transduction. In glomerular mesangial cells, PPARg agonist activated signaling leads to an upregulation of the Smad transcriptional co-repressor TGIF. Accumulated TGIF then binds to activated Smads and sequesters TGFb/Smad-mediated

gene transcription. Another mechanism of reducing muscle fibrosis mediated by PGC-1a is to inhibit myostatin activity via Gasp-1. Gasp-1 binds to myostatin through its cysteine repeat domains and inhibits its functions. PGC-1a expression is greatly increased in RN because the high stress induced from laceration activates the p38, which then phosphorylates and stabilizes the PGC-1a protein.

2) Up-regulation of follistatin expression: Follistatin sequesters myostatin and TGFb from the respective receptors and inhibits SMAD signaling in fibroblasts.

3) Up-regulation of AMPK expression: AMPK disrupts SMAD2/3 association with p300 and promotes proteosomal degradation of p300, thereby inhibiting TGFb-induced SMAD3 phosphorylation and nuclear translocation, leading to reduced aggrecan and collagen production.

4) Up-regulation of CNTF expression: CNTF increased the acetylcholinesterase expression (Boudrea-Lariviere et al, 1996) to break down excessive acetylcholine released from nerve stumps, so reducing the activation of fibroblasts in vicinity.

5) Down-regulation of CTGF, myostatin, HGF, Shh, IGF1 and R-spondin-1 expression: Reduction in expression of these proteins decreased collagen-1 and aggrecan production through both Erk1/2 and SMAD2/3 pathways in fibroblasts.

Overall, RN has the lowest fibrosis status because it can inhibit initiation of gene transcription of pro-fibrosis factors via PGC-1a which is faster and more specific than the inhibitory binding effect between decorin and the pro-fibrosis factors to reduce their availability to respective receptors.

7.1.4- Hypothesis Support

Fibrosis is initially laceration-induced. It promotes massive increase in inhibitory aggrecan and collagen-1 leading to denervation. Denervation leads to more atrophy which in turn further aggravates the fibrosis in lacerated skeletal muscles (Fig. 22 and 23).

7.2 – Atrophy

Muscle atrophy is divided into 2 different stages. Calpain-dependent proteolysis is involved in the early phase, while the lysosomal and ubiquitin-proteosome systems participate in the late phase. Both proteolytic pathways are increased in chronic denervated skeletal muscles. Muscle-specific E3 ubiquitin ligases, atrogin-1 and MuRF-1, drive the ubiquitin proteosome pathway mediated myofibrillar proteolysis (Edstrom E et al, 2007). The up-regulation of atrogin-1 and MuRF-1 can be Foxo, NFkB, p38, Erk or myogenin-dependent. Complement-3 secreted from phagocytes and dying muscle fibres at lesion site can degrade fast myosin heavy chains in skeletal muscle reperfusion injury. It is also needed for rapid Wallerian degeneration and efficient clearance of myelin after acute peripheral nerve trauma. Another important factor for loss of muscle mass is the reduced levels of IGF1, which activates Akt and mTOR phosphorylation to increase protein synthesis in muscle fibers.

7.2.1- Preserved Intra-muscular Nerve Model

PN has the lowest atrogin-1, MuRF1 and complement-3 expression levels after 12-weeks. This is due to the following reasons:

1) Atrophy in PN is AMPK-driven. AMPK induces muscle atrophy by promoting phospho-activation of Foxo1 and Foxo3, which up-regulates synthesis of atrogin-1 and MuRF-1; AMPK also inhibits the mTOR pathway and p70S6K phosphorylation for protein synthesis.

2) Up-regulation of decorin: Decorin inhibits atrophy via binding to myostatin with its core protein and sequestering myostatin from binding to its ActIIB receptor. This leads to inhibition of Foxo phosphorylation.

3) IGF1 and CNTF inhibit atrophy through Akt signaling; Akt dephosphorylates Foxo1 and Foxo3, and prevents their nuclear translocation by sequestering them to the 14-3-3 scaffold ; IGF1 and CNTF can also activate mTOR and p70S6K phosphorylation to increase protein

synthesis (Wang and Forsberg, 2000);

4) calpain-3 inhibits NFkB-induced atrophy; activation of NFkB by phosphorylation leads to NFkB translocation to the nucleus where it induces the transcriptional regulation of the MuRF1; it can also decrease IL6- induced muscle atrophy.

5) Sirt-1 up-regulation inhibits NFkB and Foxo, resulting in enhanced protection against muscle atrophy.

The calpain-3 level in PN is higher than DN and RN. The reasons are as follows:

1) higher protein turnover in response to injured myofibers as calpain-3 is needed to activate myoD and myogenin for growth and differentiation of muscle cells (Berchtold et al, 2000). As calpain-3 is known to bind with titin, increased calpain-3 abundance at 12-weeks in RN and NegC may parallel to the amounts of recently formed titin from sarcomere synthesis (Sorimachi and Suzuki, 2001);

2) high calcineurin expression, through the activation of NFAT, can increase the expression of calpain-3 as the calpain-3 promoter has a binding site for MEF2/NFAT heterodimers (Sorimachi et al, 1996).

3) high availability of nitric oxide synthase (NOS), which up-regulate calpain-3 activity via calcium/calmodulin (Berchtold et al, 2000);

4) the calpain-3 mRNA is stabilized by RNA-binding proteins, HuR and HuD.

7.2.2- Denervated Intra-muscular Nerve Model

It has the highest atrogin-1and MuRF1 expression levels after 12-weeks. This is due to the following factors:

1) High myostatin level induces the expression of atrogin-1 and MuRF1 through Foxo-dependent pathway; myostatin also auto-upregulates its transcription via p38 and Foxo signaling;

2) High follistatin level cannot inhibit atrophy via binding myostain through its heparin

sulphate domain at the extra-cellualr matrix because Foxo-independent pathways are activated to increase atrogin-1 and MuRF1 expression;

3) High NT4 and GDNF levels did not decrease atrophy because Foxo-independent pathways are activated to induce atrophy; Foxo-independent pathways to induce atrophy include activation of p38 to increase atrogin-1 expression, NFkB and Erk1/2 to increase MuRF1 expression;

4) Low IGF1 level leads to inhibition of Akt phosphorylation and mTOR activation, resulting in decreased protein synthesis;

5) A lot of dying muscle fibers leads to high complement activation, which then activates more apoptosis of muscle fibers via caspase-3. Overall, DN is in the most severe catabolic state at 12-weeks post-repair compared to other groups.

7.2.3- Re-innervated Intra-muscular Nerve Model

It has the highest complement-3 expression level after 12-weeks, while its atrogin-1 and MuRF1 levels are intermediate between PN and DN. This is because atrophy in RN is driven by myostatin, myogenin and AMPK. PGC-1a inhibits Foxo3 and so reduces the expression atrogin-1 and MuRF1. However, high PGC-1a expression cannot totally inhibit atrophy because p38 and Erk1/2 can up-regulate atrogin-1 and MuRF1 expression on their own. High myogenin expression in RN is mediated by HDAC4 upon denervation, while the high complement-3 expression is induced by the Wallerian degeneration.

7.2.4- Hypothesis Support

Atrophy is initially denervation-induced. It is both myostatin and myogenin-driven in DN and RN, but it is AMPK-driven in PN. Atrophy also arises from reduction in protein synthesis due to inhibited Akt and mTOR signaling from significant drop in IGF1, PGC-1a and CNTF levels; and concurrent increase in muscle proteolysis due to high expression of atrogin-1, MuRF1 and complement-3. Huge amounts of glutamine and leucine released from

protein degradation promotes further fibrosis, which leads back to chronic denervation and the cycle repeats itself (Fig.23).

7.3 – Myogenesis

Muscle laceration releases HGF from the ECM. HGF activates the satellite cells to down-regulate Pax7 and increase the expression of MyoD and myf5. The satellite cells then proliferate into myoblasts, then differentiate and fuse to form new adult myofibers to replace dead myofibers. Skeletal muscle regeneration requires also energy for activation of satellite cells and myoblast differentiation into adult myofibers. This needs active mitochondrial biogenesis regulated by PGC-1a. Respiration-deficient myoblasts devoid of mitochondria fail to differentiate. Also, inhibition of mitochondrial protein synthesis with chloramphenicol prevents the differentiation of myoblasts into myotubes.

7.3.1- Preserved Intra-muscular Nerve Model

PN had better myogenesis based on histology. It had more mature, fully differentiated adult muscle fibers with large cross-sectional area and multiple nuclei at the periphery. The reasons are as follows:

1) Denervation up-regulates myoD expression in PN via the activating the distal regulatory region and proximal regulatory region of its promoter. High myoD expression induced p21 and Rb synthesis to inhibit apoptosis of myoblasts. MyoD induces permanent cell cycle arrest by up-regulating p21 and p300 and activates muscle-specific gene transcription in myogenesis.

2) Increase in decorin, EGF, CNTF, Sirt1 expression coupled with lower TGFb2 and CTGF levels promoted significant myogenesis in PN. Decorin regulate TGF-β availability during skeletal muscle differentiation. Once myoblasts differentiate into myotubes, the decorin expression in the ECM is increased, and decorin binds to TGFb and myostatin to sequester the proteins to the ECM. This decreases the availability of TGFb2 and myostatin to their

transducing receptors, thus allowing myogenesis (Brandan et al, 2008). When the terminal differentiation of myoblasts into adult muscle fiber is completed, TGF-β binds to its transducing receptors and activates the Smad dependent pathway. It also binds to decorin and LRP, resulting in an activation of the PI3K dependent pathway. These two signaling pathways synergize to inhibit abnormal myogenesis. Decorin is also involved in myoblast migration (Olguin et al, 2003). It represses myoblast migration to permit skeletal muscle differentiation, independent of chemotactic growth factors. Decorin has also been demonstrated to increase expression of follistatin (Zhu J et al, 2007); so PN having higher decorin up-regulates follistatin expression simultaneously; PN has significantly greater myogenesis due to the higher follistatin expression; follistatin stimulated the myoblasts to differentiate via up-regulating myoD, myf5 and myogenin; it also blocks myostatin and TGFb2 activity, and enhances neo-vascularisation.

3) CNTF can also increase the differentiation of muscle satellite cells (Chen et al, 2005) via activation of STAT3 (Kirsch et al, 2003). Satellite cells proliferate in response to denervation. This process is stimulated by Sirt1- induced reduction of p21 activity. Sirt1 can also increase proliferation and differentiation of myoblasts as it deacetylates and inhibits NFkB, and this indirectly up-regulates myoD expression . Also, Sirt1 can activate PGC-1a to increase myoD transcription (Amat R et al, 2009). In addition, activation of p38 by stress from muscle laceration also results in enhanced PGC-1a expression and mitochondrial biogenesis. Next, PN has lower NAD+ levels as the IM nerve is intact, so Sirt1 and AMPK-1a cannot inactivate Mef2a, this promotes myogenesis.

4) Decreased CTGF and TGFb2 expression allow more terminal differentiation of myoblasts into mature muscle. This is because TGF-β2 inhibits fusion of myoblasts via down-regulating the expression of cdk6 and cyclin E-associated cdk2 activity (Tsubari et al, 1999), and it synergises with CTGF to inhibit the terminal differentiation of myoblasts into mature

muscle cells by blocking the expression of myoD and myogenin. This is achieved by 2 mechanisms: a) SMAD3 has been shown to bind to the bHLH region of myoD, interfering with myoD/E protein dimerization and subsequent cooperative binding to E-box DNA; b) SMAD3 also can bind with MEF2a, which prevent the association of the myoD/E47 dimer with Mef2a, resulting in the repression of muscle-specific gene expression.

5) High EGF levels in PN further enhance satellite cell proliferation and myoblast migration for fusion to become mature muscle fibers via Akt signaling pathway.

7.3.2- Denervated Intra-muscular Nerve Model

Denervation significantly inhibited myogenesis in DN as DN has more immature muscle fibers with small size and central nuclei at lacerated site. The reasons are listed below:

1) Depletion of satellite cell pool because the satellite cells died by apoptosis under chronic denervation, and myostatin inhibits satellite cell renewal through Erk1/2 mediated downregulation of Pax7;

2) Inhibition of myoblasts to fuse and differentiate to form mature myofibers as there is increase in myostatin, Id1, TGFb2 and CTGF expression. Myostatin, TGFb2, Id and CTGF down-regulate myoD expression. Myostatin also induces cyclin D degradation via PI3K to cause cell cycle arrest. It then inhibits the satellite cell activation and proliferation, as well as myoblast proliferation and differentiation via up-regulating p21. Also, myostatin decreases myotube formation via down-regulation of cdk6 and cyclin E-associated cdk2 activity (Tsubari et al, 1999). Myostatin also inhibits mTOR signaling and so reduces protein synthesis in myoblasts.

3) New proliferating myoblasts can only fuse with existing denervated muscle fibers but not with each other to form new fibers (Fig 22);

4) High levels of aggrecan and collagen-1 in the scar region inhibit myoblast migration;

5) Downregulation of calpain-3 leads to over-activation of caspase-3, calpain-1 and 2, inducing excessive myoblast apoptosis;

6) Decreased PGC-1a expression leads to less mitochondrial biogenesis activity;

7) Denervation increases nuclear NAD+ levels and this induces Sirt1 to deacetylate and inactivate myoD, and also high AMPK expression in DN can inactivate Mef2a, so blocking satellite cell activation and subsequent muscle differentiation (Araki et al, 2004).

8) High NT4 and GDNF expression did not improve myogenesis in DN because they mainly exerted pro-fibrosis effects (Appendix 12).

9) Denervation decreases muscle mitochondrial content and increases mitochondrial permeability, leading to elevated apoptosis in skeletal muscle.

Hence there is less viable myoblasts available to fuse and form mature adult muscle fibers. The newly regenerated adult muscle fibers are often small in size and scarce in number.

7.3.3- Re-innervated Intra-muscular Nerve Model

Myogenesis in RN is mainly promoted by R-spondin-1, Shh and galectin-1, as it has the highest expression levels of the 3 markers. Shh promotes proliferation and differentiation of myoblasts via Erk and Akt signaling. Also, the re-activation of Shh expression in adult skeletal muscle after injury can induce angiogenesis via upregulation of VEGF and SDF-1a. Galectin-1 promotes both myoblast fusion and muscle re-innervation following laceration, increasing the available myoblasts to form new myofibers. R-spondin-1 up-regulates the expression of myf5 to initiate myoblast differentiation via Wnt/beta-catenin pathway.

7.3.4- Intermediate Filaments

The expression of desmin during skeletal muscle regeneration indicates the presence of myoblasts (Bassaglia and Gautron 1995) and newly formed myotubes (Duguez et al, 2003). The higher expression of desmin in PN at 12-weeks corresponds to a higher synthesis of sacrcomeric proteins and intense fusion of myoblasts to form myotubes (Duguez et al,

2003). This is confirmed in immunohistochemistry staining of longitudinal sections of medial gastrocnemius muscle (Fig 4). The increase in desmin expression is crucial for the satellite cell activation and myoblast proliferation (Bockhold et al, 1998; Duguez et al, 2003). Also, desmin stabilizes mitochondria positioning in cells, and keep the myofibrils in register. Vimentin was used as a scar marker because it is expressed by myofiber early in development and shortly after injury at 2-weeks, then it is rapidly down-regulated during muscle differentiation and it is replaced by desmin. Vimentin is important for stabilization of collagen-1 mRNA in fibroblasts and retrograde importin-Erk signaling in regenerating neurons (Hanz et al 2003). Nestin prevents cdk5-induced apoptosis by sequestering cdk5/p35 complexes in regenerating neurons. The orchestrated dynamic expression of intermediate filaments in PN implies that intact innervation is crucial to drive the proper myogenic lineage commitment of the muscle precursor cells during muscle repair.

7.3.5- Hypothesis Support

Decrease in myogenesis is denervation-induced, then aggravated by fibrosis and atrophy, resulting in the loss of muscle mass and size. Chronic denervation leads to incomplete terminal differentiation of young myofibers into mature adult fibers to replace dead muscle fibers. The reduction in size of muscle fibers is due to myostatin inhibiting protein synthesis via mTOR signaling, while the decrease in number of mature muscle fibers is due to myostatin inhibiting satellite cell renewal via down-regulation of Pax7.

7.4 – Fiber Transformation

Denervation can alter the isometric contractile force in regenerating skeletal muscle. This process is called fiber transformation as the original expression levels of the contractile proteins are permanently modified after muscle repair.

The adult rat medial gastrocnemius expresses both fast and slow myosin heavy chains in the ratio of 1:1, and also both fast and slow troponin-I isoforms in the ratio of 12:1.

Fiber transformation in MG after denervation is denoted by a significant reduction in myosin heavy chain-2b fibers and a corresponding increase in slow myosin heavy chains expression compared with those of normal subjects. This leads to the regenerating MG muscle having weaker contractile properties than the original undamaged muscles. The regenerating rat myotubes initially express both slow and embryonic myosin heavy chains. When the myotubes get re-innervated by fast motor neurons, the embryonic myosin heavy chains are subsequently replaced by fast myosin heavy chains. Innervation is necessary to maintain fast and slow troponin-I expression since it is greatly increased in DN at 2-weeks after laceration. The expression of both the myosin heavy chain and troponin-I isoforms is dictated by the following factors:

1) Myogenin and Mef2a control the expression of slow myosin heavy chain while myoD drives the expression of fast myosin heavy chain.

2) Myostatin regulates the fiber type composition of skeletal muscles by controlling myoD and MEF2a gene expression. It up-regulates Mef2a after denervation to promote the slow muscle fiber expression, and the reverse is true for fast muscle fiber expression after the muscle is re-innervated.

3) TGFb inhibits the expression of all myosin heavy chain isoforms, while Shh and NT4 specify the slow fiber type.

4) CNTF specifies both fast and slow myosin heavy chains.

5) Sirt1 and PGC-1a control gene expression of slow fiber genes. PGC-1a activates MEF2 to up-regulate slow myosin heavy chain and slow troponin-I expression.

6) IGF1 terminates the expression of embryonic myosin heavy chain once the regenerating muscle is innervated by the fast motor neuron. It also enhances the expression of fast myosin heavy chain -2B via GSK3B signaling.

7.4.1- Preserved Intra-muscular Nerve Model

PN retained most of its fast myosin heavy chain and fast troponin-I expression after 12-weeks due to higher CNTF expression and lower atrogin-1, MuRF1 and complement-3 levels, as well as significant reduction in myostatin and TGFb2 expression.

7.4.2- Denervated Intra-muscular Nerve Model

The high expression of embryonic myosin heavy chain at 12-weeks in DN indicated that intact innervation is still absent. Also, the down-regulation of embryonic myosin heavy chain at 12-weeks implied that myoblasts in DN had differentiated (Miyabara EH et al, 2005). The high levels of myostatin, atrogin-1, complement-3, MuRF-1 and TGFb2 expression at 12-weeks greatly inhibit the expression of fast myosin heavy chain and fast troponin-I. The decreased levels of PGC-1a coupled with the increased expression of slow myosin heavy chain and slow troponin-I that retain lower oxidative capacity, and the decreased amount of mitochondria in cut muscle lead to loss of isometric contraction in the DN rats.

7.4.3- Re-innervated Intra-muscular Nerve Model

RN has also retained its myosin heavy chain-2b and fast troponin-I expression more than DN at 12-weeks post-repair due to reduction in expression of myostatin, TGFb2, atrogin-1, MuRF-1 and complement-3.

7.4.4- Hypothesis Support

With the intramuscular nerve preserved intact (PN), there is decrease in fiber transformation than DN. DN had lost most of its fast myosin heavy chain-2B as fast myosin heavy chains are less resistant to atrophy.

7.5 – Intra-Muscular Nerve Regeneration

The intra-muscular nerve can regenerate on its own after the muscle laceration. The success of muscle re-innervation depends critically on the growth environment in the distal nerve stump following the removal of axonal and myelin debris. Regenerating axons grow

toward denervated muscles within the endoneurial tubes formerly occupied by intact axons and their myelin sheaths. Few regenerating axons can successfully cross the gap between the proximal and distal nerve stumps even after micro-surgical repair due to the inhibitory collagen and proteoglycan deposited at lesion site.

7.5.1- Preserved Intra-muscular Nerve Model

PN expressed the highest GAP43 expression level after 12-weeks even though the intra-muscular nerve is preserved intact. The intact IM nerve leads to higher EGF, decorin and galectin-1 expression than DN. EGF synergises with FGF2 to inhibit TGFb2-induced apoptosis of Schwann cells. Decorin inhibits the pro-fibrotic activity of TGFb2. Administration of decorin to injured sites in the adult rat brain and spinal cord suppresses expression of aggrecan and promoted axon growth across adult spinal cord injuries. Decorin also reduces EGFR-induced synthesis of aggrecan and myelin-associated inhibitors of axon growth via RhoA/ROCK pathway. Oxidized galectin-1 from macrophages, fibroblasts and Schwann cells promotes IM nerve regeneration via neuropilin-1 signaling. Neuropilin-1 is a receptor for motor neuron guidance and survival. The strong positive correlation between HN1 expression and GAP43 level indicated the high abundance of regenerating motor neurons in PN.

7.5.2- Denervated Intra-muscular Nerve Model

It has the lowest GAP43 expression level after 12-weeks. High NT4 and GDNF did not improve IM nerve regeneration in DN due to aggressive fibrosis induced by TGFb2, myostatin and CTGF which inhibited axonal regeneration, and high complement-3 levels which destroyed the newly regenerating axons. Hence the Schwann cells cannot re-connect and re-myelinate the severed nerve stumps.

7.5.3- Re-innervated Intra-muscular Nerve Model

RN tells us that intact nerve sheaths are important for muscle regeneration after

laceration because if the nerve sheath is present, retrograde flow of neurotrophic factors and axonal guidance cues can occur to promote muscle re-innervation which then inhibits atrophy. Also, the intact nerve sheaths enhance correct targeting of nerve to specific muscle to re-establish functional neuromuscular junctions in midst of muscle scar. RN has better IM nerve regeneration than DN because it expressed high HGF to induce the proliferation of spinal motor neurons, promote survival of regenerating motor neurons and denervated Schwann cells. It also has high Shh level to stabilize structural and functional integrity of peripheral nerve.

7.5.3.1-Relevance of RN model to clinical practice:

Risk rates for crushed peripheral nerve injury in people incurring limb trauma are low (Sahjian et al, 2009). Crush skeletal muscle injuries have the highest rate of associated intra-muscular nerve injury. The overall incidence is 0.1% as the crush skeletal muscle injury is unpredictable. This model has acknowledged limitations. It can be difficult to replicate a clinical scenario of random tissue injury (ie muscle, nerve, veins and bone), nevertheless our reductionist model would better able isolate the injuries secondary to the defined markers studied in this thesis.

7.5.4- Hypothesis Support

Intra-muscular nerve regeneration in PN is better than DN as PN has the highest GAP43 expression level at 12-weeks (0.85-fold) while DN has the lowest GAP43 expression (0.59-fold).

This great reduction in GAP43 activity in DN is due to aggressive fibrosis which inhibited axonal regeneration and high complement-3 (6.61-fold) expression which destroyed the newly regenerating axons. This contributes to a reduction in number of axons that can eventually reach the denervated segment of the muscle fibers via the network of endoneurial tubes formerly occupied by intact axons and their myelin sheaths. However, no

nerve sprouts were detected at 12-weeks in all groups. The reasons are listed below:

1) Excessive high levels of collagen-1 and aggrecan in the remodeled ECM inhibit IM nerve regeneration;

2) High expression of immature neurotrophins, truncated Trk receptors and p75NTR in the injured neurons resulted in apoptosis of motor neurons upon ligand binding (Williams G et al, 2005);

3) High expression of IGFBP4 and IGFBP5 inhibits IGF1-mediated axon sprouting;

4) Insufficient levels of decorin and follistatin expressed from Schwann cells and myoblasts to inhibit pro-fibrotic activity of TGFb2, CTGF and myostatin;

5) Down-regulation of MMPs and TIMPs to degrade the excessive collagen at lesion site;

6) Lack of electrical stimulation as polyneuronal innervation of muscle fibers is activity-dependent (Skouras E 2011).

7.6 – Targets to intervene for better muscle recovery after laceration (clinical relevance)

The targets include EGF, HGF, decorin, follistatin, aggrecan, atrogin-1, MuRF-1, IGF-1, CNTF, NT4, GDNF, AMPK, PGC-1a, Sirt1, myostatin, Sonic hedgehog, CTGF, galectin-1, R-spondin-1and TGFb2. The expression trends of these targets are statistically significant at both 2- and 12-weeks, and they can modulate the fibrosis and atrophy during muscle repair via multiple signaling pathways. They can synergise or antagonize each signaling pathways.

Firstly, to reduce fibrosis in skeletal muscle after laceration, we can inhibit pro-fibrosis effect of TGF-β1 and myostatin either by suppressing the initiation of gene transcription or by altering the mRNA stability. For example, TGFb mRNA expression is reduced by anti-sense oligonucleotide, interferon-gamma and anti-oxidants (a-tocopherol). Another approach is to directly target circulating TGFb by using anti-TGFb anti-serum or

the use of chimeric protein composed of the extracellular domain of the TGFb type II receptor linked to the Fc portion of IgG that binds and inactivates TGFb. Other options include inhibiting the downstream SMAD phosphorylation in TGFb signaling by using small molecules such as trichostatin A (histone deacetylase inhibitor) and halofuginone.

Also, we need to decrease the myofibroblast activation to reduce fibrosis. This is achieved by using thiodigalactoside to disrupt the interaction between galectin-1 and glycoconjugates at the cell surface of fibroblasts. Next, we can use acetylcholine receptor inhibitors to block acetylcholine-dependent activation of fibroblasts to secrete collagen-1 at distal nerve stumps.

Secondly, to minimize atrophy of lacerated skeletal muscle, we can use proteosome inhibitor, bortezomib, to inhibit Foxo and NFkB- induced atrogin-1 and MuRF-1 activity. We can also use Class II histone deacetylase inhibitors to ameliorate myogenin-induced atrogin-1 and MuRF-1 gene transcription.

Thirdly, combinatorial neurotrophic factor administration of IGF1, NT3, FGF2 and BDNF to lacerated skeletal muscle can be used to enhance neuronal survival, promote axon regeneration through the scar tissue and increase correct targeting of intra-muscular nerve in skeletal muscle post-laceration. Also, it is technically challenging to repair the damaged nerve in lacerated skeletal muscles by micro-surgery post-trauma and impossible to do so when the nerve-muscle gap is more than 3mm wide. Hence artificial nerve conduits or nerve-muscle grafts can be employed to aid the subsequent re-innervation of the lacerated skeletal muscle. This will greatly decrease muscle fibrosis and atrophy during the recovery phase.

Lastly, we can use AMPK activators (metformin, 2-deoxyglucose, AICAR), PPAR-gamma agonists and Sirt1 agonists to activate AMPK, PPAR-gamma, Sirt1 respectively in lacerated skeletal muscle as they are the master regulators of multiple downstream targets

involved in fibrosis, atrophy and myogenesis such as myoD, NFkB, Foxo, Mef2a, SMAD7 and p300. This must be done at the correct time-point post-laceration to achieve desired outcomes. For example, we can start with Sirt1 agonists at 3 days post-laceration to expand the satellite cell pool, then switching to the Sirt1 inhibitors at 2-weeks to allow the proliferating myoblasts to differentiate to mature myofibers to replace the dead muscle fibers.

8. CONCLUSION

This study offers a rationale for repairing the concomitantly cut intra-muscular nerve in lacerated skeletal muscle, in addition to epimysial suturing of the muscle cut ends. The dynamic orchestrated expression of intermediate filaments, myogenic factors, muscle atrophy factors, fibrotic factors and neurotrophic factors in various treatment groups at the 2 time-points supports our hypothesis. It is important to repair the damaged nerve which is present in a lacerated skeletal muscle as the integrity of the nerve can modulate the functional recovery of the lacerated muscle. This is evident when comparing the severity of fibrosis formation at the lesion site and the extent of reversible and irreversible muscle atrophy and denervation between PN and DN at 12-weeks post-surgery. However, repairing a damaged nerve by micro-anastomosis is not sufficient to decrease severity of the muscle atrophy, to reduce the extent of fibrosis between two muscle stumps, and to restore the isometric contractile properties of the muscle. Appropriate anti-fibrosis agents, anti-atrophy drugs and biological axonal guidance cues must be administered at correct dosage and at very early stage post-trauma to minimize the irreversible activation of myofibroblasts, decrease the transcription of muscle atrophy genes and loss of isometric contraction.

We identified several potential endogenous biological targets which can improve both myogenic and neurogenic recovery across the lesion site to avoid irreversible muscle denervation and atrophy based on the distinct gene expression profiles in each skeletal

muscle laceration model. In brief, our results showed that the integrity of the intra-muscular nerve can regulate fibrosis, atrophy, intra-muscular nerve regeneration, fiber type transformation, and myogenesis across the lesion site. The relationship is depicted in Fig 22 and 23.

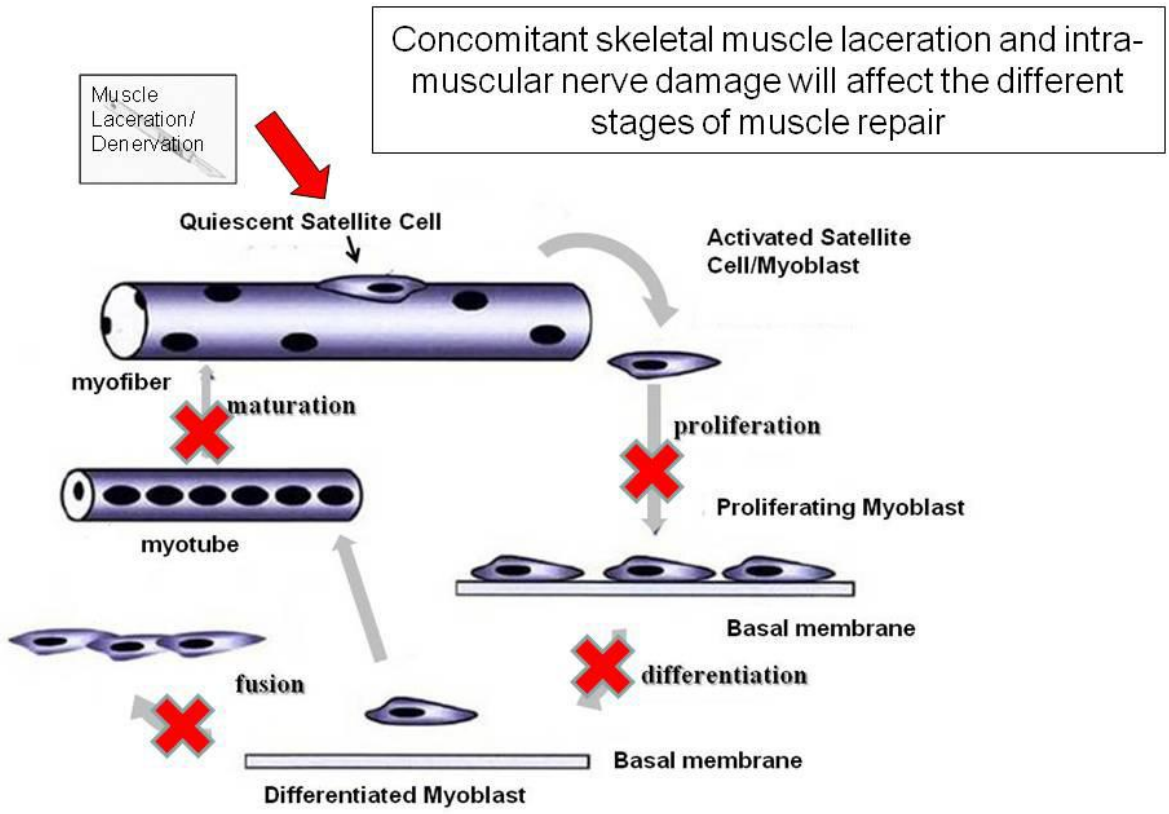

Figure 22. Possible repair cycle in a concomitant skeletal muscle laceration and intramuscular nerve damage. Although the skeletal muscle can regenerate itself post-laceration, denervation can lead to irreversible atrophy and fibrosis at the lesion site. Firstly, TGFb2, myostatin and CTGF can inhibit the proliferation and differentiation of the myoblasts. Fusion of myoblasts is also inhibited by excessive collagen-1 and aggrecan deposited during extracellular matrix remodelling, initiated by myofibroblasts, infiltrating macrophages, neutrophils, surrounding endothelial cells and platelets. In addition, atrogin-1, MuRF-1 and complement-3 degrade both the young myotubes and the regenerating nerves. Both aggressive fibrosis and severe atrophy then further resulted in chronic denervation. Thus, less number of viable myoblasts is available to mature into adult muscle fibers to replace the dead fibers. Also, the differentiated myoblasts can only fuse with existing muscle fibers, not with each other. Hence, the newly regenerated adult muscle fibers are often small in size and scarce in number. (Adapted from Kami et al. (2005) Current Drug Targets 6: 395-405).

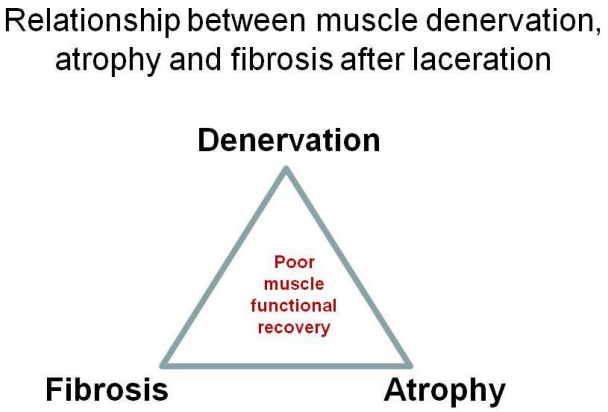

Figure 23. Skeletal muscle laceration and cut intra-muscular nerve post-trauma (as in the DN model) can cause severe fibrosis at laceration site, leading to chronic denervation, aggressive muscle atrophy and permanent fiber type transformation, and finally resulting in poor muscle functional recovery. The vicious cycle repeats itself when the damaged nerve remains unrepaired. All three processes are inter-dependent, mutually inclusive and occur simultaneously. The integrity of the intra-muscular nerve after muscle laceration will govern the magnitude of severity and duration of the atrophy and fibrosis post-repair.

9. LIMITATIONS OF THE STUDY

The study was limited by various factors. Most were unavoidable due to the nature of the experiments with animal studies and the availability of resources and time. A few are noted below for future work.

9.1-Why was the laceration model simulated with a sharp cut?

To avoid variations in muscle damage, a sharp laceration was used over a blunt laceration. This blunt model would have increase damage away from the lacerated site which may be unknown to us, and can affect the results. This is therefore only a simulated model of laceration. (Pereira et al., 2008, 2010)

9.2-Why were only 2 time points studied, and why 2-weeks and 12-weeks?

We were comparing the stage of reversible muscle atrophy (~2week) and the irreversible state (~after 3 months) (Fu and Gordon, 1995, Fnkelstein et al., 1993).

9.3-Why was the nerve crushed used as a model to simulate nerve repair?

This was an alternative model, again a simulation, as it was difficult to repair the intramuscular nerve in a rat. The intramuscular nerve is crushed damaging the axons but preserving the nerve sheath intact. Electrical stimulation was used to confirm that there was axonal damage, while integrity of the nerve sheath was also assessed to confirm continuity. This model allows for axonal regeneration within the nerve sheath and therefore can be compared with the DN where nerve and axonal regeneration may be more random, with the possibility of nerve sprouting from a neighbouring muscle which could be inappropriate. This also altered the MHC profile as shown previously (Pereira et al., 2010).

9.4-Why use medial gastrocnemius, not soleus or plantaris or other muscles?

In an experimental muscle model in an animal given the ethic requirements, the medial gastrocnemius is the most common muscle used in experiments, as it avoid the loss of mobility in the animal, given that the animal can still function the foot, with the lateral gastrocnemius and the soleus. The medial gastrocnemius is also a large muscle and that provides sufficient tissue for our study.

10. SUGGESTIONS FOR FUTURE WORK

Several suggestions are recommended for future work. Firstly, there is a need to assess suitable biological endogenous protein inhibitors and synthetic drug inhibitors for anti-fibrosis, anti-atrophy, pro-muscle re-innervation effects in animal models of skeletal muscle repair after trauma. The second potential area of research is to establish skeletal muscle-fibroblast-neuron co-culture system or skeletal muscle-fibroblast-endothelial cell-neuron co-culture system, which can be used for drug dosage studies. This is a better alternative to the animal model because it has more control of focal injury, has much less background noise arising from protein-protein interactions between different organs. In

addition, animal models have a large variability in genetic polymorphisms, and require large sample sizes for adequate power in statistical analysis. A third suggested model is to use siRNAs in either animal models or cell culture systems to inhibit collagen-1a, atrogin-1, MuRF-1, aggrecan, myostatin, CTGF and other inhibitory proteins to enhance muscle repair.

11. REFERENCES

Abe S (2009) Increased expression of decorin during the regeneration stage of mdx mouse. Anat Sci Int 84:305–311.

Abreu JG, Ketpura NI, Reversade B, De Robertis EM. (2002) Connective tissue growth factor (CTGF) modulates cell signalling by BMP and TGF-*β*. Nat. Cell Biol. 4, 599–604.

Adams D, Hathaway M, Shaw J, Burnett D, Elias E, Strain A (1991). Transforming growth factor-b induced human T lymphocyte migration in vitro. J Immunology 147: 609-614.

Alain Mauviel TGFb and TNFa: Antagonistic cytokines controlling type I collagen gene expression Cellular Signaling 16 (2004) 873-880

Alvin WC Chua, Dongrui Ma, Shu U Gan, Zhenying Fu, Hwan Chour Han, Colin Song, Kanaga Sabapathy, Toan T Phan
Journal of Investigative Dermatology 16 Dec 2010
The role of R-spondin-2 in keratinocyte proliferation and epidermal thickening in keloid scarring

Allen et al. (2005). Myocyte enhancer factor-2 and serum response factor binding elements regulate fast myosin heavy chain transcription *in Vivo.* J Biol Chem 280,17,126–17134.

Allen R, Boxhorn L (1987). Inhibition of skeletal muscle satellite cell differentiation by transforming growth factor beta. J Cell Physiol 133:567-572.

Anderson KD, Merhege MA, Morin M, Bolognani F, Perrone-Bizzozero NI
Increased expression and localization of the RNA-binding protein HuD and GAP43 mRNA to cytoplasmic granules in DRG neurons durng nerve regeneration
Exp Neurol (2003) 183: 100-108

Aoki M, Mieda M, Ikeda T, Hamada Y, Nakamura H, Okamoto H (2006). R-spondin-3 is required for mouse placental development. Dev Biol 301: 218-226.

Aoyama E. et al (2009) N-terminal domains of CCN family 2/connective tissue growth factor bind to aggrecan. Biochem. J. 420, 413–420.

Arakawa Y, Sendtner M, Thoenen H (1990). Survival effect of ciliary neurotrophic factor (CNTF) on chick embryonic motoneurons in culture: comparison with other neurotrophic factors and cytokines. J Neurosci. 10:3507-15.

Araki T, Sasaki Y, Milbrandt J (2004). Increased nuclear NAD biosynthesis and Sirt-1 activation prevent axonal degeneration. Science 5686:1010-1013

Armand AS, Della Gaspera B, Launay T, Charbonnier F, Gallien CL, Chanoine C (2003). Expression and neural control of follistatin versus myostatin genes during regeneration of mouse soleus. Dev Dyn 227:256-265.

Aspberg A, Adam S, Kostka G, Timpl R, Heinegard D (1999) Fibulin-1 is a ligand for the C-type lectin domains of aggrecan and versican. J. Biol. Chem. 274,20444–20449

Bach D, Pich S, Soriano FX, Vega N, Baumgartner B, et al (2003). Mitofusin-2 determines mitochondrial network architecture and mitochondrial metabolism. J Biol Chem 278:17190-17197.

Banzet S, Koulman N, Simler N, Birot O, Sanchez H, Chapot R, Peinnequin A and Bigard X (1985). Fibre-type specificity of IL-6 gene transcription during muscle contraction in rat : association with calcineurin activity. J Physiol 566, 839-847

Barsoum MJ, Yuan H, Gerencser A et al (2006). Nitric oxide-induced mitochondrial fission is regulated by dynamin-related GTPases in neurons. EMBO J 25:3900-3911.

Bassaglia Y, Gautron J (1995). Fast and slow rat muscles degenerate and regenerate differently after whole crush injury. J Muscle Res Cell Motil 16:420-429

Bellon G et al Glutamine increases collagen gene transcription in cultured human fibroblasts Biochimica et Biophysica Acta 1268 (1995) 311-323

Berchtold MW, Brinkmeier H, Muntener M (2000). Calcium ion in skeletal muscle: its crucial role for muscle function, plasticity, and disease. Physiol Rev 80:1215-1265

Blaydon DC et al (2006). The gene encoding R-spondin-4 (RSPO4), a secreted protein implicated in Wnt signaling, is mutated in inherited anonychia. Nat Genet 38: 1245-1247

Blough ER, Rennie ER, Zhang F, Reiser RJ (1996). Enhanced separation and resolution of myosin heavy chains in mammalian and avian skeletal muscles. J Analytical Biochem 233:31-35

Bockhold KJ, Rosenblatt JD, Partridge TA (1998). Aging normal and dystrophic mouse muscle: analysis of myogenicity in cultures of living single fibers. Muscle Nerve 21: 173-183

Bodine SC, Latres E, Baumhueter S, Lai VK, Nunez L, Clarke BA, Poueymirou WT, Panaro FJ, Na E, Dharmarajan K, et al (2001). Identification of ubiquitin ligases required for skeletal muscle atrophy. Science 294: 1704-1708.

Borisov AB, Dedkov EI, Carlson BM. (2001). Interrelations of myogenic response, progressive atrophy of muscle fibers, and cell death in denervated skeletal muscle. Anat Rec 264: 203-218.

Bornemann A, Schmalbruch, H (1992). Desmin and Vimentin in regenerating muscles. Muscle Nerve 1992, 15(1), 14-20.

Bosche W, Ewton D, Florini J (1995). Transforming growth factor-beta isoform expression in insulin-like growth factor stimulated myogenesis. J Cell Physiol 164: 324-333

Boudreau-Larivière C, Sveistrup H, Parry DJ, Jasmin BJ (1996). Ciliary neurotrophic factor: regulation of acetylcholinesterase in skeletal muscle and distribution of messenger RNA encoding its receptor in synaptic versus extrasynaptic compartments. Neuroscience. 73:613-22.

Bovolenta PI, Espinosa F (2000). Nervous system proteoglycans as modulators of neurite outgrowth. Prog Neurobiol 61:113-132

Brack AS et al. (2007). Increased Wnt signaling during aging alters muscle stem cell fate and increases fibrosis. Science 2007, 317:807-810.

Bradham DM, Igarashi A, Potter RL, Grotendorst GR (1991). Connective tissue growth factor: a cysteine-rich mitogen secreted by human vascular endothelial cells is related to the SRC-induced immediate early gene product CEF-10. J Cell Biol 114:1285-1294.

Brandan E (2008). Novel regulatory mechanisms for the proteoglycans decorin and biglycan during muscle formation and muscular dystrophy; Matrix Biology 27, 700–708.

Brigstock DR (1999). The connective tissue growth factor/cysteine-rich 61/nephroblastoma over-expressed (CCN) family. Endocrine Rev 20:189-206

Burazin TC, Gundlach AL (1998). Up-regulation of GDNFR-alpha and c-ret mRNA in facial motor neurons following facial nerve injury in the rat. Brain Res Mol Brain Res. 1998;55:331-6.

Carlson BM, Faulkner JA (1998). Muscle transplantation between young and old rats: age of host determines recovery. Am J Physiol 256: C1262-1266

Carlson C, Booth F, Gordon S (1999). Skeletal muscle myostatin mRNA expression is fiber-type specific and increases during hind limb unloading. Am J Physiol 277:R601-606.

Caroni P, Schneider C, Kiefer MC, Zapf J (1994). Role of Muscle Insulin-like Growth Factors in Nerve Sprouting: Suppression of Terminal Sprouting in Paralyzed Muscle by IGF-binding Protein 4. Journal Cell Biol 125, 893-902.

Carrasco DI, English AW (2003). Neurotrophin 4/5 is required for the normal development of the slow muscle fiber phenotype in the rat soleus. J Exp Biol. 2003; 206:2191-200.

Chen et al (2009). The scar in a jar: Studying potential anti-fibrotic compounds from the epigenetic to extracellular level in a single well. Brit J Pharmacology 158(5): 1196-1209

Chen FH., Herndon ME, Patel, N, Hecht, JT, Tuan, RS and Lawler J. (2007) Interaction of cartilage oligomeric matrix protein/thrombospondin 5 with aggrecan. J. Biol. Chem. 282, 24591–24598

Chen X, Mao Z, Liu S, Liu H, Wang X, Wu H, Wu Y, Zhao T, Fan W, Li Y, Yew DT, Kindler PM, Li L, He Q, Qian L, Wang X, Fan M (2005). Dedifferentiation of adult human myoblasts induced by ciliary neurotrophic factor in vitro. Mol Biol Cell. 16:3140-51.

Crumley RL (1998). Laryngeal synkinesis: its significance to the laryngologist. Ann Otol Rhinol Laryngol. 98(2):87-92.

Day JM, Olin AI, Murdoch AD, Canfield A, Sasaki T, Timpl R, Hardingham TE and Aspberg A (2004) Alternative splicing in the aggrecan G3 domain influences binding interactions with tenascin-C and other extracellular matrix proteins. J. Biol. Chem. **279**, 12511–12518

Dubuisson L, Desmouliere A, Decourt B, Evade L, Bedin C, Boussarie L, Barrier L, Vidaud M, Rosenbaum J (2003). Inhibition of rat liver fibrogenesis through noradrenergic antagonism. Hepatology 35:325–331.

Duguez S, Bihan MC, Gouttefangeas D, Feasson L, Freyssenet D (2003). Myogenic and non-myogenic cells differentially express proteinases, Hsc/Hsp-70 and BAG-1 during skeletal muscle regeneration. Am J Physiol Endocrinol Metab 285:E206-E215

Dulor JP, Cambon B, Vigneron P, Reyne Y, Nouguès J, Casteilla L, Bacou F (1998). Expression of specific white adipose tissue genes in denervation-induced skeletal muscle fatty degeneration. FEBS Lett. 439:89-92.

Edstrom E, Altun M, Bergman E, Johnson H, Kullberg S, Ramirez-Leon V, Ulfhake B (2007). Factors Contributing to Neuromuscular Impairment and Sarcopenia During Aging. Physiology and Behaviour 92:129-135

Edstrom E, Ulfhake B. (2005) Sarcopenia is not due to lack of regenerative drive in senescent skeletal muscle. Aging Cell 4:65-77

Engert JC, Berglund EB, Rosenthal N (1996). Proliferation precedes differentiation in IGF-I stimulated myogenesis. J Cell Biol 135:431-440

Escandón E, Soppet D, Rosenthal A, Mendoza-Ramírez JL, Szönyi E, Burton LE, Henderson CE, Parada LF, Nikolics K (1994). Regulation of neurotrophin receptor expression during embryonic and postnatal development. J Neurosci. 14:2054-68.

Fallentin N, Jorgensen K, Simosen EB (1993). Motor unit recruitment during prolonged isometric contractions. Eur J Appl Physiol Occup Physiol 67, 335-341.

Fawcett JW, Asher RA (1999). The glial scar and central nervous system repair. Brain Res Bull 49:371-391.

Filbin MT (2006). Recapitulate development to promote axonal regeneration: good or bad approach? Phil. Trans. R. Soc. B 361, 1565-1574.

Finkelstein DI et al. (1993). Recovery of muscle after different periods of denervation and treatment. Muscle Nerve 16 769-777.

Florini J, Ewton D, Falen S, van Wyk J (1986). Biphasic concentration dependency of stimulation of myoblast differentiation by somatomedins. Am J Physiol 250: C771-778

Florini J, Ewton D, Roof S (1991). Insulin-like growth factor I stimulates terminal myogenic differentiation by induction of myogenin gene expression. Mol Endocrinol 5: 718-724

Florini J, Roberts A, Ewton D, Falen S, Flanders K, Sporn M (1986). Transforming growth factor-beta, a very potent inhibitor of myoblast differentiation, identical to the differentiation inhibitor secreted by buffalo rat liver cells. J Biol Chem 261:16509-16513

Fu SY and Gordon (1995) Contributing factors to poor functional recovery after delayed nerve repair: Prolonged denervation. J Neurosci 15: 2886-2895.

Funakoshi H, Belluardo N, Arenas E, Yamamoto Y, Casabona A, Persson H, Ibáñez CF (1995). Muscle-derived neurotrophin-4 as an activity-dependent trophic signal for adult motor neurons. Science. 268:1495-9.

Funakoshi H, Frisén J, Barbany G, Timmusk T, Zachrisson O, Verge VM, Persson H. (1993) Differential expression of mRNAs for neurotrophins and their receptors after axotomy of the sciatic nerve. J Cell Biol. 123:455-65.

Gao R, Brigstock DR (2004) Connective tissue growth factor (CCN2) induces adhesion of rat activated hepatic stellate cells by binding of its C-terminal domain to integrin *αvβ*3 and heparan sulfate proteoglycan. J. Biol. Chem. 279, 8848–8855.

Gao R, Brigstock DR. (2006) A novel integrin *α*5*β*1 binding domain in module 4 of connective tissue growth factor (CCN2/CTGF) promotes adhesion and migration of activated pancreatic stellate cells. Gut **55**, 856–862.

George, Sarah Jane Regulation of myofibroblast differentiation by convergence of the Wnt and TGFb1/SMAD signaling pathways Journal of Molecular and Cellular Cardiology
46 (2009): 610-611

Gillingwater TH, Thomson D, Ribchester RR (2004). Myo-GDNF increases non-functional polyinnervation of reinnervated mouse muscle. Neuroreport. 15:21-5.

Gleghorn, L., Ramesar, R., Beighton, P. and Wallis, G. (2005) A mutation in the variable repeat region of the aggrecan gene (AGC1) causes a form of spondyloepiphyseal dysplasia associated with severe, premature osteoarthritis. Am. J. Hum. Genet. 77, 484–490.

Glinka A, Dolde C, Kirsch N, Huang YL, Kazanskaya O, Ingelfinger D, Boutros M, Cruciat CM, Niehrs C (2011). LGR4 and LGR5 are R-spondin receptors mediating Wnt/b-catenin and Wnt/PCP signaling. EMBO Reports 12:1055-1061.

Goldberg JL, JS Espinosa, Y Xu (2002). Retinal ganglion cells do not extend axons by default: promotion by neurotrophic signaling and electrical activity. Neuron 33: 689-702.

Goll DE, Thompson VF, Li H, Wei W, Cong J (2003). The Calpain System. Physiol Rev 83:731-801

Gomes MD, Lecker SH, Jagoe RT, Navon A, Goldberg AL (2001). Atrogin-1, a muscle-specific F-box protein highly expressed during muscle atrophy. Proc Natl Acad Sci USA 98:14440-14445

Gratien Dalpe et al. (1999), Dystonin-deficient mice exhibit an intrinsic muscle weakness and an Instability of skeletal muscle cytoarchitecture; Developmental Biology 210**,** 367–380.

Grötzinger J, Kurapkat G, Wollmer A, Kalai M, Rose-John S (1997). The family of the IL-6-type cytokines: specificity and promiscuity of the receptor complexes. Proteins. 27:96-109.

Grounds MD, White JD, Rosenthal N, Bogoyevitch MA (2002). The role of stem cells in skeletal and cardiac muscle repair. J Histochem Cytochem. 50:589-610.

Hartmann U, P Maurer (2001). Proteoglycans in the nervous system : the quest for functional roles in vivo. Matrix Biol 20:23-35

Helgren ME, Squinto SP, Davis HL, Parry DJ, Boulton TG, Heck CS, Zhu Y, Yancopoulos GD, Lindsay RM, DiStefano PS (1994). Trophic effect of ciliary neurotrophic factor on denervated skeletal muscle. Cell. 1994;76:493-504

Henderson CE, Phillips HS, Pollock RA, Davies AM, Lemeulle C, Armanini M, Simmons L, Moffet B, Vandlen RA, Simmons L, et al (2004). GDNF: a potent survival factor for motoneurons present in peripheral nerve and muscle. Science. 266:1062-4.

Henneman E and Olson CB (1965). Relations between structure and function in the design of skeletal muscles. J Neurophysiol 28, 581-598.

Hermanns S, Reiprich P, Muller HW (2001). A reliable method to reduce collagen scar formation in the lesioned rat spinal cord. J Neurosci Meth 110:141-146

Heuer H, Christ S, Friedrichsen S, Brauer D, Winckler M, Bauer K, Raivich G (2003). Connective Tissue Growth Factor: A novel marker of layer VII neurons in the rat cerebral cortex. Neuroscience 119:43-52

Hizz B, Gabbiani G (2003). Cell-matrix and cell-cell contacts of myofibroblast: Role in Connective Tissue Remodeling. Thromb Haemost 90(6): 993-1002.

Hoshijima M, Hattori T, Inoue M, Araki D, Hanagata H, Miyauchi A, Takigawa M. (2006) CT domain of CCN2/CTGF directly interacts with fibronectin and enhances cell adhesion of chondrocytes through integrin $\alpha 5\beta 1$. FEBS Lett. 580, 1376–1382.

Hosokawa Y (2010) Catechins inhibit CXCL10 production from oncostatin M-stimulated human gingival fibroblasts. J Nutr Biochem 21, 659–664.

Howe PH Chapter 49 Transforming Growth Factor b - The cytokine Handbook, 4th ed
Angus W Thomson and Michael T Lotze (2003)

Huang EJ, LF Reichardt (2001). Neurotrophins: roles in neuronal development and function. Annu Rev Neurosci 24: 677-736

Inoki I, Shiomi T, Hashimoto G, Enomoto H, Nakamura H, Makino Ket al. (2002) Connective tissue growth factor binds vascular endothelial growth factor (VEGF) and inhibits VEGF-induced angiogenesis.FASEB J. 16, 219–221

Jagoe RT, Goldberg AL (2001). What do we really know about the ubiquitin-proteosome pathway in muscle atrophy? Curr Opin Clin Nutr Metab care 4, 183-190

Jeanplong F, Sharma M, Bass J, Kambadur R (1999). Genomic organization of the bovine myostatin gene. Annual Scientific and Clinical Meeting, NZ Soc Endocrin May 19-22

Jennische E, Matejka GL (1992). IGF-1 binding proteins & IGF-1 expression in regenerating muscle of normal and hypo-physectomised rats. Acta Physiol Scand 146:79-86

Jerkovic R, Argentini C, Serrano-Sanchez A, Cordonnier C, Schiaffino S (1997). Early myosin switching induced by nerve activity in regenerating slow skeletal muscle. Cell Struct Funct 22:147-153

Johnson H, Mossberg K, Arvidsson U, Piehl F, Hokfelt T, Ulfhake B (1995). Increase in alpha-CGRP and GAP-43 in aged motoneurons : a study of peptides, growth factors and ChAT mrna in the lumbar spinal cord of senescent rats with symptoms of hindlimb incapacities. J Comp Neurol 359:69-89

Ju SN. (2006) Mouse Cristin/R-spondin family Proteins are Novel Ligands for the Frizz led 8 and LRP6 receptors and Activate B-catenin dependent gene expression. Journal of Biological Chemistry 281(19):13247-13257

Kami K Senba E. (2005) Galectin-1 is a novel factor that regulates myotube growth in regenerating skeletal muscles. Current Drug Targets 2005, 6, 395-405

Karna E et al The potential mechanism for glutamine-induced collagen biosynthesis in cultured human skin fibroblasts Comparative Biochemistry and Physiology Part B 130(2001) 23-32

Katada A et al (2006) A sequential double labeling technique for studying changes in motoneural projections to muscle following nerve injury and re-innervation. Journal of Neuroscience Methods 155: 20-27

Kazanskaya O, Glinka A, Del Barco Barrantes I, Stannek P, Niehrs C, Wu W (2004). R-spondin-2 is a secreted activator of Wnt/beta-catenin signaling and is required for Xenopus myogenesis. Dev Cell 7: 525-534

Kazanskaya O, Ohkawara B, Heroult M, Maltry N, Augustin HG, Niehrs C (2008). The Wnt signaling regulator R-spondin-3 acts upstream of VEGF to control the switch between angioblastic and hematopoietic cell fate determination. Development 135: 3655-3664.

Kerschensteiner, M., C. Stadelmann, G. Dechant, H. Wekerle, R. Hohlfeld. (2003). Neurotrophic cross-talk between the nervous and immune systems: implications for neurological diseases. *Ann. Neurol.* 53: 292-304.

Kiani C, Chen L, Wu YJ, Yee AJ, Yang BB (2002) Structure and function of aggrecan. Cell Res. **12**, 19–32.

Kim KA et al (2005). Mitogenic influence of human R-spondin-1 on the intestinal epithelium. Science 309:1256-1259.

Kim KA et al (2008). R-spondin family members regulate the Wnt pathway by a common mechanism. Mol Biol Cell 19: 2588-2596.

Kireeva ML, Latinkic BV, Kolesnikova TV, Chen CC, Yang GP, Abler AS, Lau LF (1997). Cyr61 and Fisp12 are both ECM-associated signaling molecules: activities, metabolism and localization during development. Exp Cell Res 233:63-77.

Kirk S, Oldham J, Kambadur R, Sharma M, Dobbie P, Bass J (2000). Myostatin regulation during skeletal muscle regeneration. J Cell Physiol 184:356-363.

Kirk S, Whittle M, Oldham J, Dobbie P, Bass J (1996). GH regulation of the type 2 IGF receptor in regenerating skeletal muscle of rats. J Endocrinol 149:81-91.

Kirsch M, Terheggen U, Hofmann HD (2003). Cilliary neurotrophic factor is an early lesion-induced retrograde signal for axotomized facial motoneurons. Mol Cell Neurosci. 24:130-8.

Kubota S, Takigawa M. (2007) Role of CCN2/CTGF/Hcs24 in bone growth. Int. Rev. Cytol. 257, 1–41.

Kragh JF, Jr., Svoboda SJ, Wenke JC, et al. (2005). Suturing of lacerations of skeletal muscle. J Bone Joint Surg Br 87: 1303-1305.

Kyung AK et al. (2008) R-spondin Family Members Regulate the Wnt Pathway by a Common Mechanism. Molecular Biology of the Cell 19:2588-2596

Larkin LM, Kuzon WM, Halter JB (2000). Synergist muscle ablation and recovery from nerve-repair grafting: contractile and metabolic function. J Appl Physiol 89:1469-1476

Lee FS, AH Kim, G Khursigara, MV Chao (2001). The uniqueness of being a neurotrophin receptor. Curr Opin Neurobiol 11:282-286

Lentz SI, CM Knudson, SJ Korsmeyer, WD Snider (1999). Neurotrophins support the development of diverse sensory axon morphologies. J Neurosci 19: 1038-1048

Li FQ et al (2005). Vital elements of the Wnt-frizzled signaling pathway in the nervous system. Curr Neurovasc Res 2(4) :331-340

Li H, Capetanaki Y (1994). An E box in the desmin promoter cooperates with the E box and MEF2 sites of a distal enhancer to direct muscle-specific transcription. EMBO J 13: 3580-3589.

Li, H., Schwartz, N. B. and Vertel, B. M. (1993) cDNA cloning of chick cartilage chondroitin sulfate (aggrecan) core protein and identification of a stop codon in the aggrecan gene associated with the chondrodystrophy, nanomelia. J. Biol. Chem. 268, 23504–23511.

Lie DC, Weis J (1998). GDNF expression is increased in denervated human skeletal muscle. Neurosci Lett. 3;250:87-90.

Lisak RP, Dusanka Skundric D, Beverly Bealmear B, Ragheb S. (1997). The Role of Cytokines in Schwann Cell Damage, Protection, and Repair. J Infect Dis 176, S173-9.

Lomo T (2002). Nerve-muscle interactions. Clinical Neuruphysiology of Disorders of Muscle and the neuromuscular Junction in adults and children Vol4 IFSCN.

Marlindo W, Nunes S, Rostom de Mello AM. (2005) Glucose metabolism in rats submitted to skeletal muscle denervation. Braz. Arch. Biol. Technol. 48(4).

Massague J, Cheifetz S, Endo T, Nadal Ginard B (1986). Type beta transforming growth factor is an inhibitor of myogenic differentiation. Proc Natl Acad Sci USA 83:8206-8210

Matheson CR, Carnahan J, Urich JL, Bocangel D, Zhang TJ, Yan Q (1997). Glial cell line-derived neurotrophic factor (GDNF) is a neurotrophic factor for sensory neurons: comparison with the effects of the neurotrophins. J Neurobiol.;32:22-32

Mendias CL et al TGFb induces skeletal muscle atrophy and fibrosis through the induction of atrogin-1 and scleraxis
Muscle and Nerve 2012 45(1): 55-59

Miyabara EH, Aoki MS, Soares AG, Moriscot AS (2005). Expression of tropism-related genes in regenerating skeletal muscle of rats treated with cyclosporin-A. Cell Tissue Res 319:479-489.

Moalem G. et al (2000). Production of Neurotrophins by Activated T Cells: Implications for Neuroprotective Autoimmunity; Journal of Autoimmunity 15**,** 331–345.

Morensi V et al (2010) Myogenin and class II HDACs control neurogenic muscle atrophy by inducing E3 ubiquitin ligases Cell 143: 35-45

Moussard EE, Brigstock DR (2000). Connective tissue growth factor: what is in a name? Mol Genet Metab 71: 276-292

Murachi T (1989). Intracellular regulatory system involving calpain and calpastatin. Biochem Int 18:263-294

Nagano M, Suzuki H (2003). Quantitative analyses of expression of GDNF and neurotrophins during postnatal development in rat skeletal muscles. Neurosci Res. 2003;45:391-9.

Nakanishi T, Nishida T, Shimo T, Kobayashi K, al. (2000) Effects of CTGF/Hcs24, a product of a hypertrophic chondrocytespecific gene, on the proliferation and differentiation of chondrocytes in culture. Endocrinology 141, 264–273.

Nam JS, Turcotte TJ, Smith PF, Choi S, Yoon JK (2006). Mouse cristin/R-spondin family proteins are novel ligands for the Frizzled 8 and LRP 6 receptors and activate b-catenin-dependent gene expression. J Biol Chem 281:13247-13257.

Nishida T, Nakanishi T, Asano M, Shimo T, Takigawa M. (2000) Effects of CTGF/Hcs24, a hypertrophic chondrocyte-specific gene product, on the proliferation and differentiation of osteoblastic cells in vitro. J. Cell. Physiol. 184, 197–206.

Nishida T, Kubota S, Nakanishi T, Kuboki T, Yosimich, G, Kondo S, Takigawa M. (2002) CTGF/Hcs24, a hypertrophic chondrocyte-specific gene product, stimulates proliferation and differentiation, but not hypertrophy of cultured articular chondrocytes. J. Cell. Physiol. 192, 55–63.

Oben JA, Roskams T, Yang S, Lin H, Sinelli N, Torbenson M, Smedh U, Moran TH, Li Z, Huang J, Thomas SA, Diehl AM (2004). Hepatic fibrogenesis requires sympathetic neurotransmitters. Gut 53:438–445.

Olson E, Sternberger E, Hu J, Spizz G, Wilcox C (1986). Regulation of myogenic differentiation by type beta transforming growth factor. J Cell Biol 103:1799-1805

Olguin HC (2003), Inhibition of myoblast migration via decorin expression is critical for normal skeletal muscle differentiation; Developmental Biology 259, 209–224.

Omura T, Sano M, Omura K, Hasegawa T, Doi M, Sawada T, Nagano A (2005). Different expressions of BDNF, NT3, and NT4 in muscle and nerve after various types of peripheral nerve injuries. J Peripher Nerv Syst. 10:293-300.

Ong CT, Khoo YT, Mukhopadhyay A, Masilamani J, Vinh DD, Lim I, Phan TT (2010). Comparative proteomic analysis between normal skin and keloid scar British J Dermatol 162:1302-1315

Otto A. Canonical Wnt signaling induces satellite cell proliferation during adult skeletal muscle regeneration. Journal of Cell Science 2008, 121(17): 2939-2950

Palazzo E et al (2012), Role of neurotrophins on dermal fibroblast survival and differentiation; J Cell Physiol 227:1017-1025.

Pallafacchina G, et al. Role of satellite cells in muscle growth and maintenance of muscle mass Nutrition, Metabolism & Cardiovascular Diseases (2012)

Pan HC. et al. (2007) Post-injury regeneration in rat sciatic nerve facilitated by neurotrophic factors secreted by amniotic fluid mesenchymal stem cells; J Clin Neuroscience 14, 1089–1098.

Parma P, Radi O, Vidal V, Chaboissier MC, Dellambra E, Valentini S, Guerra L, Schedl A, Camerino G (2006). R-spondin-1 is essential in sex determination, skin differentiation and malignancy. Nat Genet 38:1304-1309

Paves H, Saarma M (1997). Neurotrophins as in vitro growth cone guidance molecules for embryonic sensory neurons. Cell Tissue Res. 290:285-97.

Perbal B, Takigawa, M. (2005) CCN Proteins: a New Family of Cell Growth and Differentiation Regulators, World Scientific Publishers, London.

Pereira BP et al. (2008) The cut intramuscular nerve affects the recovery in the lacerated skeletal muscle. J Ortho Res. 24: 102-111.

Pereira BP et al. (2010) Myosin Heavy Chain Isoform profiles remain altered at 7 months if the lacerated medical gastrocnemius is poorly reinnervated: a Study in rabbits. J Orthop Res 28: 732-738.

Pereira BP, Tan JA, Zheng L, et al. (2006). The cut intramuscular nerve affects the recovery in the lacerated skeletal muscle. J Orthop Res 24: 102-111.

Perez-Ruiz A et al (2008). B-catenin promotes self-renewal of skeletal muscle satellite cells. Journal of Cell Science 121(17) :1373-1382.

Peterziel H. (2002). TGFb induces GDNF responsiveness in neurons by recruitment of GFRa1 to the plasma membrane Journal Cell Biol 159 157-167.

Rasbach K et al (2008) Oxidants and calicium induced PGC-1a degradation through calpain. Archives of Biochemistry and Biophysics 478: 130-135

Ranges G, Figari, Espevik T, Palladino M (1987). Inhibition of cytotoxic T cell development by transforming growth factor-B and reversal by recombinant tumor necrosis factor-a. J Exp Med 166: 991-998

Reibman J, Meixler S, Lee T, Gold L, Cronstein B, Haines K, Kolasinki S, Weissman G (1991). Transforming growth factor-b1, a potent chemoattractant for human neutrophils, bypasses classic signal-transduction pathways. Proc Natl Acad Sci USA 88: 6805-6809

Richard I, Broux O, Allamand V, Fougerousse F, Chiannikulchai N, Bourg N, Brenguier L, Devaud C, Pasturaud P, Roudaut C et al (1995). Mutations in the proteolytic enzyme calpain-3 cause limb-girdle muscular dystrophy type 2A. Cell 81:27-40

Richardson PM, UM McGuinness, AJ Aguayo (1980). Axons from CNS neurons regenerate into PNS grafts. Nature 284: 264-265

Rita M Cowell, Kathryn R Blake, Tatsuya I, Russell JW (2998). Regulation of PGC-a and PGC-1a responsive genes with forskolin-induced Schwann cell differentiation. Neuroscience Letters 439 269-274.

Rodgers BD (2005) IGF1 downregulates embryonic myosin heavy chain in myoblast nuclei. Growth Hormone & IGF Research. 15:377-383

Rockey DC (2005). Antifibrotic therapy in chronic liver disease, Clinical Gastroenterology and Hepatology, 3(2), 95-107.

Sahjian Miachael and Michael Frakes. "Crush Injuries: Pathophysiology and Current Treatment." *Advanced Emergency Nursing Journal* 29 2 (2007): 145-150. *NursingCenter.com*. 13 Mar. 2009

Sasaki Y, Araki T, Milbrandt J (2006). Stimulation of nicotinamide adenine dinucleotide biosynthetic pathways delays axonal degeneration after axotomy. J Neurosci 26:8484-8491

Schiaffino S, Serrano AL (2002). Calcineurin signaling and neural control of skeletal muscle fiber type and size. Trends in Pharmcological Sciences 23 (12): 569-575.

Schiaffino S, Reggiani C (1996). Molecular diversity of myofibrillar proteins: gene regulation and functional significance. Physiol Rev 76, 371-423.

Schwartz, M., G. Moalem, R. Leibowitz-Amit, I. R. Cohen. (1999). Innate and adaptive immune responses can be beneficial for CNS repair. *Trends Neurosci.* 22: 295-299.

Segarini PR, Nesbitt JE, Li D, Hays LG, Yates III JR, Carmichael DF. (2001) The low density lipoprotein receptor-related protein/*α*2-macroglobulin receptor is a receptor for connective tissue growth factor. J. Biol. Chem. **276**, 40659–40667.

Sendtner M, Carroll P, Holtmann B, Hughes RA, Thoenen H (1994). Ciliary neurotrophic factor. J Neurobiol. 1994;25:1436-53. Review.

Sharma M, Langley B, Bass J, Kambadur R (2001). Myostatin in muscle growth and repair. Exerc Sport Sci Rev 29:155-158.

Shimo T, Nakanish, T, Kimura Y, Nishida T, Ishizeki K, et al. (1998) Inhibition of endogenous expression of connective tissue growth factor by its antisense oligonucleotide and antisense RNA suppresses proliferation and migration of vascular endothelial cells. J. Biochem. (Tokyo) 124, 130–140.

Shimo T, Nakanishi T, Nishida T, Asano M, Kanyama M et al. (1999) Connective tissue growth factor induces the proliferation, migration, and tube formation of vascular endothelial cells in vitro, and angiogenesis in vivo. J. Biochem. (Tokyo) 126, 137–145.

Siegel SG, Patton B, English AW (2000). Ciliary neurotrophic factor is required for motoneuron sprouting. Exp Neurol. 166:205-12.

Simon M, Porter R, Brown R, Coulton GR, Terenghi G (2003). Effect of NT-4 and BDNF delivery to damaged sciatic nerves on phenotypic recovery of fast and slow muscles fibres. Eur J Neurosci. 18:2460-6.

Skouras E, Ozsoy U, Sarikcioglu L, Doychin N (2011). Angelov,Intrinsic and therapeutic factors determining the recovery of motor function after peripheral nerve transaction; Annals of Anatomy 193 286– 303.

Sofroniew MV, CL howe, WC Mobley (2001). Nerve growth factor signaling, neuroprotection and neural repair. Ann Rev Neurosci 24: 1217-1281

Sorimachi H, Forsberg NE, Lee HJ, Joeng SY, Richard I, Beckmann JS, Ishiura S, Suzuki K (1996). Highly conserved structure in the promoter region of the gene for muscle-specific calpain, p94. Biol Chem 377:859-864

Sorimachi H, Imajoh-Ohmi S, Emori Y, Kawasaki H, Ohno S, Minami Y, Suzuki K (1989). Molecular cloning of a novel mammalian calcium-dependent protease distinct from both m-types and u-types in skeletal muscle. J Biol Chem 264:20106-20111

Sorimachi H, Suzuki K (2001). The structure of calpain. J Biochem 129:653-664.

Sterne GD, Coulton GR, Brown RA, Green CJ, Terenghi G (1997). Neurotrophin-3-enhanced nerve regeneration selectively improves recovery of muscle fibers expressing myosin heavy chains 2b. J Cell Biol. 139:709-15.

Stocum D (2001), Regeneration of Musculoskeletal Tissues, Chap 9, in Yannas IV Ed. Tissue and Organ Regeneration in Adults. Springer-Verlag New York, Inc, pp221-249.

Stockholm D, Herasse M, Marchand S, Praud C, Roudaut C, Richard I, Sebille A, Beckmann JS (2001). Calpain-3 mRNA expression in mice after denervation and during muscle regeneration. Am J Physiol Cell Physiol 280:C1561-C1569

Svensson A, Tagerud S (2009). Galectin-1 Expression in Innervated and Denervated Skeletal Muscle Cellular and Molecular Biology Letters. 2009, 14, 128-138

Takigawa, M. (2003) CTGF/Hcs24 as a multifunctional growth factor for fibroblasts, chondrocytes and vascular endothelial cells. Drug News Perspect. 16, 11–21 4.

Takigawa M, Nakanishi T, Kubota S, Nishida T. (2003) Role of CTGF/HCS24/ecogenin in skeletal growth control. J. Cell. Physiol. 194, 256–266.

Tee JM et al. (2009) Regulation of slow and fast muscle myofibrillogenesis by Wnt/B-catenin and myostatin signaling. PLoS ONE 4(6):e5880.

Tollefsen S, Sadow J, Rotwein P (1989). Coordinate expression of insulin-growth factor 2 and its receptor during muscle differentiation. Proc Natl Acad Sci USA 86:1543-1547

Tsubari M, Taipale J, Tiihonen E, Keski-Oja J, Laiho M (1999) Heptocyte growth factor releases mink epithelial cells from transforming growth factor b1-induced growth arrest by restoring cdk6 expression and cyclinE-associated cdk2 activity. Mol Cell Biol 19:3654-3663

Tucker KL, Meyer M, Barde YA (2001). Neurotrophins are required for nerve growth during development. Nat Neurosci.4:29-37.

Ueki T, Kaneda Y, Tsutsui H, Nakanishi K, Sawa Y, Morishita R, Matsumoto K, Nakamura T,

Takahashi H, Okamoto E, Fujimoto J (1999) Hepatocyte growth factor gene therapy of liver cirrhosis in rats.Nature Med 5:226-230**.**

Ulfhake B, Bergman E, Edstrom E, Fundin BT, Johnson H, Kullberg S (2000). Regulation of neurotrophin signaling in aging sensory and motoneurons: dissipation of target support. Mol Neurobiol 21: 109-135

Vaittinen S et al (2001). The expression of intermediate filament protein nestin as related to vimentin and desmin in regenerating muscles. J Neuropathol Exp Neurol, 60(6), 588-597.

Vargas-Leal V et al. (2005). Expression and function of glial cell line derived neurotrophic factor family ligands and their receptors on human immune cells; J Immunol 175(4):2301-2308.

Vial C (2011) , Decorin interacts with connective tissue growth factor by LRR12 inhibiting its biological activity. J Biol Chem 2011, Jul 8;286(27):24242-24252.

Wahab NA, Weston BS , Mason RM. (2005) Connective tissue growth factor CCN2 interacts with and activates the tyrosine kinase receptor TrkA. J. Am. Soc. Nephrol.16, 340–351.

Wahl S, Hunt D, Wakefield L, McCartney-Francis N, Wahl L, Roberts A, Sporn M (1987). Transforming growth factor-b induces monocyte chemotaxis and growth factor production. Proc Natl Acad Sci USA 84:5788-5792

Wahl S, Hunt D, Wong H, Dougherty S, McCartney-Francis N, Wahl L, Ellingsworth L, Schmidt J, Hall G, Roberts A, Sporn M (1988). Transforming growth factor b is a potent immunosuppressive agent that inhibits IL-1 dependent lymphocyte proliferation. J Immunol 140:3026-3031

Walro JM, Kucera J, Narvy R (1991). Non-neural and neural expression of myosin heavy chains by regenerated intrafusal fibers of rats. Neurosci Lett 122:213-217

Wang KC, Kim JA, Sivasankaran R, Segal R, He, Z. (2002) *Nature* 420**,** 74–78.

Wang MC, Forsberg NE (2000). Effects of ciliary neurotrophic factor (CNTF) on protein turnover in cultured muscle cells. Cytokine. 2000;12:41-8.

Watanabe, H., Nakata, K., Kimata, K., Nakanishi, I. and Yamada, Y. (1997) Dwarfism and age-associated spinal degeneration of heterozygote cmd mice defective in aggrecan. Proc. Natl. Acad. Sci. U.S.A. 94, 6943–6947

Watt MJ, Dzamko N, Thomas WG, Rose-John S, Ernst M,
CNTF reverses obesity-induced insulin resistance by activating skeletal muscle AMPK
Nat Med (2006) 12, 541-548

Wehrwein EA, Roskelley EM, Spitsbergen JM (2002). GDNF is regulated in an activity-dependent manner in rat skeletal muscle. Muscle Nerve. 26:206-11.

Wells DG, McKechnie BA, Kelkar S, Fallon JR (1996). Neurotrophins regulate agrin-induced postsynaptic differentiation. Proc Natl Acad Sci U S A. 1999;96:1112-7.

Williams G (2005) Overcoming the inhibitors of myelin with a novel neurotrophin strategy, J Biol Chem. 280, No. 7, 5862–5869.

Wilson SJ, Harris AJ (1993). Formation of myotubes in aneural rat muscles. Dev Biol 156:509-518.

Yang et al. (1999) Active transforming growth factor-B in wound repair. Am J Path 154:105-111.

Yang M, Huang H, Li J et al. (2004) Tyrosine phosphorylation of the LDL receptor-related protein (LRP) and activation of the ERK pathway are required for connective tissue growth factor to potentiate myofibroblast differentiation. FASEB J. 18, 1920–1921.

Zhou FQ, Snider WD. (2006), Intracellular control of developmental and regenerative axon growth, Phil. Trans. R. Soc. B (2006) 361, 1575-1592.

Zhao J, Kim KA, De Vera J, Palencia S, Wagle M, Abo A (2009). R-spondin-1 protects mice from chemotherapy or radiation-induced oral mucositis through the canonical Wnt/beta-catenin pathway. Proc Natl Acad Sci USA 106:2331-2336.

Zhu J (2007). J Biol Chem 25852-25863.

Zwick M, Teng L, Mu X, Springer JE, Davis BM (2001). Overexpression of GDNF induces and maintains hyperinnervation of muscle fibers and multiple end-plate formation. Exp Neurol. 171:342-50.

APPENDIX

Appendix 1. List of TaqMan primers used in the real-time-PCR Assays

No	Target	Catalogue No (Amplicon size / bp)
1	Neurotrophic factor-4, NT-4	Rn01645105_m1(128)
2	Glial derived neurotrophic factor, GDNF	Rn00569510_m1 (122)
3	Ciliary neurotrophic factor CNTF	Rn00755092_m1(83)
4	Insulin-like growth factor, IGF1	Rn00710306_m1 (69)
5	Hepatocyte Growth Factor, HGF	Rn00566673_m1 (139)
6	Epidermal Growth Factor,EGF	Rn00563336_m1 (93)
7	Sonic hedgehog, Shh	Rn00568129_m1 (100)
8	MyoD	Rn00598571_m1 (85)
9	Myogenin	Rn00567418_m1 (55)
10	MEF2A	Rn01478096_m1 (118)
11	Desmin	Rn00574732_m1 (78)
12	Vimentin	Rn00579738_m1 (105)
13	Nestin	Rn00564394_m1 (78)
14	Atrogin-1	Rn00591730_m1 (61)
15	MuRF-1	Rn00590197_m1 (56)
16	Peroxisome proliferator activated receptor-gamma co-activator, alpha, PGC-1α	Rn00580241_m1 (94)
17	Sirt-1	Rn01428093_m1 (81)
18	Myostatin	Rn00569683_m1 (67)
19	Calpain-3	Rn 00482978_m1 (96)
20	Complement 3	Rn00566466_m1 (72)
21	AMP-activated protein kinase alpha 1 subuint, AMPK	Rn00569558_m1 (72)
22	Follistatin	Rn00561225_m1 (80)
23	Transforming Growth Factor beta 2, TGFβ2	Rn00579674_m1 (95)
24	Collagen Type 1 alpha	Rn01463848_m1 (115)
25	aggrecan (chondroitin sulphate proteoglycan-1)	Rn00573424_m1 (74)
26	Galectin-1	Rn00571505_m1 (98)
27	Decorin	Rn01503161_m1 (101)
28	Fast skeletal troponin-I	Rn00437157_g1 (62)
29	Embryonic myosin heavy chain 3	Rn00561539_m1 (63)
30	Fast skeletal myosin heavy chain 4	Rn01496087_m1 (65)
31	Slow skeletal myosin heavy chain 7	Rn01536269_m1 (111)
32	Slow skeletal troponin-I	Rn00567843_m1 (129)
33	Lamin A	Rn00572764_m1 (72)
34	Hematological and neurological expressed-1, HN-1	Rn01466868_g1 (137)
35	Growth associated protein 43, GAP43	Rn01474579_m1 (79)

Appendix 2. List of antibodies used for immunohistochemistry and western blot

Antigen	Host	Supplier	Cat No.	Dilution	Antigen retrieval
vimentin	mouse	SC	sc-6260	1:500	Microwave 20min, 0.01M citrate buffer, pH6.1 (Dako); Milestone Mega T/T oven, Program 21
desmin	mouse	SC	sc-52326	1:500	Microwave 20min, 0.01M citrate buffer, pH6.1 (Dako); Milestone Mega T/T oven, Program 21
nestin	mouse	SC	sc-33677	1:500	Microwave 20min, 0.01M citrate buffer, pH6.1 (Dako); Milestone Mega T/T oven, Program 21
galectin-1	rabbit	A	ab25138	1:200	Microwave 20min, 0.01M citrate buffer, pH6.1 (Dako); Milestone Mega T/T oven, Program 21
R-spondin-1	mouse	RDS	422407	1:200	Microwave 20min, 0.01M citrate buffer, pH6.1 (Dako); Milestone Mega T/T oven, Program 21
alpha tubulin	mouse	SC	sc-5286	1:1000	NA
p38	rabbit	CST	9212	1:1000	NA
phospho-p38	rabbit	CST	9211	1:1000	NA
Erk1/2	rabbit	CST	9102	!:1000	NA
phospho-Erk1/2	rabbit	CST	9106	1:1000	NA
TGFβ2	rabbit	SC	sc-90	1:1000	NA
connective tissue growth factor, CTGF	mouse	RDS	MAB660	1:1000	NA
alpha smooth muscle actin	mouse	Sig	A2547	1:1000	NA
SMAD2 and 3	rabbit	SC	sc-8332	1:1000	NA
phospho-SMAD2 and 3	goat	SC	sc-11769	1:1000	NA
Myogenin	goat	SC	Sc-31945	1:1000	NA
myoD	rabbit	SC	Sc-304	1:1000	NA
slow myosin heavy chain	mouse	Sig	M8421	1:50,000	NA
fast myosin heavy chain	mouse	Nov	NCL-MHC	1:50,000	NA

Suppliers

SC – Santa Cruz; CST – Cell Signaling Technology; RDS – R& D Systems; A – Abcam M – Milipore; Sig – Sigma & Nov – Novacastra

Appendix 3. Recipe for casting SDS-PAGE gels

Resolving gel (%)	**8**	**10**	**12**	**14**	**16**
Mass of glycine (g)	0.11	0.11	0.11	0.11	0.11
Volume of 1.5M Tris + 0.4% SDS pH8.8 buffer (mL)	3.75	3.75	3.75	3.75	3.75
Volume of 10% SDS (mL)	1	1	1	1	1
Volume of MQ water (mL)	1.518	-----	-----	-----	-----
Volume of 100% glycerol (mL)	6	6	6	4.50	4.50
Volume of 40% Bis-Acrylamide mix (mL)	3	3.75	4.50	5.25	6
Volume of 10% APS (µL)	120	120	120	120	120
Volume of TEMED (µL)	24	24	24	24	24
Total vol (mL)	15	15	15	15	15
Running buffer to use	1X with 40% glycerol	1X	1X	1X	1X

Appendix 4. Molecular weights of Protein Targets (based on antibody data sheets)

No	Protein	Molecular weight /kDA
1	galectin-1	14
2	TGFb2	25
3	α-SMA	42
4	CTGF	38
5	desmin	53
6	vimentin	57
7	Slow myosin heavy chain	220
8	Fast myosin heavy chain-2B	220
9	p38	38
10	phospho-p38	43
11	ERK1	44
12	ERK2	42
13	phospho-ERK1	44
14	phospho-ERK2	42
15	SMAD2	60
16	SMAD3	50
17	phospho-SMAD2	60
18	phospho-SMAD3	50
19	α-tubulin	55
20	R-spondin-1	39
21	myogenin	34
22	myoD	45

Appendix 5. Relative Quantification (RQ) data

RQ values are shown in means and standard deviation, n=3 per treatment group.

Post Repair Week: 2 Weeks

Group	NegC	PosC	DN	PN	RN
N	3	3	3	3	3
EGF	0.561 (0.024)	1.247 (0.041)	0.521 (0.016)	1.1400 (0.021)	0.2826 (0.001)
HGF	3.431 (0.015)	0.0317 (0.000)	2.3376 (0.048)	7.5483 (0.037)	1.2353 (0.093)
Galectin-1	0.360 (0.034)	0.024 (0.003)	0.3456 (0.002)	0.544 (0.041)	0.2463 (0.006)
Myostatin	0.954 (0.002)	0.218 (0.008)	0.1496 (0.042)	0.1653 (0.001)	0.4496 (0.031)
Aggrecan	47.869 (0.792)	0.0449 (0.007)	42.593 (1.921)	12.414 (1.225)	24.620 (0.208)
TGFβ2	0.007 (7.023)	0.0117 (0.001)	0.4363 (0.022)	0.2623 (0.006)	0.0231 (0.002)
Collagen 1A	14.718 (2.411)	0.0040 (0.003)	25.213 (4.873)	14.354 (2.560)	23.793 (4.581)
Follistatin	5.570 (0.420)	1.4783 (0.017)	18.455 (0.113)	5.5201 (0.292)	6.849 (0.048)
Decorin	1.418 (0.400)	0.7386 (0.083)	2.6396 (0.250)	2.5736 (0.014)	1.4256 (0.375)
IGF1	3.740 (0.034)	0.1343 (0.003)	0.2313 (0.011)	0.3846 (0.001)	0.3246 (0.011)
Slow Troponin-I	0.151 (0.002)	0.0353 (0.002)	0.348 (0.000)	0.0533 (0.000)	0.3796 (0.010)
Fast Troponin-I	2.2678 (0.017)	0.4483 (0.004)	0.1966 (0.007)	2.2673 (0.025)	13.329 (1.235)
GAP43	2.993 (0.164)	0.0144 (0.002)	1.438 (0.023)	1.5366 (0.015)	2.67 (0.026)
HN1	0.4773 (0.206)	0.0916 (0.002)	0.449 (0.041)	0.274 (0.004)	0.325 (0.190)
Mhc3, embryonic	156.95 (6.412)	2.0276 (0.014)	76.603 (2.269)	63.824 (1.841)	77.206 (2.081)
Myogenin	12.482 (0.100)	2.6596 (0.024)	10.371 (0.365)	1.914 (0.064)	6.66 (0.027)
MEFf2A	2.9286 (0.003)	2.4173 (0.210)	1.5726 (0.021)	0.4437 (0.018)	1.3303 (0.029)
MyoD	1.656 (0.010)	1.5143 (0.268)	1.0403 (0.015)	0.5466 (0.015)	1.7436 (0.043)
Mhc7, slow	0.3546 (0.002)	1.5528 (0.021)	0.126 (0.004)	0.1166 (0.003)	0.246 (0.002)
Mhc4,fast	0.5615 (0.024)	1.2582 (0.033)	0.2517 (0.002)	0.35 (0.020)	0.8596 (0.018)
Sirt1	2.9526 (0.026)	1.5503 (0.032)	0.648 (0.027)	0.1588 (0.018)	3.2756 (0.068)
GDNF	18.504 (0.095)	0.0288 (0.000)	45.463 (0.101)	4.3611 (0.021)	14.996 (2.750)
Shh	5.1596 (0.008)	0.0067 (0.000)	4.6673 (0.276)	8.3193 (0.486)	5.6623 (0.147)
PGC-1A	2.4663 (0.311)	1.1812 (0.060)	1.2613 (0.018)	1.7346 (0.033)	5.3616 (0.289)
MuRF-1	3.2543 (0.018)	0.0014 (3.785)	1.1063 (0.002)	0.2643 (0.003)	2.174 (0.000)
Atrogin-1	2.5396 (0.030)	0.0016 (0.000)	1.641 (0.143)	0.518 (0.000)	1.4476 (0.039)
Complement-3	22.608 (0.161)	0.0307 (0.030)	11.392 (1.064)	2.9605 (0.017)	12.286 (0.170)
Calpain-3	0.225 (0.006)	1.3406 (0.103)	0.2783 (0.020)	1.944 (0.034)	0.2943 (0.003)
CNTF	0.5506 (0.037)	1.479 (0.008)	0.256 (0.003)	0.1133 (0.013)	1.8046 (0.002)
AMPK	1.972 (0.028)	0.4676 (0.006)	1.054 (0.017)	0.354 (0.004)	4.4383 (0.022)
NT4	0.246 (0.002)	1.14 (0.026)	0.7716 (0.013)	14.280 (0.311)	1.2553 (0.089)
Desmin	0.408 (0.005)	0.077 (0.051)	0.282 (0.003)	0.190 (0.011)	0.104 (0.004)
Vimentin	1.350 (0.063)	0.063 (0.002)	0.425 (0.004)	2.817 (0.129)	0.244 (0.003)
Nestin	0.397 (0.001)	0.041 (0.001)	0.481 (0.005)	0.132 (0.002)	0.572.(0.001)

Post Repair Week: **12 Weeks**

Group	NegC	PosC	DN	PN	RN
N	3	3	3	5	3
EGF	0.2283 (0.021)	1.2168 (0.014)	2.442 (0.309)	3.2406 (0.049)	0.4313 (0.011)
HGF	0.87 (0.021)	0.0349 (0.003)	0.557 (0.036)	0.741 (0.027)	1.7323 (0.123)
Galectin-1	0.1623 (0.039)	0.023 (0.002)	0.1653 (0.028)	0.1138 (0.002)	0.197 (0.002)
Myostatin	0.771 (0.015)	0.2365 (0.037)	0.8563 (0.021)	0.1056 (0.002)	0.566 (0.004)
Aggrecan	4.6276 (0.286)	0.0226 (0.015)	7.6986 (0.133)	0.2432 (0.038)	2.158 (0.033)
TGFβ2	0.0245 (0.001)	0.0119 (0.000)	0.219 (0.008)	0.0181 (0.004)	0.0225 (0.001)
Collagen 1A	6.221 (0.065)	0.0040 (0.002)	15.765 (0.160)	3.2546 (0.337)	0.136 (0.028)
Follistatin	2.5653 (0.211)	1.423 (0.013)	8.133 (0.028)	2.3658 (0.109)	1.3883 (0.105)
Decorin	1.4186 (0.029)	0.5655 (0.349)	2.5103 (0.417)	11.286 (0.257)	0.6413 (0.045)
IGF1	0.1683 (0.023)	0.1337 (0.003)	0.154 (0.003)	0.0158 (0.002)	0.109 (0.004)
Slow Troponin-I	0.3472 (0.024)	0.0348 (0.003)	4.479 (0.337)	0.0428 (0.001)	0.3763 (0.006)
Fast Troponin-I	0.6238 (0.023)	0.4197 (0.008)	0.143 (0.021)	0.4528 (0.028)	1.6343 (0.274)
GAP43	1.3516 (0.214)	0.0146 (0.002)	0.5973 (0.065)	0.8562 (0.026)	0.8226 (0.111)
HN1	0.371 (0.050)	0.096 (0.002)	0.2326 (0.002)	0.5368 (0.005)	0.528 (0.000)
Mhc3, embryonic	17.930 (2.731)	2.0512 (0.023)	29.44 (0.426)	12.832 (1.085)	3.376 (0.012)
Myogenin	9.503 (0.041)	2.6532 (0.022)	10.816 (0.166)	1.6616 (0.042)	3.5496 (0.033)
MEF2A	2.3806 (0.016)	2.3257 (0.253)	3.1533 (0.007)	0.7274 (0.014)	1.334 (0.041)
MyoD	1.952 (0.012)	1.639 (0.069)	4.4956 (0.299)	2.4596 (0.014)	2.4883 (0.568)
Mhc7, slow	0.112 (0.001)	1.5251 (0.013)	0.4563 (0.025)	0.2248 (0.003)	0.2294 (0.005)
Mhc4,fast	0.2634 (0.042)	1.276 (0.025)	0.0433 (0.003)	1.1356 (0.029)	1.1252 (0.021)
Sirt1	0.9266 (0.020)	1.5388 (0.010)	1.5629 (0.032)	3.4362 (0.270)	1.6446 (0.042)
GDNF	11.499 (0.241)	0.0235 (0.003)	17.783 (2.040)	2.2266 (0.023)	7.496 (0.431)
Shh	1.334 (0.150)	0.0051 (0.003)	2.0489 (0.028)	1.6432 (0.032)	6.6096 (0.364)
PGC-1A	0.119 (0.023)	1.1709 (0.050)	3.4966 (0.236)	0.2608 (0.021)	14.995 (2.615)
MuRF-1	1.552 (0.029)	0.0014 (3.872)	3.4423 (0.029)	0.3646 (0.003)	1.274 (0.019)
Atrogin-1	1.3713 (0.022)	0.0013 (0.000)	3.7636 (0.026)	0.325 (0.002)	0.8763 (0.061)
Complement-3	3.6280 (0.025)	0.0419 (0.030)	6.6664 (0.110)	1.8367 (0.012)	8.418 (0.726)
Calpain-3	0.5953 (0.003)	1.4335 (0.051)	0.1496 (0.025)	0.452 (0.035)	0.9473 (0.031)
CNTF	0.8364 (0.024)	1.4287 (0.035)	1.349 (0.021)	1.9340 (0.018)	0.4886 (0.004)
AMPK	1.5496 (0.004)	0.4427 (0.034)	0.4836 (0.003)	2.9613 (0.020)	1.3478 (0.019)
NT4	0.0657 (0.004)	1.1375 (0.018)	24.869 (3.530)	0.5672 (0.014)	13.682 (0.843)
Desmin	0.216 (0.008)	0.131 (0.010)	0.128 (0.034)	0.131 (0.019)	0.205 (0.008)
Vimentin	0.107 (0.002)	0.063 (0.003)	0.821 (1.073)	0.215 (0.004)	0.024 (0.006)
Nestin	0.104 (0.002)	0.043 (0.002)	0.203 (0.001)	0.074 (0.003)	0.103 (0.002)

Appendix 6. Homogenous Subset Tables for RQ data.

ANOVA with post-hoc comparison using Scheffe's for real-time PCR data (SPSS Inc.)

MuRF1

	n	Subset for alpha = 0.05								
		1	2	3	4	5	6	7	8	9
PosC2	3	.00								
PosC12	4	.00								
PN2	3		.26							
PN12	5			.36						
DN2	3				1.11					
RN12	3					1.27				
NegC12	3						1.55			
RN2	3							2.17		
NegC2	3								3.25	
DN12	3									3.44
Sig.		1.00	1.00	1.00	1.00	1.00	1.00	1.00	1.00	1.00

Atrogin-1

	n	Subset for alpha = 0.05							
		1	2	3	4	5	6	7	8
PosC12	4	.00							
PosC2	3	.00							
PN12	5		.33						
PN2	3			.52					
RN12	3				.88				
NegC12	3					1.37			
RN2	3					1.45			
DN2	3						1.64		
NegC2	3							2.54	
DN12	3								3.76
Sig.		1.00	1.00	1.00	1.00	.91	1.00	1.00	1.00

Myostatin

	n	Subset for alpha = 0.05							
		1	2	3	4	5	6	7	8
PN12	5	.11							
DN2	3	.15	.15						
PN2	3	.17	.17	.17					
PosC2	3		.22	.22					
PosC12	4			.24					
RN2	3				.45				
RN12	3					.57			
NegC12	3						.77		
DN12	3							.86	
NegC2	3								.95
Sig.		.29	.15	.12	1.00	1.00	1.00	1.00	1.00

TGF-β2

	n	Subset for alpha = 0.05			
		1	2	3	4
NegC2	3	.0071			
PosC2	3	.0118			
PosC12	4	.0120			
PN12	5	.0182			
RN12	3	.0226			
RN2	3	.0230			
NegC12	3	.0245			
DN12	3		.2190		
PN2	3			.2623	
DN2	3				.4363
Sig.		.530	1.000	1.000	1.000

Decorin

	n	Subset for alpha = 0.05		
		1	2	3
PosC12	4	.57		
RN12	3	.64		
PosC2	3	.74		
NegC2	3	1.42		
NegC12	3	1.42		
RN2	3	1.43		
DN12	3		2.51	
PN2	3		2.57	
DN2	3		2.64	
PN12	5			11.29
Sig.		.13	1.00	1.00

Follistatin

	n	Subset for alpha = 0.05					
		1	2	3	4	5	6
RN12	3	1.39					
PosC12	4	1.42					
PosC2	3	1.48					
PN12	5		2.37				
NegC12	3		2.57				
PN2	3			5.52			
NegC2	3			5.57			
RN2	3				6.85		
DN12	3					8.13	
DN2	3						18.46
Sig.		1.00	0.99	1.00	1.00	1.00	1.00

Aggrecan

	n	Subset for alpha = 0.05						
		1	2	3	4	5	6	7
PosC12	4	.0227						
PosC2	3	.0449						
PN12	5	.2432						
RN12	3	2.1580	2.1580					
NegC12	3		4.6277					
DN12	3			7.6987				
PN2	3				12.4143			
RN2	3					24.6207		
DN2	3						42.5930	
NegC2	3							47.8697
Sig.		.185	.074	1.000	1.000	1.000	1.000	1.000

Galectin-1

	n	Subset for alpha = 0.05					
		1	2	3	4	5	6
PosC12	4	0.02					
PosC2	3	0.02					
PN12	5		0.11				
NegC12	3		0.16	0.16			
DN12	3		0.17	0.17			
RN12	3			0.20	0.20		
RN2	3				0.25		
DN2	3					0.35	
NegC2	3					0.36	
PN2	3						0.54
Sig.		1.00	0.45	0.89	0.51	1.00	1.00

CNTF

	n	Subset for alpha = 0.05							
		1	2	3	4	5	6	7	8
PN2	3	0.11							
DN2	3		0.26						
RN12	3			0.49					
NegC2	3			0.55					
NegC12	3				0.84				
DN12	3					1.35			
PosC12	4						1.43		
PosC2	3						1.48		
RN2	3							1.81	
PN12	5								1.93
Sig.		1.00	1.00	0.21	1.00	1.00	0.48	1.00	1.00

EGF

	n	Subset for alpha = 0.05			
		1	2	3	4
NegC12	3	0.23			
RN2	3	0.28			
RN12	3	0.43			
DN2	3	0.52			
NegC2	3	0.56			
PN2	3		1.14		
PosC12	4		1.22		
PosC2	3		1.25		
DN12	3			2.44	
PN12	5				3.24
Sig.		0.07	0.99	1.00	1.00

HGF

	n	Subset for alpha = 0.05							
		1	2	3	4	5	6	7	8
PosC2	3	0.03							
PosC12	4	0.04							
DN12	3		0.56						
PN12	5		0.74	0.74					
NegC12	3			0.87					
RN2	3				1.24				
RN12	3					1.73			
DN2	3						2.34		
NegC2	3							3.43	
PN2	3								7.55
Sig.		1.00	0.06	0.41	1.00	1.00	1.00	1.00	1.00

GDNF

	n	Subset for alpha = 0.05					
		1	2	3	4	5	6
PosC12	4	0.02					
PosC2	3	0.03					
PN12	5	2.23	2.23				
PN2	3		4.36	4.36			
RN12	3			7.50			
NegC12	3				11.50		
RN2	3				15.00	15.00	
DN12	3					17.78	
NegC2	3					18.50	
DN2	3						45.46
Sig.		0.60	0.64	0.15	0.07	0.07	1.00

Calpain3

	n	Subset for alpha = 0.05				
		1	2	3	4	5
DN12	3	0.15				
NegC2	3	0.23				
DN2	3	0.28				
RN2	3	0.29				
PN12	5		0.45			
NegC12	3		0.60			
RN12	3			0.95		
PosC2	3				1.34	
PosC12	4				1.43	
PN2	3					1.94
Sig.		0.07	0.08	1.00	0.57	1.00

PGC-1α

	n	Subset for alpha = 0.05			
		1	2	3	4
NegC12	3	0.12			
PN12	5	0.26			
PosC12	4	1.18	1.18		
PosC2	3	1.18	1.18		
DN2	3	1.26	1.26		
PN2	3	1.73	1.73		
NegC2	3	2.47	2.47		
DN12	3		3.50	3.50	
RN2	3			5.36	
RN12	3				15.00
Sig.		0.18	0.19	0.47	1.00

NT4

	n	Subset for alpha = 0.05		
		1	2	3
NegC12	3	0.07		
NegC2	3	0.25		
PN12	5	0.57		
DN2	3	0.77		
PosC12	4	1.14		
PosC2	3	1.14		
RN2	3	1.26		
RN12	3		13.68	
PN2	3		14.28	
DN12	3			24.87
Sig.		0.99	1.00	1.00

IGF-1

	n	Subset for alpha = 0.05						
		1	2	3	4	5	6	7
PN12	5	0.02						
RN12	3		0.11					
PosC12	4		0.13	0.13				
PosC2	3		0.13	0.13				
DN12	3		0.15	0.15				
NegC12	3			0.17				
DN2	3				0.23			
RN2	3					0.33		
PN2	3						0.39	
NegC2	3							3.74
Sig.		1.00	0.09	0.35	1.00	1.00	1.00	1.00

Complement-3

	n	Subset for alpha = 0.05						
		1	2	3	4	5	6	7
PosC2	3	0.03						
PosC12	4	0.04						
PN12	5		1.84					
PN2	3		2.96	2.96				
NegC12	3			3.63				
DN12	3				6.67			
RN12	3					8.42		
DN2	3						11.39	
RN2	3						12.29	
NegC2	3							22.61
Sig.		1.00	0.21	0.84	1.00	1.00	0.51	1.00

Myosin Heavy Chain-Embryonic

	n	Subset for alpha = 0.05					
		1	2	3	4	5	6
PosC2	3	2.03					
PosC12	4	2.05					
RN12	3	3.38					
PN12	5		12.83				
NegC12	3		17.93				
DN12	3			29.44			
PN2	3				63.82		
DN2	3					76.60	
RN2	3					77.21	
NegC2	3						156.96
Sig.		1.00	0.59	1.00	1.00	1.00	1.00

Myosin Heavy Chain-Slow

	n	Subset for alpha = 0.05				
		1	2	3	4	5
NegC12	3	0.11				
PN2	3	0.12				
DN2	3	0.13				
PN12	5		0.23			
RN12	3		0.23			
RN2	3		0.25			
NegC2	3			0.36		
DN12	3				0.46	
PosC12	4					1.53
PosC2	3					1.55
Sig.		0.98	0.78	1.00	1.00	0.45

Myosin Heavy Chain-Fast

	n	Subset for alpha = 0.05						
		1	2	3	4	5	6	7
DN12	3	0.04						
DN2	3		0.25					
NegC12	3		0.26	0.26				
PN2	3			0.35				
NegC2	3				0.56			
RN2	3					0.86		
RN12	3						1.13	
PN12	5						1.14	
PosC2	3							1.26
PosC12	4							1.28
Sig.		1.00	1.00	0.08	1.00	1.00	1.00	1.00

AMPK-1α

	n	Subset for alpha = 0.05							
		1	2	3	4	5	6	7	8
PN2	3	0.35							
PosC12	4		0.44						
PosC2	3		0.47						
DN12	3		0.48						
DN2	3			1.05					
RN12	3				1.35				
NegC12	3					1.55			
NegC2	3						1.97		
PN12	5							2.96	
RN2	3								4.44
Sig.		1.00	0.68	1.00	1.00	1.00	1.00	1.00	1.00

Sirt-1

	n	Subset for alpha = 0.05				
		1	2	3	4	5
PN2	3	0.16				
DN2	3		0.65			
NegC12	3		0.93			
PosC12	4			1.54		
PosC2	3			1.55		
DN12	3			1.56		
RN12	3			1.65		
NegC2	3				2.95	
RN2	3				3.28	3.28
PN12	5					3.44
Sig.		1.00	0.46	1.00	0.26	0.95

Slow Troponin-I

	n	Subset for alpha = 0.05	
		1	2
PosC12	4	0.04	
PosC2	3	0.04	
PN12	5	0.04	
PN2	3	0.05	
NegC2	3	0.15	
NegC12	3	0.35	
DN2	3	0.35	
RN12	3	0.38	
RN2	3	0.38	
DN12	3		4.48
Sig.		0.07	1.00

Fast Troponin-I

	n	Subset for alpha = 0.05			
		1	2	3	4
DN12	3	0.14			
DN2	3	0.20			
PosC12	4	0.42	0.42		
PosC2	3	0.45	0.45		
PN12	5	0.45	0.45		
NegC12	3	0.62	0.62		
RN12	3		1.63	1.63	
PN2	3			2.27	
NegC2	3			2.27	
RN2	3				13.33
Sig.		0.97	0.11	0.85	1.00

Sonic Hedgehog

	n	Subset for alpha = 0.05					
		1	2	3	4	5	6
PosC12	4	0.01					
PosC2	3	0.01					
NegC12	3		1.33				
PN12	5		1.64				
DN12	3		2.05				
DN2	3			4.67			
NegC2	3			5.16	5.16		
RN2	3				5.66		
RN12	3					6.61	
PN2	3						8.32
Sig.		1.00	0.07	0.46	0.43	1.00	1.00

MyoD

	n	Subset for alpha = 0.05				
		1	2	3	4	5
PN2	3	0.55				
DN2	3	1.04	1.04			
PosC2	3		1.51	1.51		
PosC12	4		1.64	1.64		
NegC2	3		1.66	1.66		
RN2	3		1.74	1.74	1.74	
NegC12	3			1.95	1.95	
PN12	5				2.46	
RN12	3				2.49	
DN12	3					4.50
Sig.		0.46	0.08	0.63	0.05	1.00

Myogenin

	n	Subset for alpha = 0.05						
		1	2	3	4	5	6	7
PN12	5	1.66						
PN2	3	1.91						
PosC12	4		2.65					
Posc2	3		2.66					
RN12	3			3.55				
RN2	3				6.66			
NegC12	3					9.50		
DN2	3						10.37	
DN12	3						10.82	
NegC2	3							12.48
Sig.		.69	1.00	1.00	1.00	1.00	.06	1.00

MEF2A

	n	Subset for alpha = 0.05			
		1	2	3	4
PN2	3	0.44			
PN12	5	0.73			
RN2	3		1.33		
RN12	3		1.33		
DN2	3		1.57		
PosC12	4			2.33	
NegC12	3			2.38	
PosC2	3			2.42	
NegC2	3				2.93
DN12	3				3.15
Sig.		0.38	0.60	1.00	0.69

Nestin

	n	Subset for alpha = 0.05							
		1	2	3	4	5	6	7	8
PosC2	3	0.04							
PosC12	4	0.04							
PN12	5		0.07						
RN12	3			0.10					
NegC12	3			0.10					
PN2	3				0.13				
DN12	3					0.20			
NegC2	3						0.40		
DN2	3							0.48	
RN2	3								0.57
Sig.		1.00	1.00	1.00	1.00	1.00	1.00	1.00	1.00

Vimentin

	n	Subset for alpha = 0.05	
		1	2
RN12	3	0.02	
PosC12	4	0.06	
PosC2	3	0.06	
NegC12	3	0.11	
NegC2	3	0.14	
PN12	5	0.22	
RN2	3	0.24	
DN2	3	0.43	
DN12	3	0.82	
PN2	3		2.82
Sig.		0.39	1.00

Desmin

	n	Subset for alpha = 0.05			
		1	2	3	4
PosC2	3	0.10			
RN2	3	0.10			
DN12	3	0.13			
PosC12	4	0.13			
PN12	5	0.13			
PN2	3		0.19		
RN12	3		0.21		
NegC12	3		0.22		
DN2	3			0.28	
NegC2	3				0.41
Sig.		0.67	0.78	1.00	1.00

Collagen-1α

	n	Subset for alpha = 0.05			
		1	2	3	4
PosC2	3	0.00			
PosC12	4	0.00			
RN12	3	0.14			
PN12	5	3.26			
NegC12	3	6.22			
PN2	3		14.36		
NegC2	3		14.72		
DN12	3		15.77	15.77	
RN2	3			23.79	23.79
DN2	3				25.21
Sig.		0.25	1.00	0.05	1.00

HN-1

	n	Subset for alpha = 0.05	
		1	2
PosC2	3	0.09	
PosC12	4	0.10	
DN12	3	0.23	0.23
PN2	3	0.27	0.27
RN2	3	0.33	0.33
NegC12	3	0.37	0.37
DN2	3		0.45
NegC2	3		0.48
RN12	3		0.53
PN12	5		0.54
Sig.		0.10	0.06

GAP43

	n	Subset for alpha = 0.05			
		1	2	3	4
PosC2	3	0.01			
PosC12	4	0.02			
DN12	3		0.60		
RN12	3		0.82		
PN12	5		0.86		
NegC12	3			1.35	
DN2	3			1.44	
PN2	3			1.54	
RN2	3				2.67
NegC2	3				2.99
Sig.		1.00	0.21	0.66	0.05

LaminA

	n	Subset for alpha = 0.05	
		1	2
RN12	3	23.30	
NegC	3	23.41	23.41
PN2	3	23.46	23.46
DN2	3	23.51	23.51
PosC12	3	23.91	23.91
NegC12	3	24.08	24.08
DN12	3	24.12	24.12
RN2	3	24.28	24.28
PosC2	3	24.35	24.35
PN12	3		24.49
Sig.		0.12	0.10

Appendix 7. Homogenous Subset Tables for Optical densitometry data

R-Spondin-1

	n	Subset for alpha = 0.05						
		1	2	3	4	5	6	7
Csham2	3	.01						
DN12	3		.47					
PN12	3			.50				
RN12	3				.59			
RN2	3					.68		
DN2	3						.92	
PN2	3							1.00
Sig.		1.00	1.00	1.00	1.00	1.00	1.00	1.00

Vimentin

	n	Subset for alpha = 0.05					
		1	2	3	4	5	6
DN12	3	.25					
RN12	3		.28				
PN12	3		.29				
RN2	3			.34			
Csham2	3				.57		
DN2	3					.75	
PN2	3						.88
Sig.		1.00	.09	1.00	1.00	1.00	1.00

Desmin

	n	Subset for alpha = 0.05					
		1	2	3	4	5	6
DN12	3	.6067					
DN2	3		.7800				
RN2	3			.8233			
PN12	3				.9800		
RN12	3					1.0867	
PosC2	3					1.0967	
PN2	3						1.3933
Sig.		1.000	1.000	1.000	1.000	.436	1.000

α-SMA

	n	Subset for alpha = 0.05				
		1	2	3	4	5
Csham2	3	.71				
RN12	3		1.33			
PN2	3		1.33			
DN12	3			1.39		
DN2	3				1.46	
RN2	3				1.47	
PN12	3					1.57
Sig.		1.00	.97	1.00	.60	1.00

Galectin-1

	n	Subset for alpha = 0.05						
		1	2	3	4	5	6	7
Csham2	3	.50						
DN12	3		.64					
PN12	3			.70				
RN12	3				.84			
RN2	3					1.71		
DN2	3						1.95	
PN2	3							2.38
Sig.		1.00	1.00	1.00	1.00	1.00	1.00	1.00

TGFβ2

	n	Subset for alpha = 0.05						
		1	2	3	4	5	6	7
Csham2	3	.34						
PN12	3		.42					
RN12	3			.57				
DN12	3				.65			
RN2	3					.71		
PN2	3						.78	
DN2	3							.85
Sig.		1.00	1.00	1.00	1.00	1.00	1.00	1.00

CTGF

	n	Subset for alpha = 0.05						
		1	2	3	4	5	6	7
Csham2	3	.87						
PN12	3		1.24					
RN2	3			1.26				
DN2	3				1.54			
DN12	3					1.62		
RN12	3						1.80	
PN2	3							1.96
Sig.		1.00	1.00	1.00	1.00	1.00	1.00	1.00

Myogenin

	n	Subset for alpha = 0.05					
		1	2	3	4	5	6
DN12	3	.31					
RN2	3		.77				
DN2	3			.80			
PN2	3				.82		
PN12	3				.83		
RN12	3					.87	
Csham2	3						1.04
Sig.		1.00	1.00	1.00	.95	1.00	1.00

MyoD

	n	Subset for alpha = 0.05			
		1	2	3	4
PN2	3	.01			
Csham2	3	.01			
DN2	3	.01			
RN2	3	.01			
RN12	3		.11		
PN12	3			.16	
DN12	3				.17
Sig.		.99	1.00	1.00	1.00

phospho-p38 vs α-Tubulin

	n	Subset for alpha = 0.05						
		1	2	3	4	5	6	7
Csham2	3	.24						
PN12	3		.98					
DN2	3			1.21				
RN12	3				1.33			
RN2	3					1.42		
DN12	3						1.63	
PN2	3							1.82
Sig.		1.00	1.00	1.00	1.00	1.00	1.00	1.00

phospho-Erk1 vs α-Tubulin

	n	Subset for alpha = 0.05						
		1	2	3	4	5	6	7
Csham2	3	.04						
RN12	3		.24					
RN2	3			.51				
DN12	3				.54			
PN2	3					.65		
PN12	3						.69	
DN2	3							.86
Sig.		1.00	1.00	1.00	1.00	1.00	1.00	1.00

phospho-Erk2 vs α-Tubulin

	n	Subset for alpha = 0.05						
		1	2	3	4	5	6	7
Csham2	3	.04						
RN12	3		.32					
DN12	3			.56				
RN2	3				.68			
PN2	3					.84		
PN12	3						.89	
DN2	3							.96
Sig.		1.00	1.00	1.00	1.00	1.00	1.00	1.00

phospho-SMAD2 vs Tubulin

	n	Subset for alpha = 0.05					
		1	2	3	4	5	6
Csham2	3	.04					
RN2	3		.50				
RN12	3		.51				

PN2	3			.61			
PN12	3				.63		
DN2	3					.84	
DN12	3						.86
Sig.		1.00	.06	1.00	1.00	1.00	1.00

phospho-SMAD3 vs α-Tubulin

	n	Subset for alpha = 0.05						
		1	2	3	4	5	6	7
Csham2	3	.04						
RN2	3		.36					
DN2	3			.41				
RN12	3				.42			
PN12	3					.43		
DN12	3						.52	
PN2	3							.64
Sig.		1.00	1.00	1.00	1.00	1.00	1.00	1.00

phospho-p38 vs Total p38

	n	Subset for alpha = 0.05					
		1	2	3	4	5	6
Csham2	3	.23					
PN12	3		.55				
RN12	3			.56			
DN12	3				.60		
DN2	3					.61	
PN2	3					.61	
RN2	3						.63
Sig.		1.00	1.00	1.00	1.00	.74	1.00

phospho-Erk1 vs Total Erk

	n	Subset for alpha = 0.05					
		1	2	3	4	5	6
Csham2	3	.03					
RN12	3		.15				
DN12	3			.45			
PN2	3				.49		
RN2	3					.65	
DN2	3						.72
PN12	3						.72

Sig.		1.00	1.00	1.00	1.00	1.00	.74

phospho-Erk2 vs Total Erk

	n	Subset for alpha = 0.05						
		1	2	3	4	5	6	7
Csham2	3	.03						
RN12	3		.20					
DN12	3			.47				
PN2	3				.63			
DN2	3					.80		
RN2	3						.86	
PN12	3							.94
Sig.		1.00	1.00	1.00	1.00	1.00	1.00	1.00

phospho-SMAD2 vs Total SMAD

	n	Subset for alpha = 0.05						
		1	2	3	4	5	6	7
Csham2	3	.07						
RN12	3		.50					
RN2	3			.56				
PN2	3				.84			
DN12	3					.98		
PN12	3						1.21	
DN2	3							1.26
Sig.		1.00	1.00	1.00	1.00	1.00	1.00	1.00

phospho-SMAD3 vs Total SMAD

	n	Subset for alpha = 0.05					
		1	2	3	4	5	6
Csham2	3	.08					
RN2	3		.40				
RN12	3		.41				
DN12	3			.59			
DN2	3				.62		
PN12	3					.83	
PN2	3						.87
Sig.		1.00	.31	1.00	1.00	1.00	1.00

Myosin Heavy Chain-Slow

	n	Subset for alpha = 0.05				
		1	2	3	4	5

PN12	3	.62				
DN12	3		.63			
RN2	3			.66		
Csham2	3			.67		
RN12	3				.78	
PN2	3					.80
DN2	3					.80
Sig.		1.00	1.00	.09	1.00	1.00

Myosin Heavy Chain-Fast (2b)

	n	Subset for alpha = 0.05						
		1	2	3	4	5	6	7
DN12	3	.14						
RN12	3		.19					
DN2	3			.26				
PN12	3				.36			
PN2	3					.38		
RN2	3						.49	
Csham2	3							.58
Sig.		1.00	1.00	1.00	1.00	1.00	1.00	1.00

Alpha-tubulin

	n	Subset for alpha = 0.05			
		1	2	3	4
PosC2	3	0.00			
NegC2	3	0.00			
NegC12	3	0.00			
PN12	3		2920.33		
DN12	3		2927.00	2927.00	
RN2	3		2940.00	2940.00	2940.00
PosC12	3			2965.00	2965.00
PN2	3			2965.00	2965.00
Sig.		1.00	0.88	0.13	0.35

Appendix 8. Overall Relative Fold Change of the Gene Expression for All Markers

	Gene	PN	DN	RN	NegC
1	Embryonic myosin HC	**-50.99***	**-47.16#**	-73.84	**-139.02***
2	Fast myosin HC	0.79	**-0.21#**	**0.27***	**-0.29***
3	Slow myosin HC	0.11	**0.33#**	-0.02	-0.24*
4	Fast troponin-I	-1.81	-0.054	-11.69*	-1.64
5	Slow troponin-I	-0.01	**4.13#**	-0.01	0.20
6	Atrogin-1	**-0.19*,#**	**2.12*,#**	**-0.57#**	**-1.17***
7	MuRF-1	0.10	**2.34*,#**	**-0.90*#**	**-1.70*,#**
8	Myogenin	-0.25	0.45	**-3.11*#**	**-2.98*,#**
9	TGFb2	**-0.24***	**-0.22*,#**	-0.01	0.02
10	AMPK	**2.61*,#**	**-0.57***	**-3.09*,#**	**-0.42*#**
11	Decorin	**8.71#**	-0.13	-0.78	0.01
12	Follistatin	-3.15	**-10.32*,#**	**-5.46***	-3.00
13	HGF	**-6.81***	**-1.78***	**0.50*,#**	**-2.56***
14	EGF	**2.10#**	**1.92#**	0.15	-0.33
15	IGF-1	**-0.37*#**	**-0.08***	**-0.22***	**-3.58***
16	NT-4	-13.71	**24.10#**	12.43	-0.18
17	GDNF	-2.13	**-27.68***	-7.51	-7.00
18	CNTF	**1.82*,#**	**1.09*,#**	**-1.32***	**0.29#**
19	Sonic Hedgehog	**-6.68***	-2.62	**0.95#**	-3.83
20	Calpain-3	**-1.49***	-0.13	**0.65#**	0.37
21	PGC-1a	-1.48	2.24	**9.64#**	-2.35
22	Sirt-1	**3.28***	0.92	-1.63	-2.03
23	Galectin-1	**-0.43***	-0.18	-0.05	-0.20
24	Complement-3	-1.12	**-4.73#**	**-3.88#**	**-18.99***
25	Collagen-1	-11.10	-9.45	-23.66	-8.50
26	Aggrecan	**-12.17***	**-34.89*,#**	**-22.46***	**-43.24***
27	myoD	1.91	**3.46#**	0.75	0.30
28	Mef-2a	0.28	1.58	0.01	-0.55
29	Desmin	0.02	**-0.15***	0.10	**-0.19***
30	Vimentin	**-1.48***	4.00	-0.22	-0.03
31	Nestin	**-0.01*#**	**-0.28*#**	**-0.47***	**-0.29***
32	GAP-43	-0.68	-0.84	-1.85	-1.64
33	HN-1	0.26	-0.21	0.20	-0.11
34	Myostatin	-0.06	**0.71#**	**0.12*,#**	**-0.18*,#**

Note: Statistics in bold: * $p<0.05$ at 2-weeks, # $p<0.05$ at 12-weeks

Appendix 9. Summary of techniques used to detect expression level of each marker

No	Marker	Real-time PCR	Western Blot	Immuno-histochemistry
1	Neurotrophic factor-4, NT-4	√		
2	Glial derived neurotrophic factor, GDNF	√		
3	Ciliary neurotrophic factor CNTF	√		
4	Insulin-like growth factor, IGF1	√		
5	Hepatocyte Growth Factor, HGF	√		
6	Epidermal Growth Factor,EGF	√		
7	Sonic hedgehog, Shh	√		
8	MyoD	√	√	
9	Myogenin	√	√	
10	MEF2A	√		
11	Desmin	√	√	√
12	Vimentin	√	√	√
13	Nestin	√		√
14	Atrogin-1	√		
15	MuRF-1	√		
16	Peroxisome proliferator activated receptor-gamma co-activator, alpha, PGC-1α	√		
17	Sirt-1	√		
18	Myostatin	√		
19	Calpain-3	√		
20	Complement 3	√		
21	AMP-activated protein kinase alpha 1 subunit, AMPK-1a	√		
22	Follistatin	√		
23	Transforming Growth Factor beta 2, TGFβ2	√	√	
24	Collagen Type 1 alpha, Col-1a	√		
25	aggrecan (chondroitin sulphate proteoglycan-1)	√		
26	Galectin-1	√	√	√
27	Decorin	√		
28	Fast skeletal troponin-I	√		
29	Embryonic myosin heavy chain 3	√		
30	Fast skeletal myosin heavy chain 4	√	√	
31	Slow skeletal myosin heavy chain 7	√	√	
32	Slow skeletal troponin-I	√		
33	Lamin A	√		
34	Hematological and neurological expressed-1, HN1	√		
35	Growth associated protein 43, GAP43	√		
36	alpha-tubulin		√	
37	Connective tissue growth factor		√	
38	alpha-smooth muscle actin, a-SMA		√	
39	Erk1 and 2 and phospho-Erk 1 and 2		√	
40	SMAD 2 and 3 and phospho-SMAD2 and 3		√	
41	p38 and phospho-p38		√	
42	R-spondin-1		√	√

Note: Gene expression assays for R-spondin-1, a-SMA and CTGF were not done because the respective Taqman primers were made-to-order.

Appendix 10. Optical Densitometry values for Western Blot Data

OD values are shown in means ± standard deviation, n=3 per treatment group. NegC is not included in the analysis because the samples were exhausted in previous projects.

2 weeks

Group	**PosC**	**DN-2**	**PN-2**	**RN-2**
Sample size	3	3	3	3
R-spondin-1	0.0053(0.00088)	0.91(0.0018)	0.99 (0.012)	0.67(0.00075)
CTGF	0.86(0.0021)	1.53(0.0026)	1.96(0.0014)	1.25(0.0014)
a-SMA	0.70 (0.0033)	1.46 (0.0012)	1.33 (0.00204)	1.46 (0.0016)
Galectin-1	0.50 (0.0030)	1.95 (0.0010)	2.37 (0.0026)	1.70 (0.0020)
TGFb2	0.34 (0.00067)	0.85 (0.0015)	0.77 (0.0024)	0.71 (0.0018)
Desmin	1.09 (0.00084)	0.77 (0.0017)	1.39 (0.0024)	0.82 (0.0026)
Vimentin	0.568 (0.0023)	0.74 (0.0011)	0.88 (0.0028)	0.34 (0.0033)
myoD	0.0052 (0.00069)	0.0073 (0.00066)	0.0059 (0.0016)	0.0068 (0.00032)
myogenin	1.03 (0.00088)	0.79 (0.012)	0.82 (0.00081)	0.77 (0.0015)
fast myosin heavy chain-2B	0.58 (0.0018)	0.26 (0.0016)	0.37 (0.0020)	0.48 (0.0011)
slow myosin heavy chain	0.66 (0.0022)	0.80 (0.002015508)	0.79 (0.0026)	0.66 (0.0020)

12 weeks

Group	**PosC**	**DN-12**	**PN-12**	**RN-12**
Sample size	3	3	3	3
R-spondin-1	0	0.46 (0.0032)	0.29 (0.28)	0.58 (0.0029)
CTGF	0	1.62 (0.0013)	0.74 (0.71)	1.79 (0.0027)
a-SMA	0	1.39 (0.0021)	0.94 (0.90)	1.32 (0.0027)
Galectin-1	0	0.64 (0.0025)	0.41 (0.40)	0.83 (0.0015)
TGFb2	0	0.65 (0.0012)	0.24 (0.23)	0.56 (0.0023)
Desmin	0	0.60 (0.0022)	0.58 (0.56)	1.08 (0.0029)
Vimentin	0	0.25 (0.0016)	0.17 (0.16)	0.27 (0.00077)
myoD	0	0.17 (0.00079)	0.092 (0.087)	0.11 (0.0016)
myogenin	0	0.30 (0.00091)	0.49 (0.48)	0.86 (0.0011)
fast myosin heavy chain-2B	0	0.14 (0.0012)	0.211 (0.206)	0.18 (0.0016)
slow myosin heavy chain	0	0.62 (0.0021)	0.37 (0.36)	0.77 (0.0039)

Appendix 11. Overall Relative Fold Change of the Protein Expression for Selected Markers

Protein	PN	p-value	DN	p-value	RN	p-value
R-spondin-1	0.298	*#	0.509	*#	0.866	*#
CTGF	0.379	*#	1.057	*#	1.430	*#
a-SMA	0.710	#	0.952	#	0.905	nil
Galectin-1	0.176	*#	0.328	*#	0.4918	*#
TGFb2	0.320	*#	0.768	*#	0.7991	*#
Desmin	0.423	*#	0.779	*#	1.3157	*
Vimentin	0.195	*	0.339	*#	0.803	*
myoD	15.603	#	23.794	#	16.445	#
myogenin	0.606	nil	0.386	*#	1.118	*#
slow myosin heavy chain	0.467	#	0.784	#	1.178	#
fast myosin heavy chain-2B	0.568	*#	0.544	*#	0.379	*#

Note:

* $p<0.05$ at 2-weeks

# $p<0.05$ at 12-weeks

Appendix 12. Pearson Correlation Analysis for Selected Markers

RQ and OD triplicates were in the Pearson correlation analysis. Selected markers from each category were set as the dependent and independent variables. Pearson correlation coefficients (r) and the significance levels are reported as follows:

1 = $0.01<p<0.05$

2 = $0.001<p<0.01$

3 = $p<0.001$

Dependent Variable	Independent Variable	r	Significance Level
Collagen-1a	CTGF	0.3566	1
	HGF	0.3903	1
	Vimentin	0.4051	1
	a-SMA	0.421	1
	Sonic Hedgehog	0.5246	2
	R-spondin-1	0.5935	3
	TGFb2	0.6407	3
	Galectin-1	0.6537	3
	GDNF	0.7735	3
	Aggrecan	0.7748	3

Dependent Variable	Independent Variable	r	Significance Level
aggrecan	CNTF	-0.4783	2
	EGF	-0.4568	2
	HGF	0.3991	1
	TGFb2	0.43	1
	Sonic Hedgehog	0.4969	2
	Galectin-1	0.6324	3
	IGF-1	0.6986	3
	Collagen-1a	0.7748	3
	GDNF	0.7856	3

Dependent Variable	Independent Variable	r	Significance Level
vimentin	Sirt-1	-0.4739	2
	CNTF	-0.4332	1
	CTGF	0.5017	2
	NT-4	0.5147	2
	TGFb2	0.5159	2
	Sonic Hedgehog	0.5335	2
	Galectin-1	0.5467	3
	HGF	0.5671	3
	R-spondin-1	0.5795	3

Dependent Variable	Independent Variable	r	Significance Level
Decorin	Myostatin	-0.4234	1
	AMPK-1a	0.4420	1
	CNTF	0.4719	2
	HN1	0.4849	2
	Sirt1	0.5334	2
	EGF	0.8214	3

Dependent Variable	Independent Variable	r	Significance Level
Follistatin	GAP43	0.3563	1
	Desmin	0.3709	1
	Embryonic myosin heavy chain	0.5010	2
	Myogenin	0.5833	3

Dependent Variable	Independent Variable	r	Significance Level
Atrogin-1	Fast myosin HC	-0.7585	3
	Calpain-3	-0.6758	3
	Slow myosin HC	-0.4102	1
	Myostatin	0.7753	3
	Myogenin	0.8659	3
	MuRF1	0.9471	3

Dependent Variable	Independent Variable	r	Significance Level
MuRF1	Calpain-3	-0.7066	3
	Fast myosin HC	-0.6068	3
	Slow myosin HC	-0.4108	1
	Myogenin	0.8476	3
	Myostatin	0.8712	3
	Atrogin-1	0.9471	3

Dependent Variable	Independent Variable	r	Significance Level
myoD	CTGF	-0.4227	1
	TGFb2	-0.3873	1
	AMPK-1a	-0.3653	1
	Mef-2a	0.3788	1
	IGF1	0.3864	1
	CNTF	0.4168	1
	Myostatin	0.4611	2
	EGF	0.4899	2
	NT-4	0.5492	3

Dependent Variable	Independent Variable	r	Significance Level
myogenin	Fast myosin HC	-0.7349	3
	Myostatin	-0.4499	2
	EGF	-0.3928	1
	CNTF	-0.3479	1
	Slow troponin-I	0.4508	2
	IGF-1	0.5418	2
	Follistatin	0.5833	3
	Mef-2a	0.633	3
	Desmin	0.6338	3
	GDNF	0.7514	3
	Slow MHC	0.9229	3

Dependent Variable	Independent Variable	r	Significance Level
GAP43	Follistatin	0.3563	1
	HN-1	0.4349	1
	GDNF	0.4441	2
	HGF	0.4788	2
	Sonic Hedgehog	0.6429	3
	IGF-1	0.6643	3
	Galectin-1	0.6718	3

Dependent Variable	Independent Variable	r	Significance Level
Embryonic myosin heavy chain	CNTF	-0.4195	1
	myostatin	0.3958	1
	Follistatin	0.501	2
	HGF	0.535	2
	GDNF	0.5478	3
	Sonic Hedgehog	0.5566	3
	Myogenin	0.6373	3
	IGF-1	0.8378	3

Dependent Variable	Independent Variable	r	Significance Level
Fast myosin heavy chain	Atrogin-1	-0.7585	3
	Myogenin	-0.7349	3
	TGFb2	-0.6738	3
	MuRF-1	-0.6068	3
	Myostatin	-0.4796	2
	NT-4	-0.4297	1
	Mef-2a	-0.3777	1
	Complement-3	-0.3773	1
	Sonic Hedgehog	-0.3502	1
	CNTF	0.5359	2

Dependent Variable	Independent Variable	r	Significance Level
Slow myosin heavy chain	TGFb2	-0.3466	2
	Complement-3	-0.438	1
	MuRF-1	-0.4108	1
	Atrogin-1	-0.4102	1
	IGF-1	-0.3741	1
	CNTF	0.3479	1
	PGC-1a	0.3872	1
	Mef-2a	0.4309	1
	NT-4	0.4504	2
	Sonic Hedgehog	0.4912	2
	Myogenin	0.9229	3

Dependent Variable	Independent Variable	r	Significance Level
Fast troponin-I	Sirt-1	-0.388	1
	Sonic Hedgehog	-0.4169	1

Dependent Variable	Independent Variable	r	Significance Level
Slow troponin-I	Myogenin	0.4508	2
	Mef-2a	0.4847	2
	Myostatin	0.4988	2
	NT-4	0.7736	3

Dependent Variable	Independent Variable	r	Significance Level
AMPK-1a	CNTF	0.4909	2
	Sirt1	0.7985	3

Dependent Variable	Independent Variable	r	Significance Level
CNTF	TGFb2	-0.5564	3
	AMPK-1a	0.4909	2
	EGF	0.5861	3
	Sirt1	0.7013	3

Appendix 13. Loss of Muscle Mass over 12-weeks

Muscle mass is shown in means ± standard deviation, n=3 per treatment group.

Group	Mean muscle mass (g)	Difference	Loss of muscle mass (%)
PN-2 PN-12	0.544 (0.041) 0.325 (0.002)	-0.219	21.90
DN-2 DN-12	1.054 (0.017) 0.4836 (0.003)	-0.5704	57.04
RN-2 RN-12	0.481 (0.005) 0.203 (0.001)	-0.278	27.80